University of Southern Queensland
Faculty of Health, Engineering and Sciences

ANALYTICAL MODELLING OF COMPOSITE SANDWICH PANELS

A Dissertation submitted by
Jordan Picton

In fulfilment of the requirements of
Course ENG4111/4112 – Research Project

towards the degree of
Bachelor of Engineering (Civil)

ABSTRACT

With the use of recycled materials within construction becoming more expansive and varied, there is an increased interest in further developing these materials and processes. This paper will focus on investigating the mechanical behaviours recycled wood composite material and will explore improving the suitability of combining wood composite materials into a sandwich panel, adding a layer of skin on either side to help improve the inefficiencies of the product. An analytical model has been created to determine how the product can be enhanced by the addition of these skin layers, and the model has been expanded to include other recycled material options to select from for the core and skin, to be able to determine the maximum load that a panel can withstand in a simple three-point bending test set-up. This model aims to create a design tool which makes it easy to determine the suitability of sandwich panel products for differing design scenarios. This research will determine the suitability of wood composite products as well as other recycled materials for use as a solid core or as skin layers of a sandwich panel. From this outcome, the paper hopes to improve the prove the mechanical properties of recycled materials, increasing the usage rates and leading to more sustainable engineering design.

University of Southern Queensland

Faculty of Health, Engineering and Sciences

ENG4111/ENG4112 Research Project

LIMITATIONS OF USE

The Council of the University of Southern Queensland, its Faculty of Health, Engineering & Sciences, and the staff of the University of Southern Queensland, do not accept any responsibility for the truth, accuracy or completeness of material contained within or associated with this dissertation.

Persons using all or any part of this material do so at their own risk, and not at the risk of the Council of the University of Southern Queensland, its Faculty of Health, Engineering & Sciences or the staff of the University of Southern Queensland.

This dissertation reports an educational exercise and has no purpose or validity beyond this exercise. The sole purpose of the course pair entitled "Research Project" is to contribute to the overall education within the student's chosen degree program. This document, the associated hardware, software, drawings, and other material set out in the associated appendices should not be used for any other purpose: if they are so used, it is entirely at the risk of the user.

CERTIFICATION OF DISSERTATION

I certify that the ideas, designs and experimental work, results, analyses and conclusions set out in this dissertation are entirely my own effort, except where otherwise indicated and acknowledged.

I further certify that the work is original and has not been previously submitted for assessment in any other course or institution, except where specifically stated.

Jordan Picton

Student Number: [redacted]

ACKNOWLEDGEMENTS

I would like to thank and acknowledge my supervisor, Dr Wahid Ferdous for his guidance, support, and reassurance throughout this project.

To Ashiqul Islam, who I completed the experimentation alongside, I would like to offer a sincere thank you, as without agreeing to allow myself to assist and observe your experimentation and use the data within this project, it would not have been possible.

I would also like to thank the University of Southern Queensland, for allowing use of the facilities and machinery to perform the testing required.

And finally, thanks to my family and my partner, Rhianna, for their continuous support throughout my studies.

TABLE OF CONTENTS

LIST OF FIGURES

LIST OF TABLES

CHAPTER 1 – INTRODUCTION

1.1 PROJECT BACKGROUND

Helping to protect our natural environment is becoming more important as population growth continues to increase and the demand for resource and material usage increases every year. Timber is one of these resources which is in decline, with the UN FAO estimating that an average of 10 million hectares of forests are being cut down each year (since 2010) and only 5.3 million hectares of forest are being replanted. (Ritchie & Roser 2021) This significant deforestation rate will make it ever more difficult for future generations demand to meet the supply and at this rate the natural resource will eventually become depleted.

Currently Australia is going through a significant timber shortage which is predicted to continue for the next few years, and there is a general timber shortage which is expected to last until 2035, if not beyond. (Timber and Forestry eNews 2022) New timber plantations have been sponsored by the Australian government, investing $86 million to help alleviate the shortage, but the benefits of these plantations will not be realised until at least 2047. (Timber and Forestry eNews 2022)

The construction industry currently produces enormous amounts of physical waste, being the main consumer of natural resources, and energy, also being the largest producer of physical waste products, including timber. The Australian construction industry spent $2 billion on waste services, which has increased by 35% since 2017, but this waste from construction materials has the most potential to be reused or recycled. (ABS 2020) The waste category with the lowest recovery rate according to (ABS 2020) was plastics, being only 19%, with the rest being sent to landfill. Landfills within Australia are running out of space due to the high amount of waste being produced each year, with many of the major landfills within Melbourne expected to be out of space within 5 years. (Waste Sense 2022) This emphasises the need to find sustainable materials and practices and increase rates and methods of recycling to help maintain and better our current environment and that of the future generations.

This is why it is important that alternate solutions for timber products are explored and improved upon to help alleviate the timber crisis, for a more short-term solution and to increase rates of recycling, particularly for plastic waste materials. A solution to help these problems can be found in using composite lumber technologies, which combine recycled products of cellulose fibre (wood) and industrial grade polymers (thermoplastics) with a bonding agent. (Klyosov 2007) To help alleviate any typically deficiencies of the product, additives are included in the mixture (lubricants, coupling agents, pigments, antioxidants, UV stabilizers,

antimicrobial agents, etc.) and is then manufactured in a similar process to plastics, using a high-volume process such as extrusion, compression, or injection moulding, to create a wood composite material (Klyosov 2007).

Wood composites have been typically used as a decking or railing, but are also a practical option for profiles, sheathing, roof tiles and window trims. (Wechsler & Hiziroglu 2007) The market size for wood plastic composite was USD 4.77 billion in 2019, and Fortune Business Insights (2020) predicts this to rise to 9.3 billion by 2027. (Market Research Report 2020) The reason for the market rise is due to the advantages provided by wood composites for the environment and for the consumer. Not only is the product made of recycled materials, but also can be made from unusable timber, as more than half of the wood from a tree in unsuitable for making planks and typical timber products as the branches are too thin but has the potential to be used as wood flour in wood composites. (Pritchard 2004) This will reduce the rate at which forests need to be felled and the recycling of plastic reduces a major component global municipal solid waste while providing a low-cost, high-volume material source. (Najafi 2013) The downside of the product is the additional cost to traditional timber, but it offsets this by providing numerous advantages over timber. Wood composites have a good durability, low maintenance, aesthetic qualities (no knots, splinters, warping or checking), termite and fungal resistance, as well as fire resistance qualities due to the addition of the plastic and other additives (Klyosov 2007). A downfall of the product is the strength and stiffness performance being lower than timber, requiring more structural support and being unusable in many applications. This problem may be able to be solved through the adaptation of the product into the core material of a sandwich panel.

Sandwich panels behave differently as they have a structural composition and cannot be considered as a homogenous material. Sandwich panels consist of an interior core, usually being of a lower density, and have a thin skin layer on each side of this core, secured by adhesive bonding. They offer a relatively lower density and a high rigidity (Polmear et al. 2017), having the potential to negate some of the mechanical shortcomings of the composite wood product, and can help further improve the durability through the addition of the skin material. The facing materials of the sandwich panel will carry the axial compressive and tensile forces, and the core (composite wood product) will carry the shear load.

In this study, sandwich panel mechanical properties are being tested for the viability of using a wood-composite material as the core of the panel, and this research paper will determine whether the failure mode of the material can be predicted based on the available theory. Two different types of specimens were prepared for testing, each comprising of a different skin material, either hemp fibre or recycled PET fabric.

1.2 PROJECT AIM

The aim of this project is to create an analytical model to predict the failure mode of a composite wood sandwich panel. This model will be based on the basic properties of the wood composite and of the skin material, such as the tensile, flexural and shear strength and modulus parameters to predict the load-displacement behaviour and ultimately predict the failure mode. Analytical equations will be used to predict the ultimate load for a wood composite sandwich panel for shear failure, bending failure, and a general equation to roughly predict the load for both cases simultaneously. A previous analytical model, created by Ferdous, et. al. (2017) will be used as a starting point for the shear, bending, and combined shear-bending failure model equations and will be tested against the experimental data for validation. Alterations to these models will be made as seen fit, and then the general equation will be created based on the materials behaviour in both flexure and shear. This model will then be validated against the experimental data of the wood composite sandwich panel, and the success of the model will be determined from these results.

1.3 SIGNIFICANCE OF THE STUDY

If the project aims are successful, this research will help contribute to the overall scientific knowledge in the topic of the rapidly expanding sector that is wood composite products. Being able to predict at what loads the product will reach failure would be useful in determining the suitability for the application of the product.

This research will also help in determining the viability of composite wood as a sandwich panel core and will help optimise the use of materials to obtain a stronger and stiffer product, to be able to be used for more varied and numerous applications, removing the current the reliance on fresh, non-recycled timber products, reducing deforestation, and helping to alleviate the current timber shortage for construction.

This research into other developments and applications of composite wood could serve as a starting point for other researchers who wish to explore this product further, further enhancing the material or the sandwich panels, which would help bring popularity to the composite wood products as a renowned structural alternative. This research into composite wood sandwich panels could also branch out for other environmentally friendly alternatives in construction such as recycled plastic, which could use this research to develop similar products, improving the materials mechanical downfalls.

1.4 SCOPE AND LIMITATIONS

Due to limitations in time and resources, the scope will be refined to only analyse one wood composite product, to prove that the properties are possible to be predicted. Further studies should be completed in the future to determine the validity of the experiment using several different products, that have a range of manufacturing processes, matrix composition, wood and plastic types used and additives in the mixture. This will be able to translate the research conducted in this experiment to create predictions of expected material performance for any possibility of wood composite product in the future, to allow potential consumers or companies to know how to best use wood composites in construction and their homes to increase the amount of product sold and continue helping the environment.

The mechanical properties being tested are limited to flexural strength in a three-point bending set-up, through static testing methods. Other tests such as impact and any dynamic testing will not be included in this research. There will also be no analysis of how the product performs after degradation.

All materials will be sourced directly from the supplier, and the limitations of time, restrict any long-term durability analyses of the products.

1.5 THESIS STRUCTURE

This thesis will consist of 6 chapters, consisting of the following:

Chapter 1: This chapter will provide the background necessary into the wood composite material and its advantages and show how the inclusion of the material in a sandwich panel could be beneficial, potentially becoming next stage in developing the wood composite product. It also includes the aims and objectives of the study, with the significance of the research to the overall knowledge.

Chapter 2: This chapter provides a literature review of varying scientific papers previously conducted on wood composite materials, particularly referring to the way different properties are seen to affect the materials mechanical strength. There will also be a brief analysis on the skin materials being used and will detail out the other previous analytical models developed for both wood composites and sandwich panels as useful information for the study.

Chapter 3: This chapter will provide the details of the materials being used in the study and the methodology of the experimentation that will be occurring. This will be for both the initial experimentation of the wood composite panel under three-point bending, as well as the final

experimentation of the composite sandwich panel for model validation. The composition of the final sandwich panel is also shown in diagram to be referred to in the model equations.

Chapter 4: This chapter will provide information about the theoretical analysis conducted of the results from initial experimentation as well as the theory behind the model equations. This chapter outlines each of the failure modes which will be modelled for, including how they would be predicted to occur.

Chapter 5: This chapter of the research will analyse the results from the model and compare against the theory from prior literature. The model will also be used to determine the effects of each parameter within the model equations and summarise a recommended range for each parameter to get the optimal output. This chapter will also end with the validation of the analytical model, using the experimental results of the final experimentation.

Chapter 6: This chapter will serve as a summary of the paper, re-iterating the major findings from this paper. It will summarise whether the goals of this paper were met and how it could have been improved. The paper will also conclude with recommendations and future studies which can be conducted to continue and improve upon the analytical model and to best achieve the goals this paper has set out to do using this research.

CHAPTER 2 – LITERATURE REVIEW

2.1 – WOOD COMPOSITE PRODUCTS

A literature review shows that the creation of wood composites is not a recent development, with the first uses dating back to 1916, finding limited success, and then being reborn with new processing technologies to create a successful wood substitute which became extremely popular in North America from the 1990's. (Pritchard 2004) Over the last 30 years a large quantity of studies and research has been conducted into the product to better understand and improve the product to increase its viability in a variety of ways. Due to the vast quantity of research, the most relevant literature to this potential research will be covered in this review. This will include previous studies into the differing mechanical properties, being tensile, bending, and shear properties, analysing use of recycled plastics in wood composites and the material's durability.

2.1.1 - Mechanical Properties of Wood Composites

Original testing of the mechanical properties of wood composites has occurred for a long period of time, with experimental results found dating back to 1977 for the 19th volume of the 'Radiation Physics and Chemistry' book. (Gouloubandi 1982) Since the popularisation of the product, many more studies have been conducted regarding the tensile, compressive, and flexural strength of wood composites.

The book "*Wood-Plastic Composites"* by Klyosov (2007) summarises all previous literature and experimentation data prior to its publishing. Most studies can be seen to focus on flexural strength of wood composites and how different factors affect the strength in bending. Klyosov looks at the mechanical properties of Trex boards, the most popular supplier in the US, giving the equation for flexural strength:

$$S = \frac{PLh}{8I} \qquad (1)$$

Where, S = flexural strength (N), P = load at fracture (N), L = span (mm), h = board hight/thickness (mm) and I = second moment of inertia, being $bh^3/12$. (mm^4)

Experimenting on Trex TM boards finding out they were able to withstand an ultimate distributed load of 1667 lb/sq. ft. (79.8kN/m^2), being "more than 6 times higher than the ICC required load including the necessary safety factor." (Kylosov 2007) The flexural modulus was also predicted using the equation:

$$D = \frac{PL^3}{48} * EI \tag{2}$$

Where: D = deflection (mm), and E = flexural modulus (MPa).

Later studies were conducted by Leu et al. (2012) testing effects of wood flour size and addition of coupling agents and lubricants. Formulas used to get results after testing were similar, being related to the modulus of elasticity and modulus of rupture in bending:

$$MOE = \frac{\Delta P_b}{\Delta y} * \frac{L^3}{4bd^3} \tag{3}$$

$$MOE = \frac{3P_b^{max}L}{2bd^2} \tag{4}$$

Where, ΔP_b is the difference between the upper and lower limits of the bending loading (N), Δy is the deflection in the vertical axis about the loading point, and P_b^{max} is the maximum allowable loading in bending.

Vedrtnam, Kumar & Chaturvedi (2019) performed more recent experimental studies, testing the mechanical behaviour of wood composites. The injection moulded samples were tested under tensile, three-point bending and impact, to record the properties of specimens with different woods and wood percentages. The bending tests were performed under the ASTM standard D143-14, tensile under ASTM D638-99, and the Charpy and Izod test were used for impact strength to standard of ASTM D6110-10.

Maximum load before fracture varied from 846-828N and maximum deflection was 12.8-14.4 mm. (Vedrtnam, Kumar & Chaturvedi 2019) Other literature also follows their tensile, flexural, and notched Izod impact strength testing to the ASTM standards, but Nourbakhsh & Ashori (2010), use slightly differing standards being D638, D790 and D 256 respectively. The reason for this is that there are standard configurations for testing behaviours of differing materials, but due to the material is a composite, there is no set standard to perform to. Both testing standards for tensile tests are for testing plastics, but Vedrtnam tests the flexural based on wood standards and Kumar does so based on plastics. (ASTM International n.d.)

Keskisaari & Kärki (2018a) analysed the tensile and impact strength of wood composites that use recycled plastic. Flexural properties were found to decrease, but impact resistance increased from use of recycled polymer (PW).

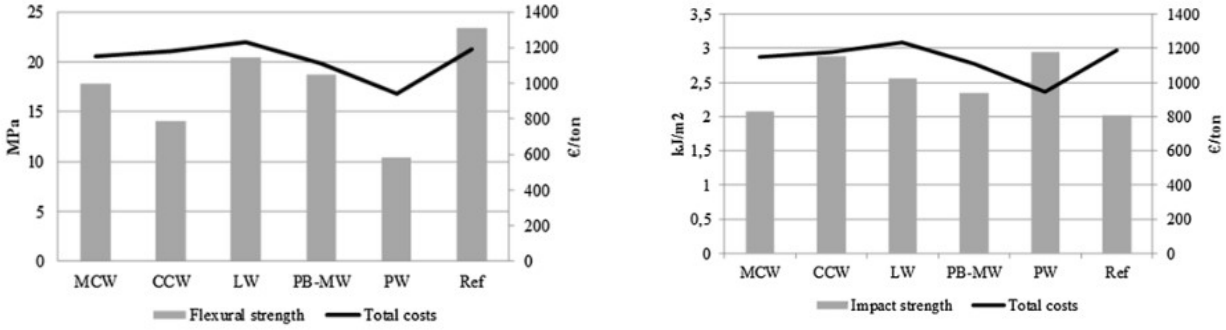

Figure 1: Difference in flexural strength (left) and impact strength (right) based on changing plastic type. (Keskisaari & Kärki 2018a)

The purpose of this study was to evaluate the influence of different recycled materials on the price of wood composite materials, and it found the price of recycled raw material is not that influential on the overall properties. However, the pricing of virgin plastics does represent the overall quality of the properties of the final wood composite product.

Not many researchers discuss the compressive strength properties of wood composites, but one study by Hamel, Hermanson & Cramer (2012) tested the composites via creep tests in tension and compression until ultimate failure. Compressive strengths were found to be close to double of the tensile strengths if not more. Due to the high compressive strengths of wood composites, the failure mode in compression of the material should not be considered as a critical failure mode. Hamel, Hermanson and Cramer then applied mathematical models to the experimental results. The mathematical expression for instantaneous strain was expressed as:

$$\varepsilon(\sigma) = A_0 \sinh\left(\frac{\sigma}{\sigma_0}\right) \tag{5}$$

Where the instantaneous strain, ε is dependent on the original cross-sectional area of the panel, A_0, the height of the panel, h, and the stress in the panel pre- (σ_0) and post- (σ) load application.

These mathematical models of strain can be very helpful in determining an analytical model for shear failure based upon the load-displacement relationship of the material.

Hugot & Cazaurang (2010) submitted composite products to tension and compression tests to the standards of wood specimens and three-point bending tests to standards designated for plastics. The results obtained were analysed using the Curve Fitting Toolbox in MATLAB for stress-strain behaviour of the material.

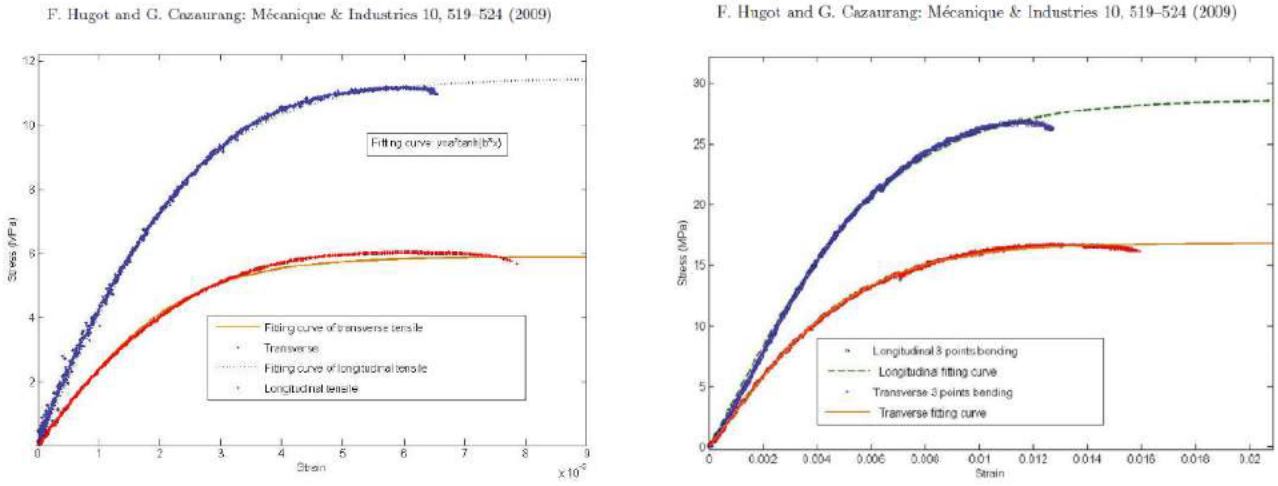

Figure 2: Experimental and fitted tension stress strain curves. Tension (left) and bending (right). (Hugot & Cazaurang 2010)

The stress-strain behaviour seen in the graph above (Figure 2), is non-linear, being closer to typical thermoplastic behaviour than the brittle behaviour of wood. The behaviour of the material is described by Zawlocki (2003) exhibiting "a constant accumulation of residual strain that can be well described using a hyperbolic tangent function." These curves are also difficult to find a yield point of the material.

From analysing the curves based on a tangent function created in MATLAB, it fits the three-point bending curve to an R^2 value of 0.99, describing the dataset very accurately, while the tensile curve has an R^2 value of 0.85 being less accurate. This shows the level of uncertainty for bending behaviour to be less than that of tension and shear, making the probability of predicting behaviour in bending the most accurate due to the patterns of material behaviour. The tensile strength was also found to be greater than compressive strength, being the opposite of its components (wood and plastic) and Hugot & Cazaurang believe this to be caused by the "mechanical entanglement of wood fibres and HDPE polymer, allowing benefit during compression testing." (Hugot & Cazaurang 2010)

The maximum tensile and bending stresses were halved in the transverse direction, but compression was seemingly unaffected by direction. The maximum tensile stress for the wood composite (σtl = 11.6MPa) was lower than HDPE (σtl = 25MPa) and wood (σtl = 50 MPa) in

the testing, leading to the conclusion that the wood product is acting as a filler in the matrix, rather than as reinforcement. (Hugot & Cazaurang 2010) From the fractured appearance of the material, evidence of fibre pull out is present (Figure 3), being characteristic of poor interfacial adhesion. This is a well-known problem for composite products due to the incompatible nature of both components, and Hugot and Cazuarang (2010) suggest "additional improvements should be done to link wood fibre to thermoplastic in order to prevent the fibre pull out leading to a better load transfer."

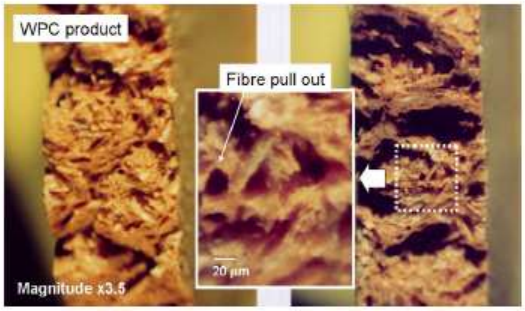

Figure 3: Failure appearance of wood composite material. (Hugot & Cazaurang 2010)

2.1.2 - Analysis of Plastics for use in WPC

Almost any type of plastic has the capabilities of being used as the plastic component of a wood composite, but only three major types are used today, being polyethylene (PE), polypropylene (PP), or polyvinyl chloride (PVC). Klyosov (2007) suggests the reason these plastics are used is due to the low pricing of the materials, while still having the required properties to allow the finished material to pass the building code.

Najafi (2013) and Basalp et. al (2020) both stress the importance of recycling plastic waste products, with wood-plastic composites (WPCs) being an important way to increase the amount of material recycled each year. Najafi (2013) discussed the effects that the conditions of the recycled plastic have on the mechanical properties of WPC. Because recycled plastics are exposed to differing storage and reprocessing conditions, it is found to be important that proper and efficient collection, separation, and recycling processes are established to reduce a level of variability as to not have poor performing plastics within the final product mix. Basalp et. al (2020) examines the difference in performance of WPC with recycled plastic (r-WPCs) versus virgin plastic (v-WPCs). Five differing types of PP or PE based recycled plastics were tested, and specimens were created at differing wood flour contents to provide a dataset, different additives were used as well to determine the optimum compound for the WPC. Basalp performed tensile tests of WPCs, carried out according to ASTM D638 standard in Shimadzu AG-I mechanical test equipment at a 10 mm/min tensile test speed and 5 kN load cell. Notched

Charpy Impact strength tests were conducted by using a V-notch CEAST Resil Impactor and three-point flexural bending tests were performed by using AGS-J Shimadzu mechanical testing machine with 5 kN load cell and support span length of 62 mm. The tensile test found 30 % wt of plastic to be the optimum amount, having the greatest tensile strength (24.8 MPa). It was also found that the r-WPCs had lower impact strength, decreased flexibility, but the most flexural strength.

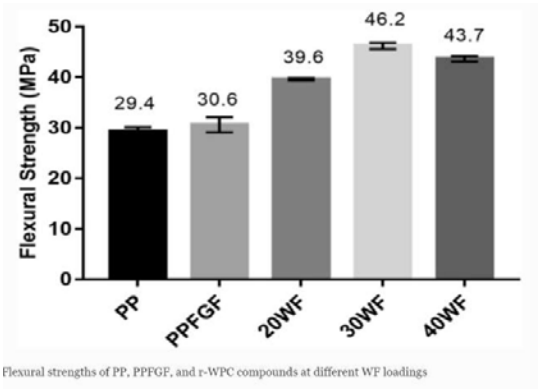

Figure 4: Flexural strengths of differing plastics, and with differing wood fibre percentages. (Basalp et. al 2020)

Basalp attributed this increase in flexural strength from the recycled plastic to be due to the improvement on interfacial adhesion between the wood and plastic from the bonding of the matrix and improved dispersion of the wood particles throughout. (Basalp et. al 2020) This research shows the differing strengths between virgin and recycled plastic in WPCs, having differing strengths and weaknesses, yet both have acceptable properties to use in the wood composite.

The lead company in supply of WPC, are one of the largest plastic recyclers in the US, saving over 800 million pounds of reclaimed timber and recycled plastic annually, with each standard 16-foot Trex board containing the equivalent of 2250 plastic bags. (Trex 2022) This shows the potential benefit using r-WPCs over v-WPCs can have on the environment, contributing to the circular economy. From this research into recycled versus virgin polymers in wood composites, the recycled plastics are determined to have high potential for use while still maintaining comparable mechanical strength properties. With the cheaper recycled plastic having similar performance to the more expensive recycled and virgin options, the potential for using recycled plastics is high, with efficient processes needing to be established to reduce variability of the plastics strength properties by ensuring effective storage and separation of the recycled materials.

2.1.3 - Durability

Studies on wood composites are predominantly from the United States, due to the popularity of the product within the country. Many studies assessed the durability of the composite, and this information is important for application in Australia due to the differing conditions that will need to be endured under the Australian climate and environment. Wood composites are typically marketed as highly durable, even more so than timber, due to the necessity of high durability because of the typical outdoor application of the product. Early studies by Caulfield et al. (2005) showed the nature of the product to absorb moisture slower than timber, which helps protect itself from issues like dimensional changes as a result of moisture as well as protecting the material from fungal attacks.

Wood composites were originally depicted as impervious to biological attack due to the nature of the plastic surrounding the wood particles. Many later studies proved this fact to be false, showing wood composites to be susceptible to degradation. Pendleton et al. (2002) found fungal decay to have a very low leach rate, but still could affect the product under the right condition, and suggested zinc borate as an additive to help prevent fungal intrusion. Investigation into wood materials using zinc borate were conducted around the same time by Verhey, Laks & Richter (2001), which found similar mechanical strength deterioration in all specimens regardless of the amount of zinc borate used. The result of this research concluded that the predominant strength losses were caused by the thickness swelling from moisture absorption, rather than fungal attack.

Despite Caulfield's findings of slower absorption rate, if moisture is allowed to enter the lattice, the effects are quite devastating to the product. A study into moisture absorption's effects on mechanical properties has showed an injection-moulded wood composite containing 40 percent wood flour was soaked for 2,000 hours that the moisture increased to 9%, resulting in the flexural modulus and strength decreasing by 39 percent and 22 percent, respectively (Stark 2001). Schirp et al. (2008) recommends into how to improve the durability of WPCs, by moisture exclusion, via complete encapsulation of the wood particles by the plastic matrix, hydrophobation of the material surface or chemical modification of the wood substrate. Schirp also disagrees with Pendelton's recommendation of zinc borate, claiming "no reasonable amount of zinc borate will prevent moisture entry into the composite." (Schirp et al. 2008)

Morell et al. (2006) provides a summary of many other works into the durability of wood-plastic composites and suggests an ulterior method of degradation by photodegradation caused by ultra-violet (UV) light. This was though not to be a potential issue due to the plastic matrix, but residual solvent and other impurities allow photodegradation of the lignin in the wood. This results in changes in colour, surface composition, and small changes in mechanical properties.

These affects are not too major, but photodegradation may be a common issue for long term use of wood composites under the weather conditions in Australia.

Due to the plastic within the matrix, the materials are also resistant to termite attacks, and improved resistivity to chemical intrusions and fires. The strong durability of the product can make wood composites a resilient and resistive material, suitable for interior use as panelling within homes, having a greater resistivity to fire than traditional foam panel materials.

2.2 - PREVIOUS WOOD COMPOSITE ANALYTICAL MODELS

A summation of models used for wood composite products, prior to 2008, was detailed by Hugot & Cazaurang (2008). The differing models analysed and compared were the series, parallel, Hirsch (and modified Hirsch), Cox/Bigg/Kelly and Halpin/Tsai models, which all relate to predicting elastic properties of two discontinuous phases. The comparison was made against experimental data completed by Hugot & Cazaurang, where the modified Hirsch model and Cox/Kelly/Briggs model were seen to be in best agreement with the experimental data (See Figure 5).

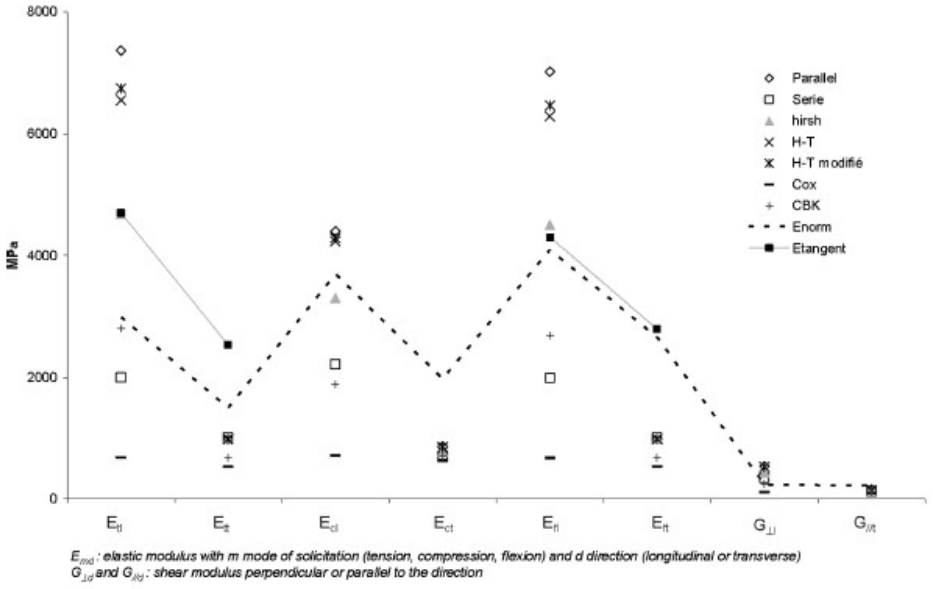

Figure 5: Evaluation of MOE from analytical models compared to experimental (Hugot & Cazaurang, 2008).

Due to the inefficiency of wood composites in tension, having a lower performance than both wood and HDPE, limits the differing model's accuracy in many cases.

2.3 SANDWICH PANELS

2.3.1 Key Papers for Model Preparation

The analytical model that will be used as a starting point for the wood composite sandwich panels will be based on the model created by Ferdous, Manalo & Aravinthan (2017), which will be adapted as required. Ferdous created this model for phenolic core sandwich panels under 4-point bending to determine the theoretical failure load of the panels. This model tested the effect of beam orientation and shear span-to-depth ratios on the failure loads and the predicted failure mode of each panel depending on these two factors. This research featured analytical models using equations relating to the nature and structure of the sandwich panel consisting of two outer layers of GFRP (skin) and a softer middle layer (phonetic core). The wood composite sandwich panel is expected to behave differently under loading due to the dramatic increase in density of the core material, being the composite wood, being atypical compared to the phonetic core in Ferdous' experimentation.

It was observed that the shear span-to-depth ratio of the panels in application is important for the moment capacity, with this ratio increasing would result in significantly reducing the moment able to be carried due to the nature of the skin wrinkling from compression (Mathieson and Fam 2015). Due to this nature, the shear span-to-depth ration will be kept the same for all materials being tested, so that differing thicknesses will have less of an effect on the results obtained.

Other papers within the literature have created analytical model equations for sandwich panels under three-point bending, being based upon the stress within the core material reaching the allowable limit under midpoint loading. These papers are by Steeves & Fleck (2004b) and Ouled Ahmed Ben Ali & Chatti (2020) who base the equations upon differing beam theories.

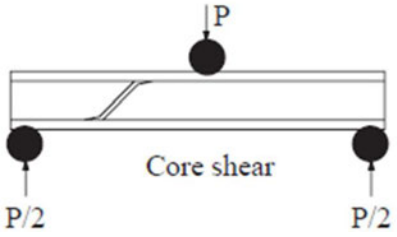

Figure 6: Diagram of core shear failure in a three-point bending test set-up. (Steeves & Fleck 2004b)

In the model by Steeves and Fleck, the analytical equation used in this study, considers a simple equation, based on the shear strength (τ_c) of the core material, and its width (b) and depth (d).

$$P = 2\tau_c bd \tag{6}$$

This equation does not consider any effects of the skin and treats the panel as homogenous, due to the failure criterion of the panel by shear, being considered of the core alone. In their analytical models (2004a) Steeves and Fleck treat the sandwich panel as a non-linear Timoshenko beam, having a rigid core and elastic face sheets. This allows contribution of a post-yielding hardening response, controlled by the bending stiffness of the face sheets (skin), increasing the load required before shear failure.

$$P = 2\tau_c bd + 8E_f b\left(\frac{t_f}{L}\right)^3 \delta \tag{7}$$

This equation is the same as before but with the addition of load required due to the skins response to loading, requiring the elastic modulus of the skin layer (E_f), the thickness of the skin layer (t_f) and the vertical displacement about the midpoint (δ).

The other model equation for shear by Ouled Ahmed Ben Ali & Chatti based the analytical equation upon the modified Gibson's model. In this model, the panels failure load in shear is considered to just be affected by the properties of the core, with no benefit provided by the skin layers. The critical shear load (P_{cr3}) of the core is expressed in the equation:

$$P_{cr3} = 2be_c\left[2.32\left(\frac{\rho_c}{\rho_s}\right)^{3/2} - 0.28\frac{\rho_c}{\rho_s}\right]\sigma_{ys} \tag{8}$$

Being based upon the dimensions of the core, with *b* referring to the width of the panel and e_c being the thickness of the core. The equation is based upon the yield strength of the core material (σ_{ys}) and is multiplied by a factor of dimensionless relative density of the core (ρ_c/ρ_s). Both of these equations will be later used to compare against the equation based upon four-point bending by Ferdous (2017) to determine the accuracy of each model's prediction for the shear failure load.

For comparison of the four-point bending failure load analytical equation by Ferdous, it will be compared against a separate model from Ouled Ahmed Ben Ali & Chatti (2020), considering the tolerance of the yield strength of the skin layers being exceeded by the normal stress at the load point, from rearranging the bending moment equation. This gives Equation 9 for the critical bending load (P_{cr1}):

$$P_{cr1} = \frac{4be_p e_c}{L}\sigma_{yp} \tag{9}$$

Being based upon the modified Gibson's model, where σ_{ys} is the yield strength of the skin material. This results from this equation will be compared against those from the four-point bending equation for the effects from altering the skin thickness.

2.3.3 Other Key Sandwich Panel Papers

The analytical equations used in this paper will be tested against many other credited examples of sandwich panels already existing within the literature. This will be done to determine the viability of the analytical modelling equations against a variety of differing sandwich panel types and using various materials to determine the suitability of the model equations to describe the behaviour of any sandwich panel material, and to know the strengths and limitations of the models. The existing papers within the literature that the model will be tested against will need to have done practical experimentation on a created sandwich panel, determining the behaviour of the material under three-point bending.

The papers that were selected for analysis, were required to have the material properties of both skin and core materials, and the details of the test set-up shown. Photos of the panels after failure has occurred were also required so that the failure mode can be seen or inferred based on the condition and failure planes seen on the material to perform a proper analysis and comparison. If all required inputs for the model were not found within the paper, the values were taken from manufacturers of the products listed by the paper, or other academic research papers that used an identical material were sourced for the required information. To help determine allowable stresses of materials an arbitrary Factor of Safety of 1.5 was chosen for all examples.

2.3.3.1 – Sandwich Panel Experimentation for Verification of Model Equations

The differing papers chosen for the analytical modelling were selected to contain as wide of a variety of sandwich panel types, materials, and compositions as possible from the literature available, while following the required guidelines that are detailed in Section 4.5 of this paper.

Paper number 1 by Xia et al. (2022) creates 5 different sandwich panels with differing core types, including some with differing materials, layouts, and thicknesses, while keeping the same skin material (Al5005-H34) and overall dimensions and loading conditions of the panels. The reason this paper was chosen was to discover the limitations of the model against a variety of sandwich panel types, instead of the solid core that it was originally modelled for. Cores like honeycomb cores and transverse and truss hollow cores all respond differently under loading,

and this paper will help display the inaccuracies due to these differences and will determine if the model equations are at all suitable in these cases.

The next paper by Mohammadabi et al. (2020) investigates using a composite wood product for both the core and the skin material. This will show the effects of having materials of the same properties of both skin and core, and the overall effects of sandwich panel creation in this manner will be analysed. The composite wood core is a corrugated core, so predictions by the model may not be relevant due to the model being based on homogenous core panel types. The level of accuracy of the prediction for this different core type will be known from using comparisons with the previous paper by Xia et al. (2022).

Another key paper for validation is by Ma et al. (2020), where sandwich panels were tested for fatigue behaviour under three-point bending. Within this paper, static testing under three-point bending is conducted as a reference point for the fatigue loading, and this experimental data is what will be used to compare against the model equations to determine the accuracy and help validate the prediction of failure load. Ma created two sandwich panel types, consisting of the same materials, being a 15 mm thick Nomex honeycomb core, at a modulus of 10.5 GPa, with differing face sheets (skin layers) for each panel configuration, with a differing laminate skin, having a modulus of 36.2 GPa. The length between the supports of all tests was 200 mm, and a width of 75 mm. A summary of the thickness of the skin layers, the modulus of the skin materials and the ultimate failure load for each panel type is in Table 1. The honeycomb core is tested in two differing configurations, to test how the core behaves when the thicker walls of the Nomex honeycomb are in the longitudinal direction (L) or the transverse direction (W).

Table 1: Summary of ultimate load of different sandwich panels from Ma et al. (2020)

Honeycomb Configuration	Skin thickness (mm)	Ultimate Load (kN)
L	1.1	9.38
L	2.42	10.78
W	1.1	5.69
W	2.42	5.82

Another paper which will be used for verification is by Giglio, Giglio & Manes (2012), that performed a numerical investigation of sandwich panels with an aluminium skin and Nomex honeycomb core. The analytical model is not created for honeycomb core types, however the results are expected to be similar due to the strong performance of honeycomb cores, acting with similar mechanical properties to solid core panel types. The panel has dimensions of 70 mm width and 200 mm length, with the core material being 19.05 mm thick, with an elastic modulus of 1.878 GPa, and a yield strength of 40 MPa. The skin material is 0.25 mm thick, with an elastic modulus of 72.4 GPa. With data not being provided for the yield or shear strength of the skin, the data values for Al5052 will be used, having a similar modulus. Four

experimental tests were performed on the created panels, with the average peak load from the three-point bending test being 0.455 kN, with a 0.3% error.

Papers also need to be analysed that consist of a solid or foam cores for direct comparison to the model. One of these papers to be used for verification of the model equations is from Huang et al. (2022) who tested composite sandwich panels with an aluminium foam core in three-point bending. The experimental results from this study can be directly compared against the model, as the model's creation was based on solid and foam homogenous core panel types. The length of the samples is 120 mm, by 50 mm width, with the aluminium foam core being 28 mm thick and the Aluminium alloy 3003 skin layers being roughly 1.6 mm thick. The required material properties are not provided within the paper, so will be taken from Matweb (n.d.), giving an elastic modulus of the Al 3003 skin at 68.9 GPa, yield strength of 296 MPa, and a shear strength of 110 MPa. The core will be taken as ALPORAS aluminium foam, for which the properties will be included within the final model as standard.

The panels within Huang's study mostly failed via indentation failure, so the allowable load for bending, shear, and combined failure should be greater than the failure load of roughly 0.8 kN.

The final paper being compared to the model is by Crupi & Montanini (2007), which also analyses an aluminium foam sandwich panel in three-point bending. Crupi & Montanini analyse the collapse mode of panels under static and dynamic loading, but for the purposes of this research, only the static loading tests will be analysed. Two differing sandwich panel materials compositions are being tested, Alulight AFS and Schunk panels. The Alulight panels consist of an AlSi10 foam core, and two Aluminium (99%) face sheets, and the Schunk panels consist of an AlSi7 core and AlMn1 faces. The dimensions of both panels are identical, being 50 mm wide and 20 mm thick, with face sheets of 1 mm. It was found that the failure mode of the panels was dependent on the support span of the panels, and many different spans were trialled, with the differing failure modes of the panels being documented. For the purposes of this analysis, the span of 110 mm for the panel composition will be used, as this produced a core shear failure found for the Alulight panels, aligning with one of the failure prediction modes within the model. At this panel width, the panel failed at an ultimate load of to fail around 1.20 kN for the Alulight panels, and 2.2 kN for the Shunk panels under static bending.

2.3.3.2 – Sandwich Panel Experimentation for Analysis of Model Equations

Xia et al. (2022) performed bending tests on various sandwich panels with different types of cores. The four types of cores focused on in this study were corrugated, truss, honeycomb, and aluminium foam cores. This paper is very useful to test how the analytical equations used in this paper perform for differing sandwich panel core types, other than the solid core of the composite wood being focused on in this study.

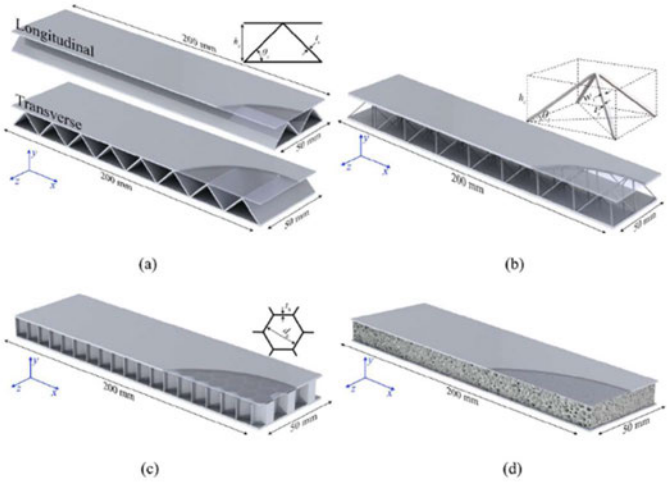

Figure 7: Schematics of differing sandwich panels. (a) corrugated, (b) truss, (c) honeycomb, and (d) aluminium foam core.

(Xia et al. 2022)

The three-point bending tests were performed on each of these panel types, set up as in Figure 8.

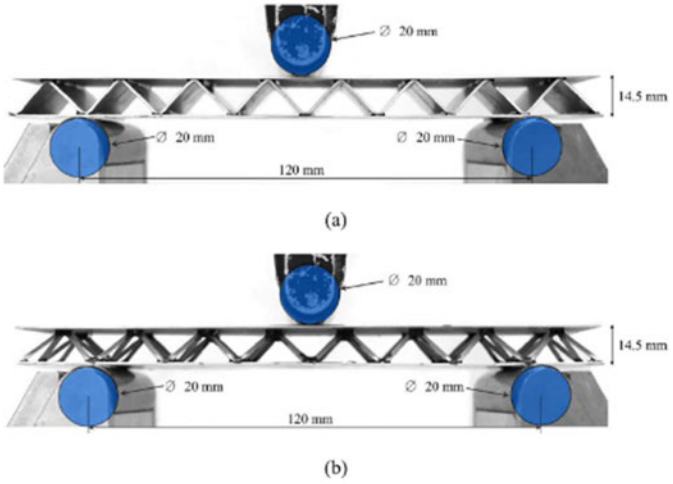

Figure 8: Three-point bending test set-up on corrugated core and truss panels.

(Xia et al. 2022)

Using the parameters of the test set-up and the materials described in the paper as the inputs of the model, it will be tested against both the bending, shear, and combined failure modes. The parameters that were required but not mentioned in the study will be taken from the product

information of ALPORAS aluminium foam in Table 2 below, being the flexural strength and Modulus of Elasticity of the foam core.

Table 2: Material Properties of ALPORAS aluminium foam. (Shen, Lu & Ruan 2010)

ALPORAS® aluminium foam Composition (%)	Density (kg/m^3)	Young's modulus (GPa)	Shear modulus (GPa)	Shear strength (MPa)	Tensile strength (MPa)
Al + 1.5%Ca + 1.5%Ti	230 ± 20	1.1 ± 0.1	0.33 ± 0.02	1.2 ± 0.05	1.6 ± 0.2
Bending strength (MPa)		**Poisson's ratio**	**Compressive peak stress (MPa)**		**Average cell size (mm)**
2.8 ± 0.3		0.33	1.9 ± 0.3		2.88

Three-point bending tests were conducted for all created panels with the load vs displacement data being seen in the various graphs in Figure 9. The tests were conducted on a 50kN MTS machine loaded at a rate of 1.5 mm/min. The maximum load experienced from Figure 9 for each core type will be used as the loading at panel failure, being the ultimate load to be predicted and compared against by the final model.

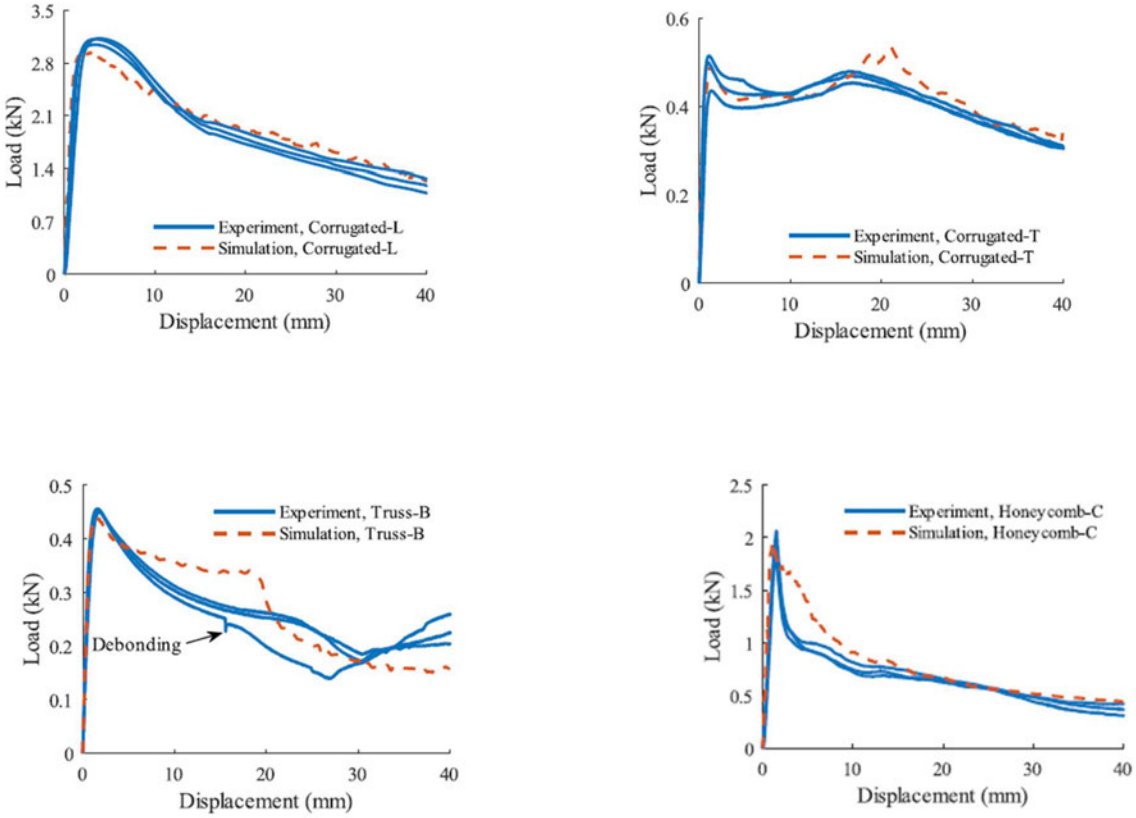

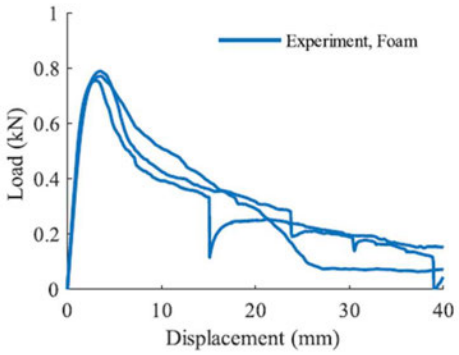

Figure 9: Experimental results of bending tests by Xia et al.

(Xia et al. 2022)

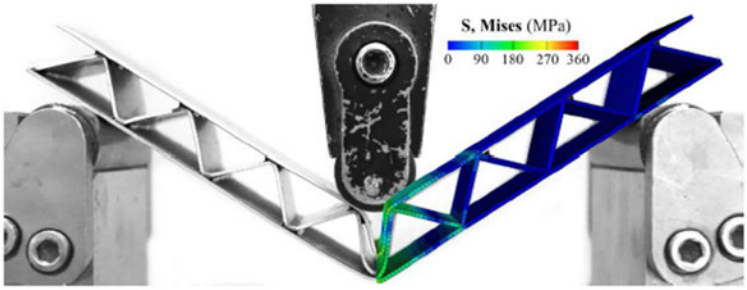

Figure 10: Failure mode of corrugated Al5005 core.

(Xia et al. 2022)

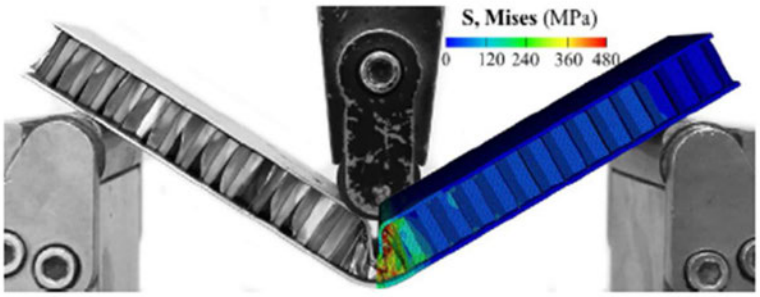

Figure 11: Failure mode of honeycomb Al5052 core.

(Xia et al. 2022)

Corrugated core panel types were seen to experience global bending failure or indentation failure, aluminium foam core panel failed in shear failure, and honeycomb panels failed by

global bending failure with some indentation occurring. Truss core typed panels were observed to have two failure modes, by asymmetrical deformation of the core struts, leading to failure or by bending of the face sheets leading to deformation of the core struts resulting in collapse.

These failure modes and ultimate failure loads observed by the experimentation by Xia will be compared against the predicted results by the final model and compared to determine the viability of the model predictions for differing sandwich panel core types.

The next sandwich panel being tested against the model was created by Mohammadabadi et al. (2020), where predictive models were created for elastic bending behaviour of a 'wood composite sandwich panel'. This model is different to the planned experimentation and model creation in this study as a composite wood product was made into a sandwich panel in a hollow core geometry in the configuration as seen in Figure 12.

Figure 12: Composite wood sandwich panel structure by Mohammadabadi.
(Mohammadabadi et al. 2020)

As seen in this figure, the panel is made of a composite wood material which is used as both the outer skin layers and as the core material, being differentiated by being a corrugated core construction to improve the material performance. In this study the wood composite was turned made into unit cells, with only wood strands from small timber used to fabricate the panel for uniformity. The Modulus of elasticity was determined from these unit cells in both the longitudinal and transverse directions, with the bending stiffness being determined from a 4-point bending test, conducted as per ASTM D7249. The corrugated core in isolation and the created sandwich panel were tested for comparative purposes and the bending stiffness was determined by the equation below:

$$EI = \frac{23mL^3}{1296} \tag{10}$$

Two theoretical models were then derived and compared against finite element analysis of the material. The two models were the classical beam theory (Euler Bernoulli) and the first-order

shear deformation beam theory (Timoshenko) to investigate the bending behaviour of the product and material. These theories were derived using displacement fields, the principal of minimum potential energy, and the variational method to arrive at the governing equations used below,

$$\text{Euler–Bernoulli}: \; Q_{11} I \frac{\partial^4 w}{\partial x^4} = q(x)$$

$$\text{Timoshenko}: \begin{cases} Q_{11} I \frac{\partial^2 \phi}{\partial x^2} - k_s Q_{55} A\left(\phi_x + \frac{\partial w}{\partial x}\right) = 0 \\ k_s Q_{55} A\left(\frac{\partial^2 w}{\partial x^2} + \frac{\partial \phi}{\partial x}\right) + q(x) = 0 \end{cases}$$

Figure 13: Euler-Bernoulli and Timoshenko equation used by Mohammadabadi.
(Mohammadabadi et al. 2020)

Where w represents beam deflection and Φ represents rotation of the cross section about the y-axis, with Q_{11} and Q_{55} being components of the stiffness matrix, and k_s is the shear correlation factor.

The results of this paper found both the two models, Euler and Bernoulli both followed the experimental deflection curve to a greater extent than finite element analysis, being very accurate until reaching a higher load/deflection. The bending stiffness determined of the material in experimentation was numerically between the two model equations (being lower) and the finite element analysis (being higher), with the Euler model derivation having the closest result.

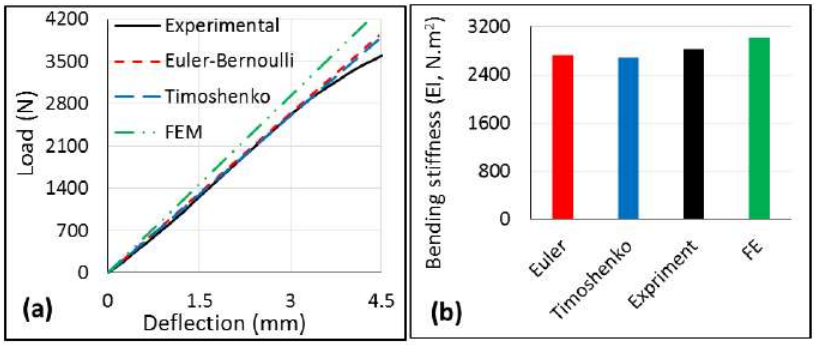

Figure 14: (a) Comparison of load-deflection curves and (b) comparison of bending stiffness results by Mohammadabadi.

(Mohammadabadi et al. 2020)

From a sensitivity analysis performed by Mohammadabi, the Euler model was observed to have the most differentiation when changing the E values of the specimen, and the finite element analysis had the greatest change in stiffness when altering G values, being far greater than the two models. This shows that the Timoshenko model is the safest for differing material

properties, being mostly in-between the percentage of change of the other two models in these categories.

Table 3: Sensitivity analysis performed by Mohammadabadi. (Mohammadabadi et al. 2020)

Property	% Change in Material Properties	% Change in Bending Stiffness		
		FE	Euler	Timoshenko
E1	9.4% increase: E_1 = 10.72 GPa	8.8	9.3	9.2
	9.4% decrease: E_1 = 8.88 GPa	−8.7	−9.2	−9.1
E2 = E3	13.4% increase: E_2 = 1.94 GPa	0.41	0.89	0.34
	13.4% decrease: E_2 = 1.48 GPa	−0.5	−0.85	−0.25
G12 = G13	37.8% increase: G_{12} = 3.53 GPa	3.3	0.57	0.97
	37.8% decrease: G_{12} = 1.59 GPa	−5.9	−0.47	−1.5

2.3.3.3 – Analysis of Shear-Span-to-Depth Ratios of Sandwich Panels

In the model to be created, the differing failure loads of a sandwich panel are to be predicted, to determine which failure mode will be the minimum and the ultimate cause of panel failure, either by bending, shear or combined bending and shear failure. One of the properties which will help indicate the expected failure mode is the shear-span-to-depth ratio, or a/D, where “a” represents the distance from each support to the loading point, and D representing the total depth of the composite sandwich panel. Some examples of determining the effects of the a/D ratio for sandwich panels can be found in the literature.

From testing a phonetic cored sandwich panel with GFRP skin, Ferdous et al (2017) analysed the effects of a/D ratio for a sandwich panel, and the expected failure mode of panels with different a/D ratios. From testing in differing orientations and at differing different load points in a four-point bending test to alter the a/D ratio, the effects could be seen.

From the many different a/D ratios tested, Ferdous concluded that the beams in the vertical orientation failed in a more brittle manner. Indentation failure is likely to have occurred at lower a/D ratios, due to the reduced width at the loading positions, creating less contact area to distribute the load effectively. In relation to the a/D ratio, shear failure was expected to occur when the ratio was less than 2 and bending failure (skin compression) was expected when greater than 6. A transitional zone was observed when a/D ratios were between 2 and 6 where both the effects of bending and shear can be seen contributing to the sandwich panels failure.

Zhang et al. (2020) analysed the effects of a/D ratio for a composite sandwich beam, consisting of GFRP skin and a balsa wood core. In this study the panels were subjected to three-point loading.

The results showed that shear failure was experienced at the lower a/D ratios and bending failure at the higher (roughly 6). This paper concluded that when a/D < 4, it is predicted to fail

in shear, and for a/D > 6, it would be expected to fail in bending. There is no mention of combined shear and bending failure, but it would be expected at an a/D ratio between 4 and 6 for this material setup.

Both papers had a similar conclusion about the relationship between a/D ratio and the expected failure mode. There was agreement that at a/D > 6, the panel should be predicted to fail in bending, but there was slight disagreement on the shear failure, so any panel that has an a/D between 2 and 4 will be acceptable to either be predicted to fail in shear or combined failure in the model. Any panel with an a/D less than 2, should be predicted to fail in shear.

The a/D ratio will be used to help validate the model results, as the properties of other tests can be inputted into the model, and the failure mode that was seen should also be predicted by the model, and at a similar load. If failure mode experienced is not noted, it will be predicted by the relationship from Ferdous et al., (2017), being shear failure predicted for a/D < 2, combined bending and shear failure for 2 < a/D < 6 and bending failure for a/D > 6. The papers used for validation will need to supply the required material properties of the core and skin and the experimental failure load under three-point bending.

2.3.4 Material Properties for Use Within Final Model

The final model created will have many differing material options for both the core and the skin. For use of differing material options within the model, certain properties will need to be known for each, including the Young's Modulus, yield strength, shear strength, and the optional parameter of the shear modulus of the material. For the model, different recycled material options are desired to be included as well as traditional sandwich panel materials which are being currently used.

The recycled materials for the core are to be the wood composite product and recycled plastic, also including traditional materials of foam and phenolic core materials. For the skin, hemp fibre and recycled PET will be the recycled options, with Aluminium, AL5052 and GFRP being traditional skin layers also included. The data for the wood composite is determined from the experimentation under three-point bending within this paper, and the other material options parameters will be taken from published literature, being referenced within the model.

Recycled plastic lumber is the other sustainable material choice for within the model. The modulus of elasticity of the recycled plastic for 100% recycled fibres will be 620 MPa (Yin et al. 2013), the yield strength is 24 MPa (Barbosa, Piaia & Ceni 2017), and the shear strength is taken from Resco Plastics (1997), where the average of the three tests was taken, being 6.19 MPa. Other more recent testing was found of recycled plastic materials for shear strength, but the materials undertaking conditioning to determine effects under extreme temperatures to measure performance, so the values of these tests will not be considered.

Hemp fibre is the chosen skin material for the sandwich panel creation within the model. This material was chosen due the availability of the recycled material for the potential to physically create the sandwich panel for future verification of the theoretical model. Hemp fibres have an elastic modulus of 75 GPa, being similar to the stiffness of glass fibres, which vary from 50-75 GPa, and are much more practical in fabrication. (Thygesen et al. 2006) Hemp fibres are a highly ductile material, allowable large deformations before reaching their yield. The shear strength of the hemp fibres used within the model is to be 8.86 MPa (Dhaliwal, Dueck & Newaz 2019). The density of hemp fibres was also required for use in the model, for use in the modified Gibson shear failure model equation which is to be used as comparison to the other shear model equations. The density used is taken from Liu et al. (2017), who compares many differing research papers into hemp fibres and the average of these results was taken at 1500 kg/m^3. This parameter is only required for hemp fibre as this is the skin material that is used in the test model and is not required for any material in the created final composite sandwich panel model.

For the Recycled PET skin material, the flexural modulus and yield strength were obtained at 10.5 GPa (Tapia-Picazo et al. 2017) and 45 MPa (Ror, Negi & Mishra 2023) respectfully with Tapier Picaso et al. finding the mechanical properties of the recycled PET fibres being found to have almost twice the mechanical performance of the virgin PET fibres. The shear strength was not able to be obtained, however the relationship of shear strength being roughly equal to between 0.58-0.6 times the ultimate tensile strength, the final shear strength was calculated at 60% of 49MPa, equalling a shear strength of 29.4 MPa.

For the non-recycled materials, the AL5052 and AL5005-H34 skin layers and the foam core layers were chosen due to their use within the paper by Xia et al. (2020) for the modulus and the yield strength, where different sandwich panel core types and materials were tested. The elastic modulus of these materials used is 73 GPa for the Al5052, 53.5 GPa for the AL5005-H34 skin material, and 1.1 GPa for the foam core and the yield strength of each of the materials will be 96.5 MPa for AL5052, 114 MPa for AL5005-H34, and 2.8 MPa for the foam material. The shear strengths were included in the paper, being not relevant to the study and will be taken from other sources. The Shear strength for Al5052 will be 138 MPa, (Cavallo n.d.), 96.5 for AL5005-H34 (Matweb n.d. a) and 1.7 for the foam material (Matweb n.d. b).

The other non-recycled materials are the phonetic core material and GFRP skin, both of which will have the required properties taken from Ferdous, Manalo & Aravinthan's (2017) paper investigating the effects of differing shear span to depth ratios on ultimate failure load of sandwich panels. From this paper, all required material properties are listed, with an excerpt being provided in Table 4. Of note the properties of the GFRP skin are being taken from testing on the material in the longitudinal orientation, to align with the modelled sandwich panels.

Table 4: Properties of GFRP skin and phenolic core materials.

Test	GFRP	Phenolic core
Elastic Modulus (GPa)	14.28	1.33
Yield Strength (MPa)	450.39	14.32
Shear Strength (MPa)	23.19	4.25

2.4 KNOWLEDGE GAP/CHAPTER SUMMARY

From the literature, a clear gap within the existing knowledge can be seen, with no research into solid sandwich core panel types. Using a material with a high density and modulus compared to a foam panel will have a much greater stiffness and can improve the mechanical performance of panels in shear. Exploring solid sandwich panels, using recycled alternatives as core materials will be analysed in this paper, with a wood composite material being used as an example, which will be explored for its performance to determine the structural performance of this material, and many other solid core sandwich panels. Based on the various simple model equations of homogenous materials, the use of a validated analytical model can generate results and be used for analysis in a simple manner.

Various model equations for predicting the load allowable of sandwich panels exist within the literature, however, none are applied and compared to differing scenarios and there is no research into using a model to optimise a product based on the theoretical predictions from the model equations.

Wood composite was found to be a suitable choice for use in a sandwich panel, due to the materials nature, being a highly durable product, with many great qualities, but studies have been inconsistent in finding the performance of the material to be less than traditional timber products, being suitable for use within a sandwich panel to help improve the mechanical deficiencies of the product, and will be tested within the created model for optimisation of material thicknesses, dimensions and skin materials to improve mechanical performance. With the wood composite panels becoming more popular, further studies conducted on the materials are analysing effects of different agents, mechanical processing, and more to further improve and simplify the manufacturing and cost of the product, while maintaining its effectiveness.

The model will be based upon the features of the materials and dimensions, created using and testing the various existing models outlined in the literature review, and will be tested and altered based on other studies into homogenous materials and sandwich panel studies. The model will be validated using the various paper found within the literature which performed practical three-point bending experimentation on sandwich panels, comparing the ultimate failure loads from the studies to the predicted results from the model using the material data given within each paper, outlined within this chapter.

CHAPTER 3 – MATERIALS AND METHODOLOGY

3.1 INTRODUCTION

Before the sandwich panels can be tested, the wood composite was measured and weighed to get the dimensions and densities of each specimen, and then a tested to be able to obtain the required input parameters for the model, notably, the elastic modulus, shear modulus, peak stress, and subsequent. To do this a 3-point bending test will be conducted.

3.2 WOOD COMPOSITE

3.2.1 – Preparation of Wood Composite

The wood composite was sourced directly from the supplier COEN, being their 'Solid Composite Timber Screening', of dimensions 75 x 25 x 900mm. These panels were sawn down to be 350mm in length, to be of appropriate size for testing in the universal testing machine (UTM). Three samples of both the wood composite product (WC1-3) and polystyrene (SF1-3) were made and numbered on both ends for the preliminary testing at this 350mm length. The samples were measured using callipers at 5 differing points along the length, width and depth of each sample and the averages of each measurement were taken, and the volumes were calculated. The samples were then weighed, so that the densities could be calculated by dividing the weight of each sample by its volume. The results of which can be seen in Table 5 below.

Table 5: Testing material sample quantities.

Sample	Volume (mm^3)	Mass (g)	Density (kg/m^3)
WC1	6.6104×10^5	875.4	1324.3
WC2	6.7191×10^5	879.3	1308.7
WC3	6.7127×10^5	872.0	1299.0
Average			1310.7
SF1	4.3774×10^5	6.7	15.306
SF2	4.3617×10^5	6.5	14.902
SF3	4.4433×10^5	6.9	15.530

3.2.2 - Test Set-up

Due to the differing thicknesses of the material, both were to be tested at the same a/D ratio of 6. This made the length between supports of the 3-point bending test (L), equal to 300mm for the wood composite and 200mm for the Styrofoam. Due to the greater length required for the wood composite tests, a different clamp was required to properly secure the material in place.

3.2.3 - Test Procedure

The tests were carried out in the UTM, with the specimen being placed in the centre of the machine and clamped at the supports, ensuring the centre of each support was at 150 mm from the load application point. Once in place, the load is then applied to the material at the midspan and slowly increased in magnitude. The extensometer on the UTM measures the displacement of the midpoint, continuously recording the position as the load is increased. The load is continually applied and increased until failure of the specimen. The failure load is noted, and the test is repeated for the other two specimens, so that an average can be obtained. This testing was also repeated for the Styrofoam samples (ensuring the same a/D ratio to the wood composite), but this data is not being analysed in this paper, however the data of the Modulus of Elasticity will be used in the final model for the material option of a foam core.

The test setup can be seen in Figure 15. The notations of each dimension in this figure will be used in the equations in Section 5 of this paper.

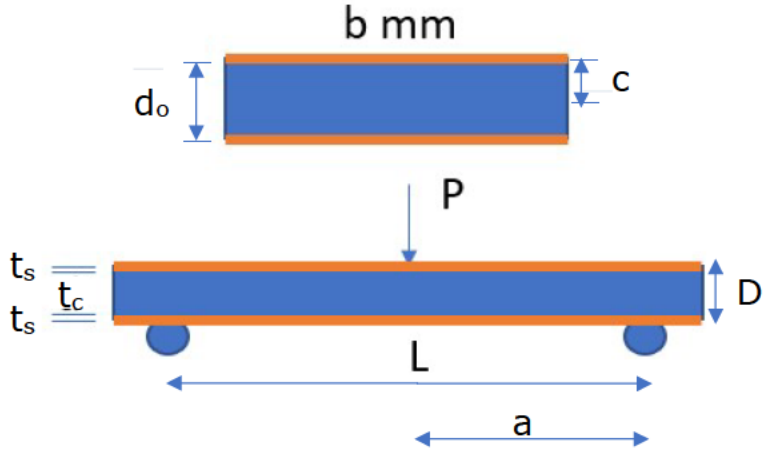

Figure 15: Diagram of material in three-point bending test set-up.

3.3 - RISK MANAGEMENT

For the preliminary experimentation, a risk management plan was completed by Ashiqul Islam for this testing and was approved by the University of Southern Queensland before commencement. This plan can be found in Appendix A.

3.4 – CREATION OF ANALYTICAL MODEL EQUATIONS

The analytical model equations will then be created for a wood composite sandwich panel using the experimental data obtained from the three-point bending test on the homogenous material. These equations will mathematically predict the allowable load the panel can withstand, by calculating the allowable stress of the combined materials of the panel, and their composition and will compare against the maximum stress induced to determine if the panel will fail in a design scenario. The model equation will be based on material parameters; created, tested, and refined from various beam theories, material behaviours and limits, and the predicted effects of combining differing materials together to act as a composite sandwich panel.

CHAPTER 4 – THEORETICAL ANALYSIS

4.1 – METHODS OF RESULTS ANALYSIS

From the obtained data of the three-point bending tests on the wood composite specimens, the experimental stress, strain, and flexural modulus will be calculated. This is done as to compare against the model equations and the prediction of stress within the sandwich panels with 0 mm of skin to verify that the model is appropriate for homogenous panels.

Equation for stress:

$$\sigma = \frac{3FL}{2bd^2} \tag{11}$$

Equation for strain:

$$\epsilon_f = \frac{6Dd}{L^2} \tag{12}$$

Equation for flexural modulus:

$$E_f = \frac{L^3 m}{4bd^3} \tag{13}$$

The mean of the three specimens for Equations 11, 12, & 13 will be derived, and standard deviation of the datasets will be calculated using Equation 14.

$$\sigma \equiv \sqrt{E[(X-\mu)^2)]} \tag{14}$$

Where, E represents summation, μ = the average of the dataset, and X represents each variable.

The average load at fracture point of three panels will also be used to verify the predicted failure load within the model for a homogenous wood composite panel.

The shear stress of the wood-composite is also needed for the model for determining the allowable shear stress of the core. To obtain this, the shear stress at the fracture point is obtained, also known as the shear strength. The shear stress of a sandwich panel is calculated using Equation 15.

$$\tau_c = \frac{\frac{P}{2}}{\left[t_c + 2t_s\left(\frac{G_s}{G_c}\right)\right] b} \quad (15)$$

Where G_s and G_c are the Modulus of Rigidity of the skin and core respectively. When obtaining the shear stress of the core material, t_s will be inputted as 0, not requiring the rigid modulus of the shear or core materials, but these will be useful parameters for the model equation for shear failure. To obtain the Modulus of Rigidity for the material, Equation 16 will be used.

$$G \overset{\text{def}}{=} \frac{F/A}{\Delta y/d} \quad (16)$$

Where, Δy is the change in length in the y axis.

Verification of the analytical model for the combined sandwich panel will be obtained from a similar three-point flexural test, in the same setup as the homogenous wood composite product, with the addition of the skin material, being a hemp fibre skin. These created panels average load at fracture point will be compared against the output from the model for the same composition, materials, and skin thickness. The margin of error for the prediction equation will be determined from the variation of failure load of the three wood-composite specimens. If the experimental result falls within this range it will be verified that the model can be used to predict the allowable load of a sandwich panel, provided a reasonable factor of safety is used.

4.2 – FAILURE MODES

The main failure methods that are expected to be exhibited by the product under three-point testing will be shear failure, bending failure, and a combined shear and bending failure. Other modes which may be seen include indentation failure and compression face wrinkling, which will be noted if observed, but will not be analysed in this study.

Shear failure is expected to occur when the panel has a lower shear resistance than the shear force being applied. The same applies to the bending failure, for if the bending moment inflicted by the central load exceeds the capacity of the beam, it will fail in bending. If both the shear force and bending moment applied to the beam are both significant, and close to reaching capacity, a combined shear-bending failure will occur.

Shear failure of the material will show through long diagonal cracks forming through either the skin material or the composite-wood core, at a point between the loading point and one or both supports. This failure is expected to occur in the wood composite core material, due to the

horizontal orientation of the beam, therefore the bending strength of the core will be modelled against the applied bending stresses from three-point testing.

Bending failure will be seen through a compressive failure of the top skin, with the skin and core debonding after. Another bending failure type may be observed from the core cracking from the bottom in the vertical direction, beneath the loading point in the centre of the material. This bending failure will most likely be from a comptonization of the skin, meaning the applied shear stress versus the allowable skin stress will be modelled.

Combined failure can be spotted by beginning with core shear failure before the cracks are propagated to the edge of the material and debonding occurs between the skin and the core.

4.3 – ANALYTICAL MODEL EQUATIONS

Bending Failure

These equations, as stated previously, will be initially based off the equations created by Ferdous et al. (2017). The equation for estimation of bending failure loads is based on the panel failing when the bending stress of the skin exceeds the allowable bending stress of the skin, being:

$$P_b = \frac{4(EI)\sigma_{s(all)}}{aDE_s} \tag{16}$$

Where, P_b is the ultimate failure load of the sandwich beam in bending, $\sigma_{s(all)}$ is the allowable bending stress of the skin, and EI can be calculated as in skin thickness influence calculations.

Shear Failure

The equation for shear failure is based on the similar principle, expecting that the beam will fail when the shear stress of the core exceeds the allowable. The shear failure of the skin is not expected, but this will be checked by analysing the failure method post testing of the specimens which failed in shear, and a different model for failure of the skin in shear will be made.

$$P_s = \frac{16(EI)\tau_{s(all)}}{4E_s t d_0 + E_c d^2} \tag{17}$$

Where, P_s is the ultimate failure load of the sandwich beam in shear, $\tau_{s(all)}$ is the allowable shear stress of the skin, and d_0 is the distance form centre to centre of the top and bottom skin.

Combined Failure

Failure under combined action of both shear and bending stresses is expected when the sum of the ratios of actual stresses to allowable stresses of both bending and shear equal to 1 or above, as shown in equation (3) below.

$$\frac{\tau_{act}}{\tau_{all}} + \frac{\sigma_{act}}{\sigma_{all}} = 1 \tag{18}$$

So, by substituting in equations (1) and (2) into (3) gives equation (4):

$$P_{s\text{-}b} = \frac{1}{\frac{4E_S t d_0 + E_C d^2}{16(EI)\tau_{s(all)}} + \frac{aD_s}{4(EI)\sigma_{s(all)}}} \tag{19}$$

4.4 – GENERAL SOLUTION

These three equations are useful in determining in which method a sandwich panel will fail, and what the failure limit should be based on the properties of the panel and its materials, however, a general equation can be useful to give a rough estimation under any of the three failure methods for the ultimate stress of the product. This will be useful in generating faster results as the product will not have to be tested separately in three models and compared. This will allow for more differing analyses of products to be done over the same span of time to quickly determine if a product will work under a certain application, and if not, what product or change to the existing product will. Once the product required has been established, then the more in-depth modelling under each of the failure modes can commence to check the failure stress of the product more thoroughly.

4.5 – ALTERNATE ANALYTICAL EQUATIONS

The analytical model equation for shear from Ferdous (17) will be compared against the two other model equations outlined in Section 2.3.2.1 of the paper, being based on the Timoshenko non-linear elastic beam theory (6)(7) and the modified Gibson's model (8).

Each of the three models will be compared against their effects from altering the skin thickness of the panels on the returned shear failure load to be compared against the theory from the literature and the stress and stiffness analysis. The three models will also be compared for the effects from altering the length between supports of the panels, changing the shear-span-to-

depth ratio (a/D) to be compared against the bending failure load. From this, the most suitable panel will be selected for use in the final model for all other panel configurations.

The alternate analytical equation for bending failure load prediction based upon the modified Gibson's model as seen in (9) will be compared against the equation form Ferdous (16), to determine the similarities and advantages of each when altering the skin thickness.

After comparing both equations, the bending moment equations will be decided upon for use in the final model.

4.6 – MODEL VALIDATION

Differing papers were chosen for analysis, as detailed out previously in Section 2, each being chosen for a specific reason, as to allow for a wide sample variety of sandwich panel products analysed to fully understand the scope of the analytical model equations. For comparison, the linear section of load vs displacement graph (elastic deformation) will be relevant, as the models only predict to the point before the yield stress is reached.

All selected papers are relevant, being three-point bending tests on sandwich panels, which include the parameters of the materials being used to be directly inputted within the created final model of this paper. The predicted failure load and failure mode outputted from the model will be compared against the experimental results from within the source papers. If the results are seen to be similar, the model will be taken as validated to a degree, and if the results do not align, the reason for the differentiation will be investigated.

4.7 – CHAPTER SUMMARY

This section of the paper outlines the equations used to get the parameters required from the experimental data of the wood composite material in three-point bending to use within the model equations. It then explores the three failure modes being analysed, of bending, shear, and combined failure, detailing the failure criteria of each, how each failure mode will be expected to occur, and the failure plane that will be seen from each failure mode. The analytical equations are then listed and discussed for each of the failure modes which will be originally testes, as well as some alternate analytical equations from other papers that will be explored within Section 5 of the paper. Then it details how each of these equations will be analysed and compared to be decided upon and verified for use in the final model.

CHAPTER 5 – RESULTS AND DISCUSSION

5.1 – EXPERIMENTAL RESULTS OF WOOD COMPOSITES

All specimens of wood composite material were tested in the UTM, and the recorded data was used for analysis. Photos of the setup for experimentation (Figure 16) and photos of each specimen post-failure (Figures 17 - 20) can be seen below. Failure occurred suddenly, with no splintering and little elastic failure observed from the high density, with the created tightly packed lattice and low modulus, making the material brittle in nature. The photos reveal similar failure modes for all three specimens to be similar, with the specimens having experienced bending failure, with the cracks resulting from the underneath of the specimen (tension face) and propagating upwards to the compressive face or the cracks starting to form from the compressive face. These flexural cracks take the path of least resistance, being a similar pattern in specimens 1 and 2, being a notched failure, which indicates cacks from the top and bottom propagating towards each other. Specimen 3 has a straight into diagonal failure plane, which indicates the major cracking from the underside was the sole perpetrator for the failure of the material. No shear cracking is seen in the materials, and there were no signs of indentation failure.

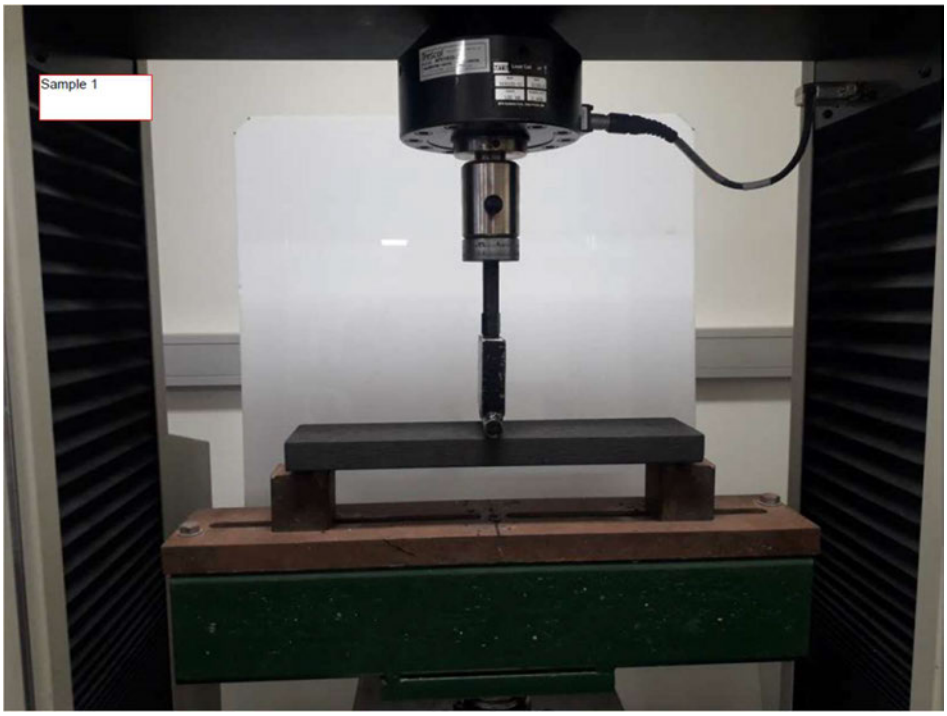

Figure 16: Three-point bending test setup.

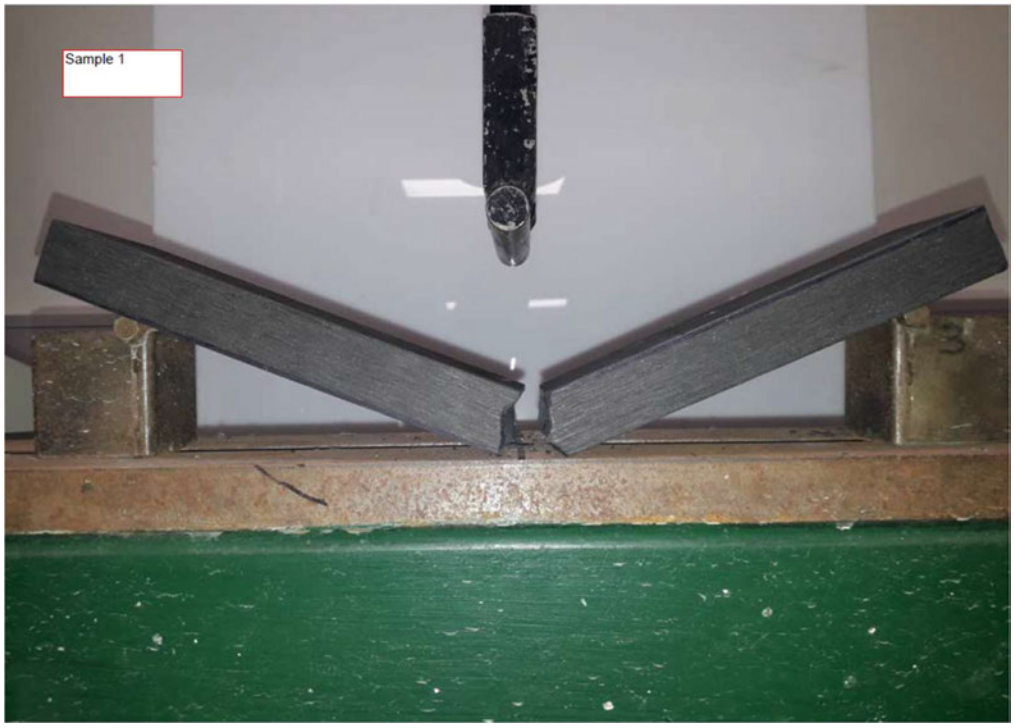

Figure 17: Failure plane of Sample 1.

Figure 18: Failure plane of Sample 2.

Figure 19: Failure plane of Sample 3.

Figure 20: Failure of all three wood composite specimens (top-down view)

Figure 21: Failure of all three wood composite specimens.

The data from the Universal Testing Machine recorded the load vs displacement data which can be seen in Figure 22. Each specimen can be seen to have a similar relationship curve between load and displacement, with that of Specimens 1 & 3, having a near identical curve, but failing at differing loads (Figure 22). The applied load at the midspan has a lesser influence on the displacement to begin at loads less than 200N, and then the wood composite begins to displace at a higher rate as higher loading is applied. The displacement to load relationship then begins to decrease before failure occurs (seen in Figure 22 when displacement drops back to 0).

The average load at failure was found to be 2978.8kN, being rounded to the integer of 5 below, at 2975kN for use in the model. This value is what will be used for the base value for the applied load in the stress and strain theoretical analysis of the composite sandwich panels.

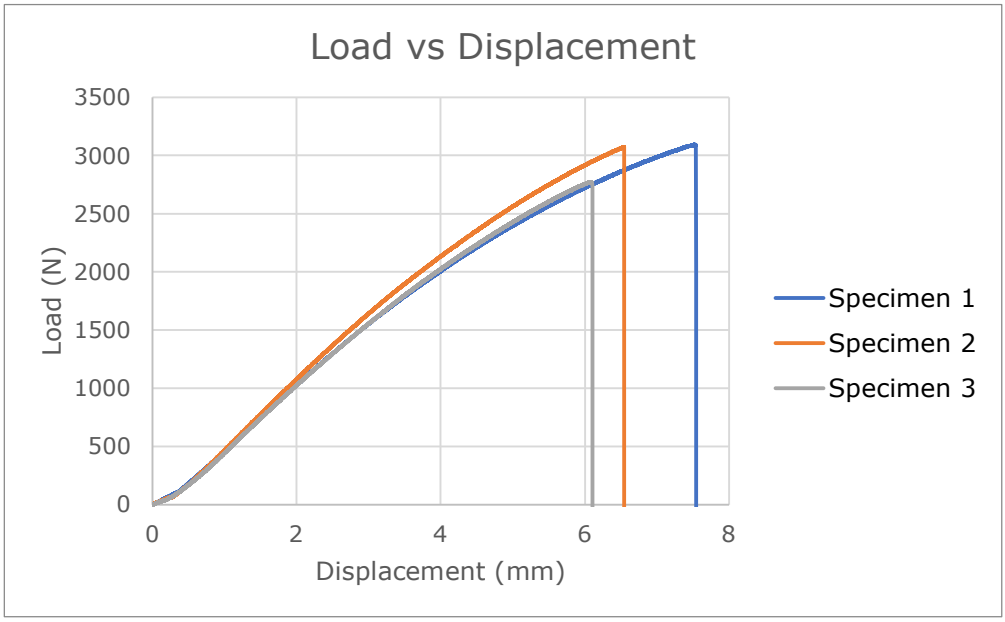

Figure 22: Load vs displacement data from three-point bending experimentation on wood composite material.

From using the equations in Section 4.1, the mean and standard deviation of the load at fracture point, stress, strain, and elastic modulus of the three wood-composite specimens tested will be represented in Table 6.

Table 6: Calculated parameters of wood composite specimens based on experimental data.

Specimen	Load at Fracture Point, F (N)	Stress, σf (MPa)	Strain, ϵf	Elastic Modulus, Ef (Mpa)
1	3093.9	29.347	0.0126	2978.5
2	3071.8	28.553	0.0111	3109.0
3	2770.9	25.656	0.0103	2898.7
Mean	2978.9	27.852	0.0113	2995.4
Std. deviation	180.5	1.943	0.0012	106.2
% deviation	6.06	6.98	10.29	3.54

The values recorded from the three specimens are similar to each other, with the standard deviation of strain being the greatest, being most likely from the measuring method, requiring recordings of very small changes, making the accuracy worse from slight variation. Each sample is also not of precisely identical measurements as seen in Section 3.2.2, with slightly altering dimensions and densities of each specimen recorded, leading to differences in the failure load for each and the resultant ultimate stress and strain. The maximum stress and strain

were used to determine the elastic modulus of each specimen, and the average of the three will be used in the model. The variation of this elastic modulus can be seen to be very similar at a 3% difference from the mean. This is due as when a panel endures less stress before failure it is also seen to endure less strain. This relationship can be seen in Figure 23, where all samples follow a similar curve.

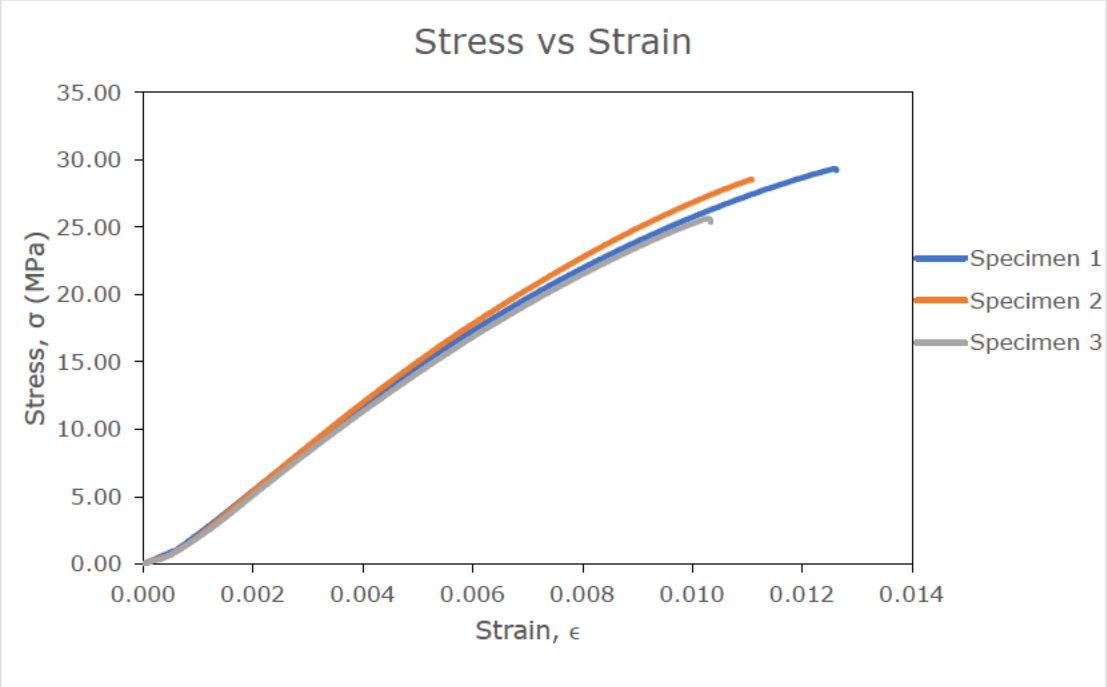

Figure 23: Stress vs strain of wood composite materials until fracture point.

The shear stress of the panel and modulus of rigidity were calculated from the average failure load, strain, and material dimensions. When calculated the results obtained are as follows:

Modulus of Rigidity, $G_{(wc)} = 3490$ MPa

Shear Strength, $\tau_{(wc)} = 0.778$ MPa

These quantities are for use in the model equation for shear failure.

From comparison with other sandwich panel materials identified and discussed in Section 2.3.4, the wood composite material has a higher Modulus of Elasticity compared to other standard core material. Both foam and the phenolic core materials have an elastic modulus less than half of that for the wood-composite, with lower yield strength, but higher shear strengths. The other recycled material that is being included in the model of recycled plastic lumber has a greatly lower modulus of elasticity than all other products, also having a high yield and shear strength.

Table 7: Material properties of core materials for final model.

Material	Wood Composite	Foam	Recycled Plastic	Phenolic core	Custom
Young's Modulus (MPa)	2995	1100	619	1330	0
Yield Strength (MPa)	27.852	2.8	24	14.32	0
Shear Strength (MPa)	0.778	1.7	6.89	4.25	0

The effects of these differences will be investigated further in the model.

5.2 – EFFECTS OF VARIABLES TO MATERIAL STRESS AND STIFFNESS

The effects of differing variables within the model equations can be analysed by theoretically predicting the benefits to both strength and stiffness of the sandwich panel, in relation to a changing each parameter. Each parameter being investigated will be the variables of the sandwich panel that are included in the final model equations that affect the strength and stiffness, being:

- Skin thickness, t
- Length of panel, L
- Width of panel, b
- Core thickness, d
- Core Modulus of Elasticity, E_c
- Skin Modulus of Elasticity, E_s

The strength will be tested by calculating the amount of stress acting on the material, using the equation:

$$\sigma = Mc/I \tag{20}$$

where σ = total stress, M = maximum moment acting on material (PL/4), c = distance from neutral axis to face of skin material (d/2+t), and I = second moment of inertia. Refer to Figure 15 for dimensional references in the test set-up.

The stiffness of the material will be calculated by the formula:

$$\Sigma = EI \tag{21}$$

where Σ = stiffness and E = Modulus of Elasticity.

The second moment of inertia I, will be calculated for both materials, core (I_c) and skin (I_s), separately:

(22)

$$I = I_C + I_S$$

Due to the sandwich panel consisting of the two differing materials, the modulus of elasticity of the product will not be constant. The second moment of inertia for the skin is assumed to have a greater modulus of elasticity to that of the core as to create an efficient sandwich panel. Due to this, the width of the skin will be multiplied by a the modular ratio skin and core (E_s/E_c) to create an effective width of the skin material, to allow second moment of inertia be equal to the amount of area that would be required to get the same I value if the skin had the same modulus as the core, without effecting the distance from the x-axis (origin at mid-point of panel). The properties of each component of the cross-section need to be scaled by the modular ratio of the corresponding material to determine the total cross-section stiffness. (Anwar & Najam 2017) This gives equations 23 & 24.

$$I_c = \frac{bd^3}{12} \tag{23}$$

$$I_s = 2 * \left[\frac{b\left(\frac{E_s}{E_c}\right)t^3}{12} + \left(b\left(\frac{E_s}{E_c}\right)t\right) * \left(\frac{d}{2} + \frac{t}{2}\right)^2 \right] \tag{24}$$

To get the stiffness of each panel the modulus of the core (E_c) and skin (E_s) materials shall be multiplied by the respective second moment of inertia, making the equation for stiffness:

$$EI = E_c I_c + E_s I_s \tag{25}$$

For the purposes of each analysis, a standard value was used for each parameter in the equations, other than the parameter being investigated. The standard values used will be those of the experimental test on the wood-composite material, the researched E value of hemp fibre for the Modulus of Elasticity of the skin, and an assumed skin thickness based on the skin thickness analysis which will be performed first.

These base standard values are as follows:

Table 8: Base values of parameters used in model equations.

Variable	Base Value
Length, L	300 mm
Width, b	75 mm
Core height, d	25mm
Skin thickness, t	1 mm
Skin Modulus, E_s	75000 MPa
Core Modulus, E_c	2995 MPa

The load is a dependent variable in the final model equations and is not a variable of the sandwich panel itself and therefore will not be analysed in this section. The standard value for load for the strength and stiffness equations has been taken as the average of the failure load of the wood-composite specimens from the experimental analysis, making; Load, P = 2974 N for all stress equations.

5.2.1 – Effects of Skin Thickness on Stress and Stiffness

For the purposes of this analysis, the skin thickness was analysed at every 1mm of thickness between 0 and 10 mm, and the effects on the strength and stiffness were analysed. From this it was seen that adding additional millimetres of skin was seen to be decreasing the stress on the panel an insignificant amount after 5 mm of skin. It was also seen that the greatest decrease in stress was between 0 and 1 mm being over an 85% reduction, so the skin thickness in this zone was then analysed in smaller increments at every 0.1 mm of additional skin thickness on both sides between 0 and 1 mm to see the effects. From performing this analysis in excel, the final graph can be seen in Figure 24.

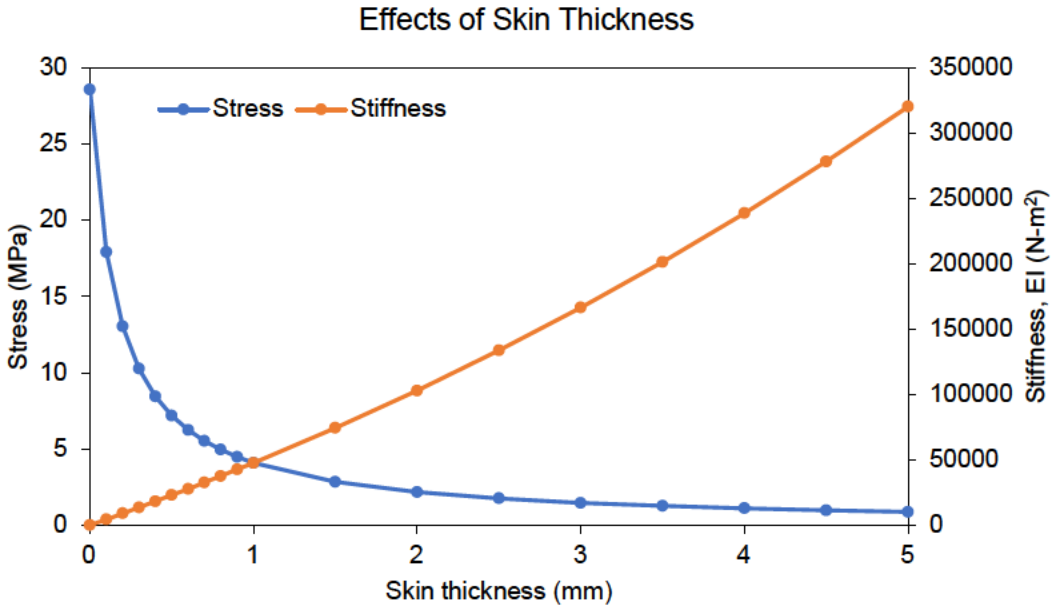

Figure 24: Graph of skin thickness theoretical influence on stress and stiffness.

As seen from Figure 24, the stress experienced by the panel decreases and the stiffness decreases when the skin thickness increases, both being positive for the sandwich panel. The stiffness of the panel increases almost linearly, with a similar amount of increase experienced

from each subsequent increase of skin thickness. The decrease in the amount of stress experienced by the sandwich panel for each subsequent increase in skin thickness is seen to lessen the higher the thickness of skin becomes. This makes the amount of benefit per millimetre of skin become lesser as it increases, making the range of skin thickness which seems to be optimal is between 0.3 and 1.5 mm for each skin. This range allows values give a balanced amount of stress experienced and stiffness of the material, before the decreases in stress for the panel is not worth the extra thickness.

This graph also shows that increasing the skin thickness (t) will continuously benefit the sandwich panel, increasing the stiffness and reducing the stress experienced. The amount of benefit to stiffness in the wood composite with no skin is very low in comparison to the amount with any skin added, showing the benefit gained from the addition of skin layers to the wood composite.

However, the stress is the key component in the sandwich panel, and the decrease experienced from increasing the skin thickness gradually lessens. This relationship can be seen in Table 9.

Table 9: Percentage of stress decrease from additional skin thickness.

Skin thickness (mm)	Stress (MPa)	% decrease from initial stress
0	28.56	-
0.1	17.93	37.2
0.2	13.06	54.3
0.3	10.27	64.0
0.4	8.47	70.4
0.5	7.20	74.8
0.6	6.26	78.1
0.7	5.54	80.6
0.8	4.96	82.6
0.9	4.50	84.3
1	4.11	85.6
1.5	2.87	89.9
2	2.20	92.3
2.5	1.78	93.8
3	1.49	94.8
3.5	1.28	95.5
4	1.12	96.1
4.5	1.00	96.5
5	0.90	96.9

The efficiency of using the wood composite as a sandwich panel can be seen in Figure 24 and Table 9, with only 0.1mm of skin added to each side reduces the stress experienced from the ultimate load on the wood composite panel by 37% and 0.2mm reduces it by over half. The

benefits of combining the wood composite material with a skin layer with increased stiffness are evident, offsetting the shortcomings of the material alone.

As seen in Table 9, the greatest decrease in stress is seen when just 0.1mm of skin material is added, turning the product from a homogenous material to a sandwich panel. After the first millimetre of skin, there is an 85.6% decrease in stress experienced by the material. This decrease greatly lessens for the next additional millimetre of skin, as at 2mm an additional reduction of 6.7% is seen, and the amount of stress reduction continually decreases for each additional millimetre of skin material added to either side of the sandwich panel. After 3.5 mm of hemp fibre skin on each face, the reduction becomes less than 0.5% for each subsequent millimetre added compared to the original stress experienced, and the benefits become negligible.

The decided optimal skin thickness reduces the total stress experienced from between 64.0 to 89.9%. This is an extreme benefit for the little total addition in thickness. The amount of hemp fibre skin added is not recommended to go above the 1.5 mm on either side, but if a slightly higher capacity is required then it can still be a possibility. A thickness greater than 2mm would be seen as becoming unreasonable for this sandwich panel, and that any further increase would not be valuable enough in stress decrease to justify the extra material, and to still provide decent stiffness to the composite panel.

From these findings, our model will consider 0.1 to 2.0 mm of skin thickness of hemp fibre skin on each face of the sandwich panel. For the purposes of all future evaluations of model parameter effects on panel strength and stiffness, the standard dimension for skin thickness has been chosen at 1mm. This value gives great benefit to the wood composites strength and stiffness, being between the recommended range of 0.3-1.5 mm. With this decent skin thickness chosen, each parameter can be analysed for the effects on strength and stiffness on both the core and skin materials.

5.2.2 – Effects of Panel Length on Stress and Stiffness

From altering the length of the panel, the modulus and cross section of the panel will remain constant, making the stiffness of the panel unaltered. The stress in the panel will be increased as the length between supports increases, as the moment will increase from the increased lever arm distance (equal to a).

The increase in stress is seen to have a linear relationship (Figure 25) from the increase in moment, as expected from a point load. If the load was distributed, it would be expected to increase in exponentially.

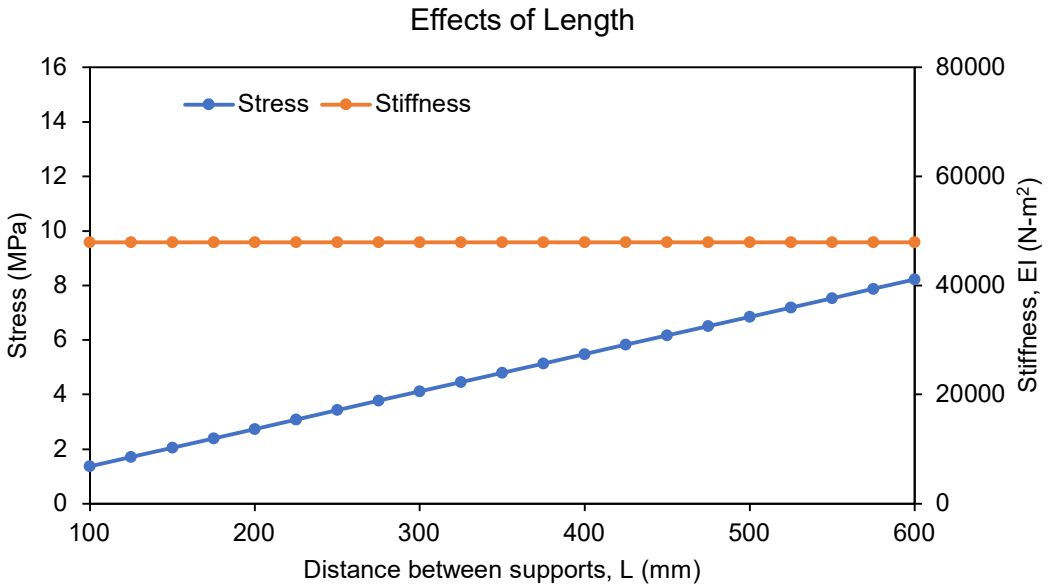

Figure 25: Theoretical influence of length on stress and stiffness of panel.

5.2.3 – Effects of Panel Width on Stress and Stiffness

From increasing the width of the panels, the second moment of inertia will increase linearly, due to the increasing of the cross section, in turn increasing the stiffness. This increase is quite small in comparison to the amount of stiffness gained from increasing the skin thickness due to the high modulus value of the skin in comparison to the core, greatly increasing the second moment of inertia (I) value.

The stress in the panels also decreases with additional width, with the reduction seen to be exponential, with a greater decrease at the start. The benefit gained from additional increases to panel width after a certain point would become negligible, not having a noticeable effect. This effect can begin to be seen after 100 mm of width, making the decreases in stress small. This aligns with the theory in practice, as width is considered to play a negligible effect after a certain level, allowing materials to be analysed per metre width as this yields similar results. The analysis shows that the panels should not be less than 50 mm in width as this increases the stress experienced by the panels greatly compared to the presumed cost of having a wider panel.

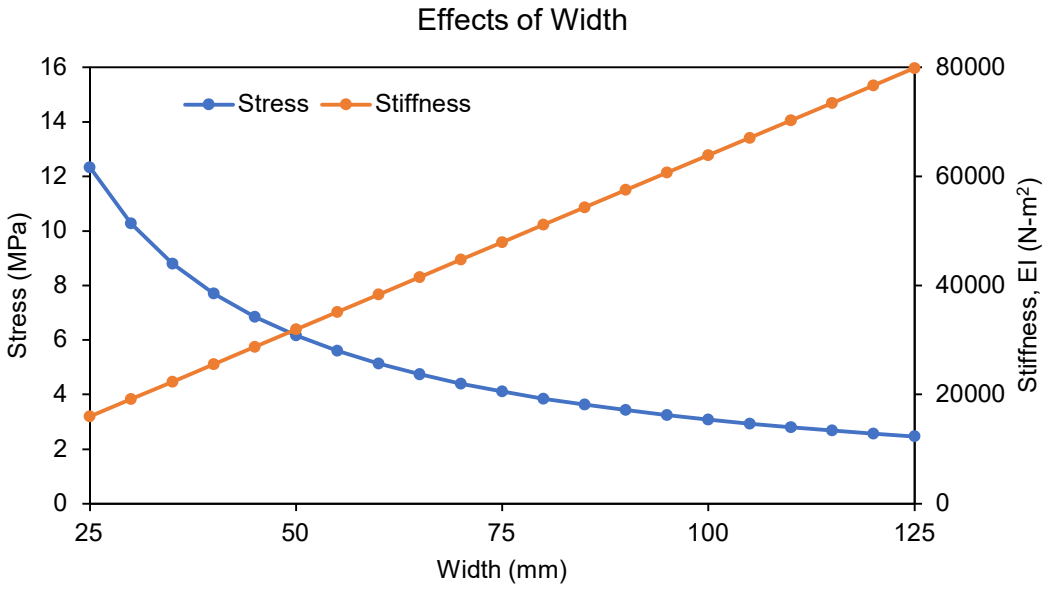

Figure 26: Theoretical influence of width on stress and stiffness of panel.

5.2.4 – Effects of Core Height on Stress and Stiffness

Increasing the core height has a positive effect on both the stress and stiffness of the composite sandwich panel. From increasing the cross section, the second moment of inertia is increased, and the stiffness will increase, and the stress will decrease, but at a lesser rate than from the skin thickness as the core height has a lower modulus, making the increase in I be less comparatively to the same thickness of skin thickness added. This shows that to increase the strength and stiffness properties of the panel, less skin would need to be added than core to have an equivalent benefit. The cost of materials may be a factor, and the greater amount of core material required for the same benefit as that of the skin could be more cost effective and be the preferred choice.

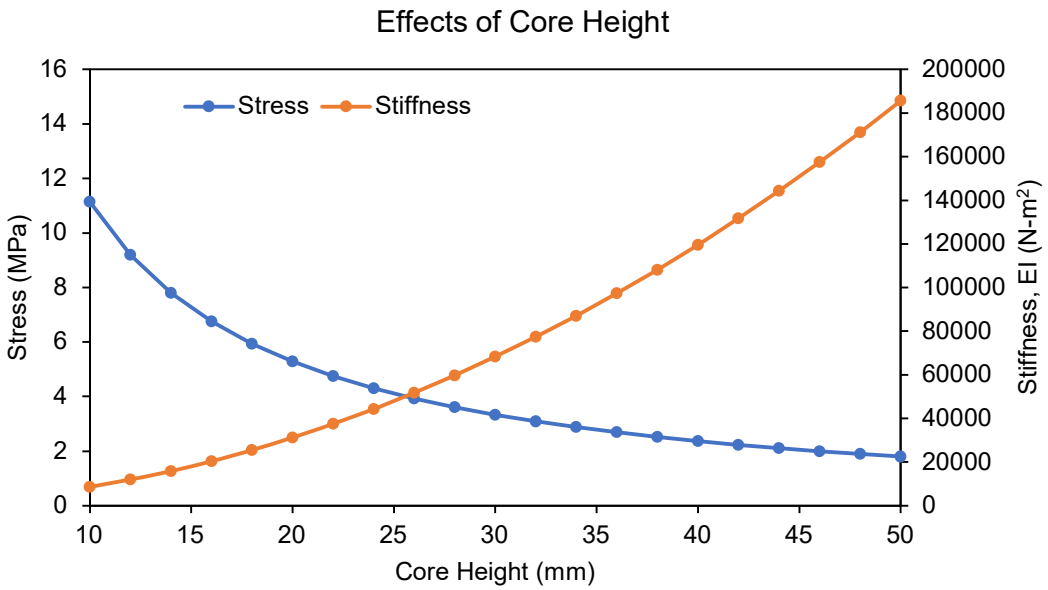

Figure 27: Theoretical influence of core height on stress and stiffness of panel.

5.2.5 – Effects of Skin Modulus on Stress and Stiffness

When the modulus of elasticity of the skin is increased the bending stress within the panel reduces and the stiffness increases, making it optimal for a higher modulus of the skin layers to obtain the most effective sandwich panel. The effects on stress are exponentially reducing as the modulus of the skin increased while the effects on stiffness are exponentially increasing. This would make the optimal range vary depending on which property is being required as more valuable. The modulus of the skin being increased above 75 000 MPa can be seen to start having diminishing returns on the reduction in stress experienced. The stiffness of the panel can be seen to roughly double from increasing the bending modulus of the material by 30 000 MPa. This amount of increase in stiffness is not likely to be necessary, making the theoretical optimum skin modulus for a wood composite core sandwich panel to be 65 000 – 85 000 MPa.

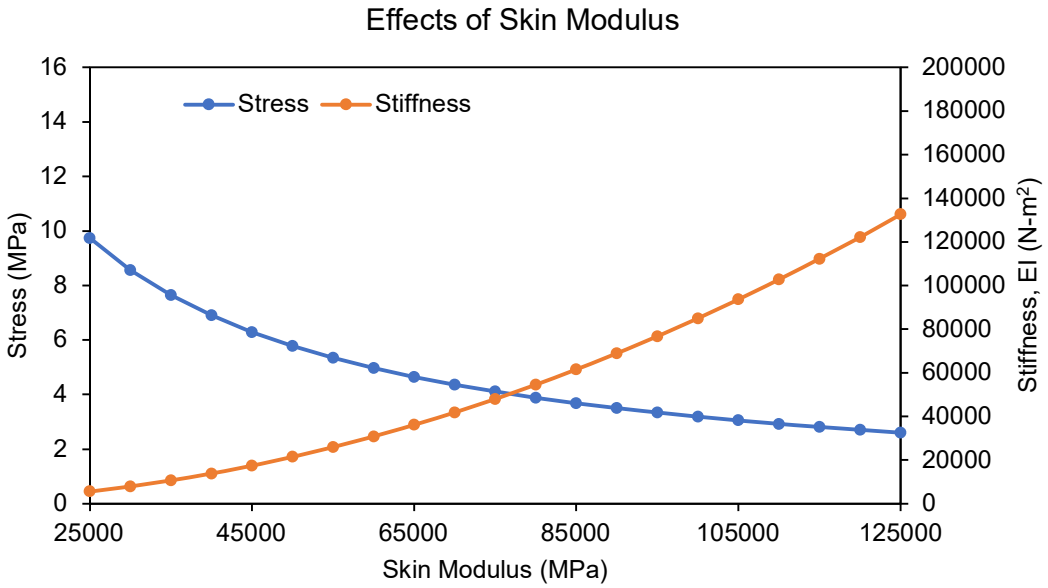

Figure 28: Theoretical influence of skin modulus on stress and stiffness of panel.

5.2.6 – Effects of Core Modulus on Stress and Stiffness

Increasing the modulus of the core can be found to have a negative effect on both the strength and the stiffness of the composite sandwich panel in bending as the stress experienced within the panel will increase and the stiffness of the composite panel will decrease. Figure 29 shows that the core stiffness decreases rapidly as the modulus of the core decreases initially before rapidly beginning to plateau after the initial increase to core modulus. Reduction of the core modulus will therefore have minimal negative effects on the panel composition for stiffness after the core material increases above 10 000 MPa. This high core modulus would be seen as unreasonable for use in a sandwich panel as the benefits of combining the material would not be reasonable for the additional cost. The core modulus value of the wood composite at roughly 3000 MPa can be seen to offer a reasonable value of stiffness at roughly 5000 Nmm^2, while the stress experienced is still low. The optimum modulus for the core for the chosen sandwich panel composition will be 1000 – 3000 MPa, with the wood composite value being on the outer limits of this optimum range from Figure 29.

The relationship between the core modulus and skin modulus is a critical factor in maximising the bending strength of the material. If the modulus of the sandwich panel core increases to a similar level of the skin, the material will begin to act more towards a homogenous state, with similar material properties of both the core and skin and will lose the benefits to bending strength and stiffness offered from being a sandwich panel composition.

Although the benefits to bending stiffness appear to continue to improve by lowering the core modulus (Figure 29), the performance in shear will worsen as core shear is a major failure mode of composite sandwich panels. To obtain an optimum design, a balance will need to be obtained between having a high enough core modulus to prevent core shear and a great enough difference between core and skin modulus for the benefits to bending strength of the panels.

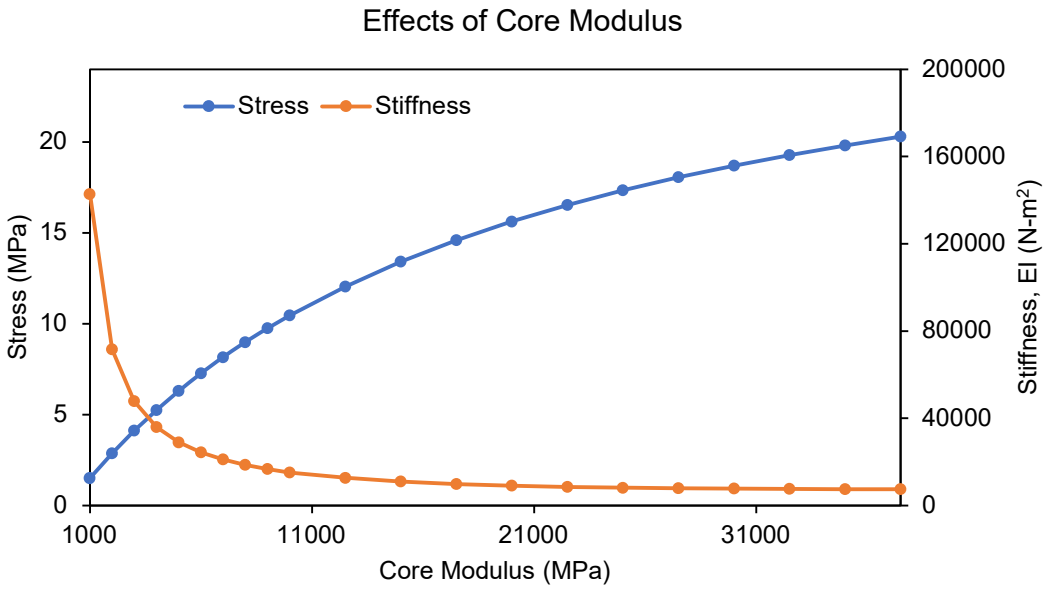

Figure 29: Theoretical influence of core modulus on stress and stiffness of panel.

5.3 – MODEL VALIDATION

5.3.1 – Validation of No Skin Layer Applied

From analysing the model outputs, it was determined that the model was accurately predicting data for the wood composite product with no skin layers applied. Through the altered equation for when no skin is applied, the predicted failure load is to be between that of combined failure 2.15 kN, (Equation 19) and bending failure 3.40kN (Equation 16). The average failure load from the experimental results was 2.95 kN, being between the predicted range for the model, verifying the model for predicting the ultimate failure load required about the midpoint (in bending, shear, and combined bending-shear) of a homogenous material.

5.3.2 – Investigation of Bending Failure Load Modelling

From investigating the two differing equations for bending failure load outlined in Section 2.3.2.1 within the model based upon to skin thickness, the results can be seen in Figure 30. Both equations can be seen to produce similar results, having a similar starting failure load and a similar linear increase based upon increasing skin thickness. The four-point bending analytical equation produces slightly higher failure loads at all skin thicknesses and has a slightly greater linear relationship between skin thickness and failure load. Due to the similarities between the results of both equations, either would be fine to use within the model, so the model equation from Ferdous will be used, as the modified Gibson model is simpler in nature, and treats the skin and core layers separately, not considering the effects of the distance from the centroid to the middle of the skin layers.

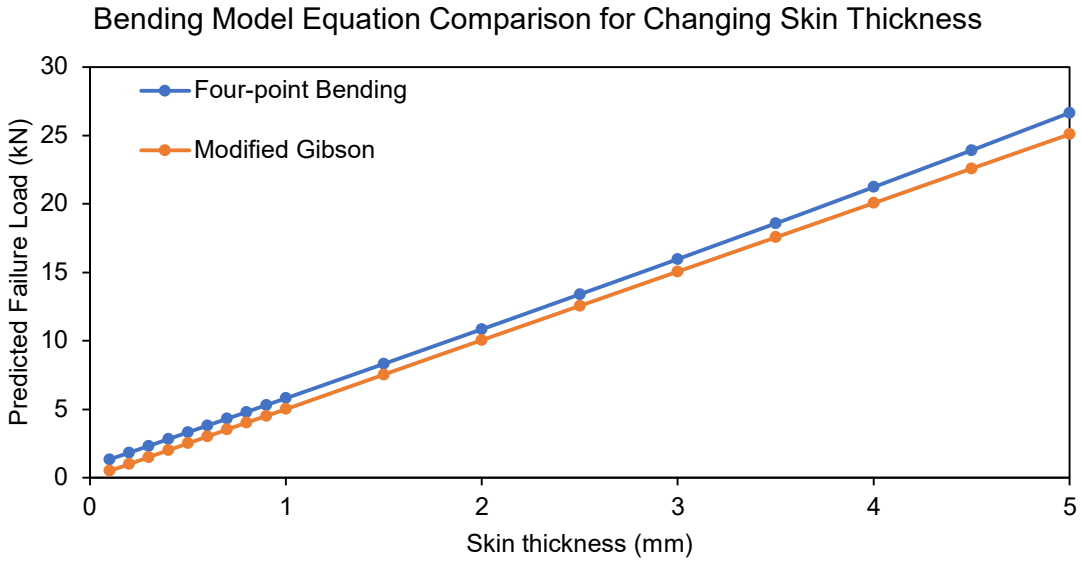

Figure 30: Comparison between bending failure mode model predictions per skin thickness.

5.3.3 – Investigation of Shear Failure Load Modelling

Due to the nature of the equations being derived from another paper by Ferdous (2017) who investigated sandwich panels failure under four-point bending, the model equations may not directly transfer across to this study with analysis of composite panels under three-point bending. The model equation for ultimate shear failure of the panels will be investigated, by comparing against results from other shear failure load prediction equations under three-point bending conditions of sandwich panels. The model by Ferdous will be compared against models based on the non-linear 'Timoshenko Beam' theory and the 'Modified Gibson Model'.

After comparison, each will be evaluated for their predictions based on changes to skin thickness and length to determine the best shear failure load prediction equation to use within the final model.

When comparing the differing models for shear for the effects of skin thickness, the differences between the models are portrayed in Figure 31. The model equation based upon four-point bending is affected the most by changing the skin thickness, having an inverse exponential to the skin thickness, becoming less of an increase as the skin is additionally increased. The modified Gibson equation has a constant predicted failure load, being unaffected by any increase to skin thickness, this is due to the failure criterion of the panel, with the panel predicted to fail solely based upon when the shear stress in the core is greater than the allowable shear stress and is therefore unaffected by the skin layers. The Timoshenko model also has a similar failure criterion, however there is a predicted minor increase to the predicted failure load, with the failure load presumed to be slightly benefitted by the addition of skin layers, reducing the amount of shear stress within the panels. As seen from Figure 31, the amount of increase is minimal in this panel scenario and could be seen as negligible. All three analytical prediction equations have a similar prediction for the shear failure load. With the modified Gibson equation predicting the lowest failure load after 0.3 mm of skin applied, and the Timoshenko model is higher, but is less than the prediction of the four-point bending model after 1.5 mm of skin. Due to the panels being predicted to fail when the shear within the panel is greater than the allowable of the core material, the failure load should not be majorly affected by the addition of skin layers.

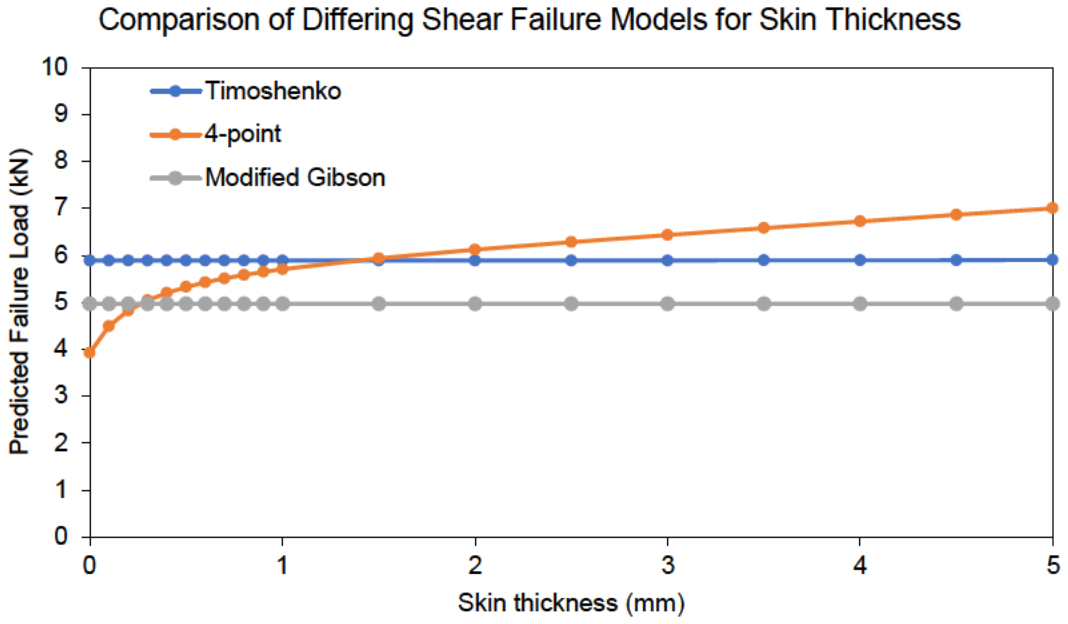

Figure 31: Comparison between shear failure mode model predictions per skin thickness.

Comparing the different shear prediction equations based on altering the length of the panels against the bending model equation (Figure 32), the different equations can be analysed based on the predicted failure mode at certain shear-span-to-depth ratios. Figure 32 shows the effects of altering the a/D ratio by altering the length and keeping a constant core height of 25mm and skin thickness of 1mm on each face.

Each shear prediction equation is not affected by the length of the panel, having a constant failure load. The Timoshenko equation has the highest prediction for this panel configuration at just over 6 kN, and the Modified Gibson has the least, at roughly 5 kN. From the literature (Section 2.3.1), the predominant failure mode of composite panels depends on the shear span to depth ratio (a/D), predicted to be bending failure at a/D > 6, shear failure in the range of a/D < 2-4, and combined failure at 6 > a/D > 2-4.

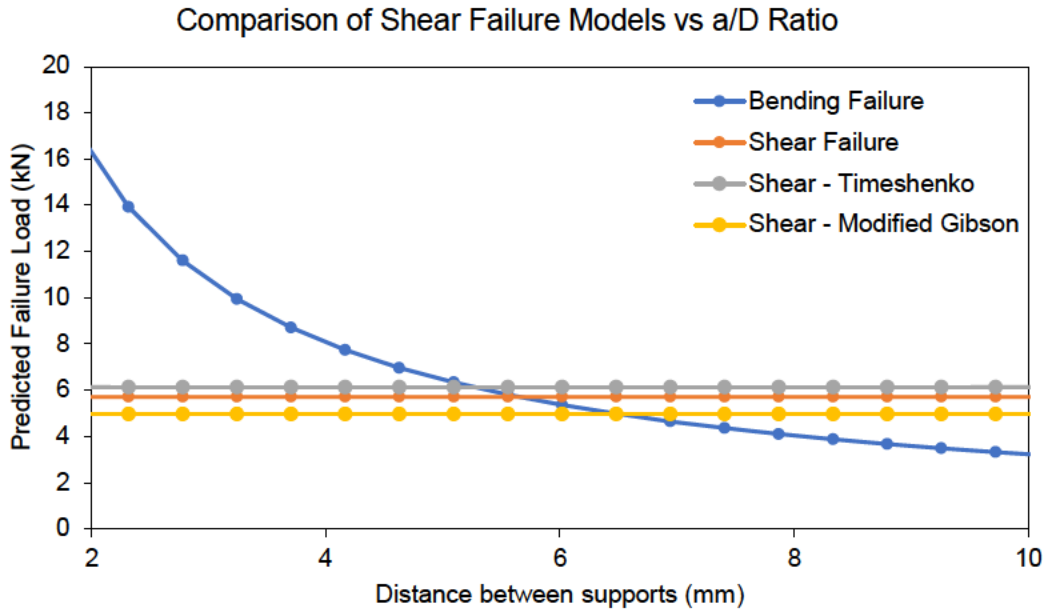

Figure 32: Comparison between shear failure mode model predictions per a/D ratio.

In the load vs shear-span-to-depth graph (Figure 32), the bending failure load is predicted to be less than the shear failure load of the at an a/D of roughly 7.0 for the Modified Gibson method, and at roughly 5.5 for the four-point bending prediction and at roughly 5.0 for the Timoshenko method. This shows that the Modified Gibsin equation is underpredicting the shear failure load, with the panel being expected to fail in shear over bending for a span to depth ratio greater than expected. Taking into account that there will be roughly a combined shear bending failure predicted at an a/D of approximately ± 1 at the curve intersection makes both the four-point and Timoshenko model equations fit within the theory. With both model equations being acceptable within the theory, the Timoshenko and four-point equations will be

more likely to return bending failure as the ultimate failure load and the modified Gibson method will be more likely to output shear failure as the ultimate failure mode.

Ultimately, the model equation for shear is decided to be based upon the modified Timoshenko method. This is due to the equation being based on the prediction of three-point bending, rather than for four-point bending testing, and produces results that align more accurately with the literature than the Modified Gibson equation. While the Timoshenko method is less conservative, the model will have an appropriate factor of safety in the calculations due to the uncertainties of the model, being of an analytical nature. The Timoshenko model aligns best within the predicted failure mode based on shear-span-to-depth ratio from Ferdous (2017), being predicted to fail via shear fail at an a/D less than 4, by combined shear and bending failure from 4 to 6 and by bending failure for any panel with an a/D greater than 6. The Timoshenko method also does not require yield strength of the core or skin, for which experimentation of each skin material will be required, lowering the ease of use for quick preliminary checking of composite panels for design applications.

Due to these reasons the analytical model prediction equation for the shear failure load of a composite panel under three-point bending will be predicted based on the Timoshenko method. Any mention of the shear model equation will be referring to the Timoshenko equation from this point forwards within the paper.

5.4 – MODEL VERIFICATION

The results from the experimental results on the homogenous wood composite material have a close resemblance to the predictions from the model. The failure mode observed from experimentation was bending failure, as was predicted in the model using the same parameters, with a skin thickness of 0 mm in the equations, and the allowable stress of the skin as that of the wood composite (as this material is taken as the skin when no other skin is applied). The model predicts the load at fracture to be 3.40 kN using the bending model equation (16), 5.89 kN in shear (17) and 2.15kN in combined failure (19). This means that the model predicts the failure load to be between 3.40 kN for when no effects of shear influence the panel, and no lower than 2.15 kN when true combined failure is in effect. The average failure load from the experimentation was roughly 3.0 kN, falling within the predicted range, predicting that the wood composite had some influence on the failure load from the presence of shear stress within the material. The model's failure load and failure mode predictions are considered verified to be accurate for the wood composite material for when no skin layers are applied.

With the model being verified for the wood composite product homogenous material, it also needs to be verified as a sandwich panel and for differing materials and compositions to know

the strengths and limitations of the model. From comparing the model with experimental results from other three-point bending tests on sandwich panels from within the literature, a variety of results can be seen, with Figures 33-38 showing the inputs and predicted failure loads of the panels from the respective literature which tested sandwich panels within a three-point bending test set-up.

The first papers being compared by Ma et al. (2020) and Giglio, Giglio & Manes (2012) both consist of honeycomb core panel types. In the testing by Ma et al., the honeycomb core had stiffening along the edges of the hexagonal lattice in a particular direction, being longitudinal or horizontal. Shear failure was observed to be the determining failure mode of the honeycomb panels for both skin thicknesses of panels (1.1 and 2.42 mm) and for both stiffened directions of core. The panels with 1.1 mm of skin thickness failed in Ma's static three-point bending tests at 9.5 kN with longitudinal stiffening and 5.5 kN with transverse stiffening and the panels with 2.42 mm of skin failed at 11 kN with longitudinal stiffening and 5.75 kN for the transverse stiffened core panels. From the model predictions in Figures 33 & 34, the predicted range for the 1.1 mm panel 4.0-5.2 kN and 6.1-9.1 kN for the 2.42 mm skin panels. The model is underpredicting the failure load of both panels, with the prediction being closer to the upper limit of the 2.42 mm skin panels, and below the lower limit for the 1.1 mm skin panel. This shows that the effects of changing the skin thickness to the model have a greater affect then what is seen in Ma's experimentation. The model also has predicted combined failure/bending failure to be the ultimate failure load of the panel, most likely from the assumption of greater core stiffness from the assumed homogeneity of the core by the model equation. The stiffening of the core within a certain direction is not applicable within the model equation, making the predictions compared to this panel less accurate.

From the experimental results of the paper from Giglio, Giglio & Manes, the average peak load was 0.455 kN, being lower than the predicted peak load from the model at 0.6 kN. This behaviour is expected from a honeycomb core being expected to have a slightly lower value than for the same panel configuration with a solid homogenous core of the same material. With similar results from this paper, with no directional stiffening of the panels, the model is seen to be accurate to a degree, of predicting the failure load of a honeycomb panel type, being a common sandwich panel core. To use honeycomb sandwich panel core types within the model, the factor of safety inputted to the model should be increased to be conservative for the unknown decrease in ultimate load by the honeycomb core composition.

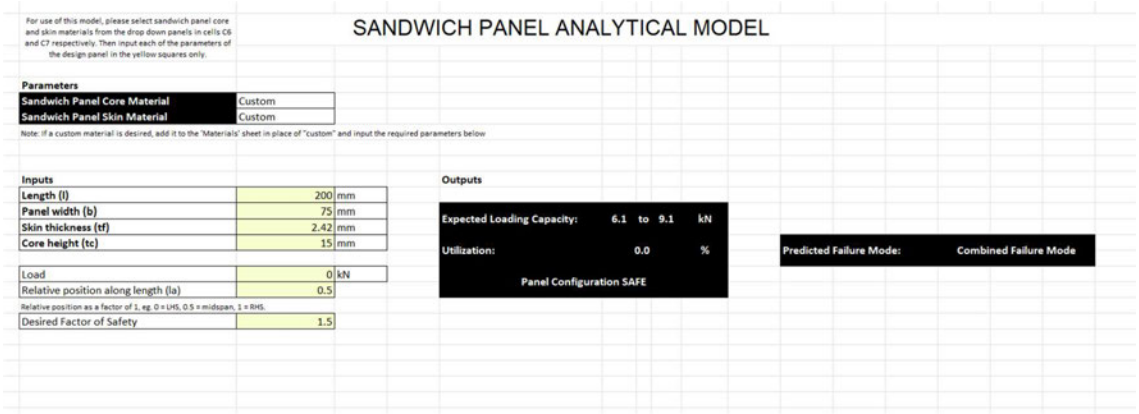

Figure 33: Model output for paper by Ma et al. (2020) for honeycomb core, 2.42mm of skin.

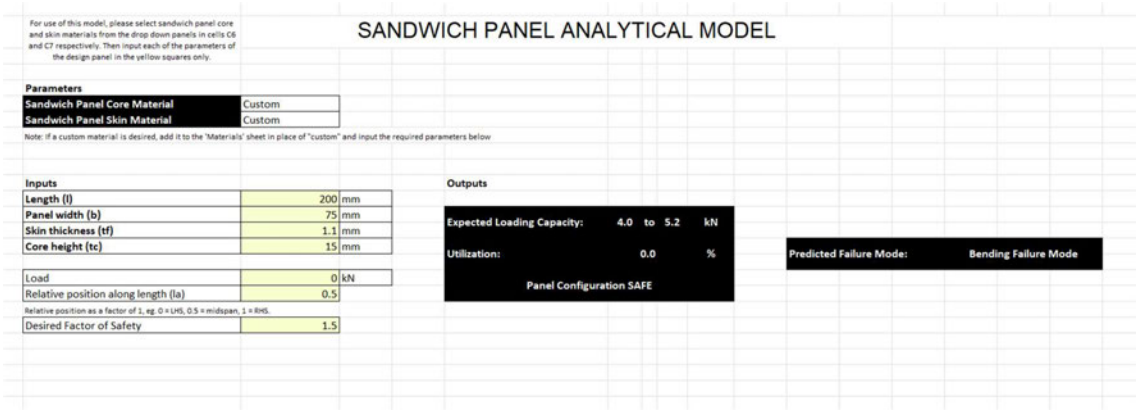

Figure 34: Model output for paper by Ma et al. (2020) for honeycomb core, 1.1 mm skin.

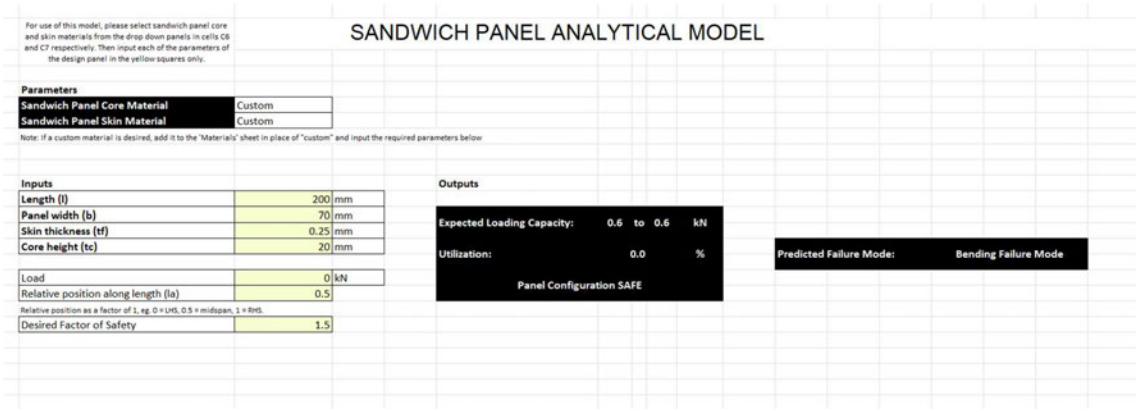

Figure 35: Model output for paper by Giglio, Giglio & Manes (2012).

The next papers to be compared against the model are those which conducted static three-point bending experimentation on foam core panel types, by Huang et al. (2022) and Crupi & Montanini (2007). In Huang's experimentation, the panels failed via indentation, at an average of 0.8 kN. This means that the load required for indentation must be lower than the required load to cause bending, shear, and combined failure of the panels. From the model, the failure load is predicted to be between 3.2-4.1 kN (Figure 36), being far greater than the minimum 0.8 kN of indentation failure. However, due to the panels failing in indentation, not much can be gained in validating the model from this study.

The paper by Crupi & Montanini sandwich panels failed via shear failure at 1.2 kN for the Alulight panels, and by bending failure at 2.2 kN for the Schunk panels, being able to be directly compared against the model's predictions. For these two differing foam cored panels, the model predicts that the Alulight panels will fail at an ultimate load of 1.1-2.0 kN by shear (Figure 37), and the Schunk panels will fail between 1.7 and 2.8 kN via combined failure (Figure 38). These predictions are accurate with the experimental values falling within the ranges predicted by the model with similar failure modes being predicted to the modes that occurred in Crupi & Monanini's experimentation.

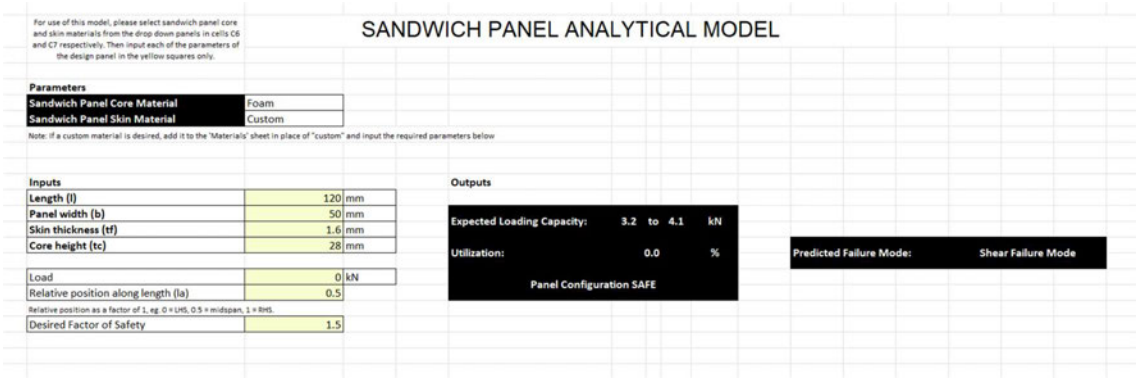

Figure 36: Model output for Huang et al. (2022).

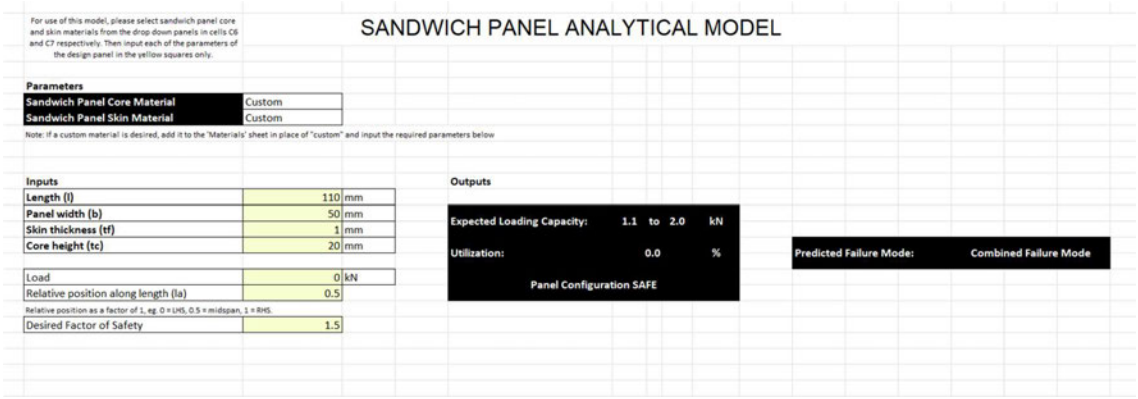

Figure 37: Model output for Crupi & Montanini (2007), Alulight panels.

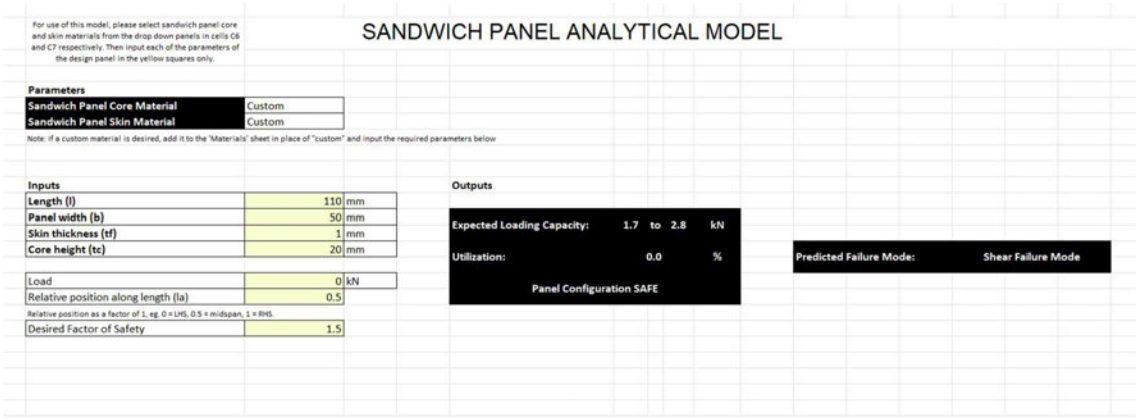

Figure 38: Model output for Crupi & Montanini (2007), Schunk panels.

From these comparisons, it shows that the analytical equations of the model are closely accurate to the experimental data, being more accurate for foam core panel types compared to honeycomb cores, with the failure mode for honeycomb cores being more likely to predict bending failure over shear than what would be observed, and at a higher ultimate load. No papers undertaking three-point bending static experimentation of solid sandwich panel types exist within the literature for direct comparison, however due to the nature of foam panels being a homogenous material, the panels are expected to perform in a similar manner, but with a higher core stiffness and resistance to shear failure. From the accurate predictions of the foam core panel types, the model equations are taken to be verified for use for the solid wood-composite core as well as other solid core and foam panel types.

5.5 – FINAL MODEL OVERVIEW

With the final model prediction equations decided and verified for homogenous core panels, the model for use was generated. This model simplified the process of the model equations into an excel spreadsheet of three sheets, being easy to understand and use. The practical use of the model, the main sheet that is needed is the “Summary” page, being sheet 1. In the “Summary” sheet, the instructions for use are in the top left explaining how to use the model (Figure 39).

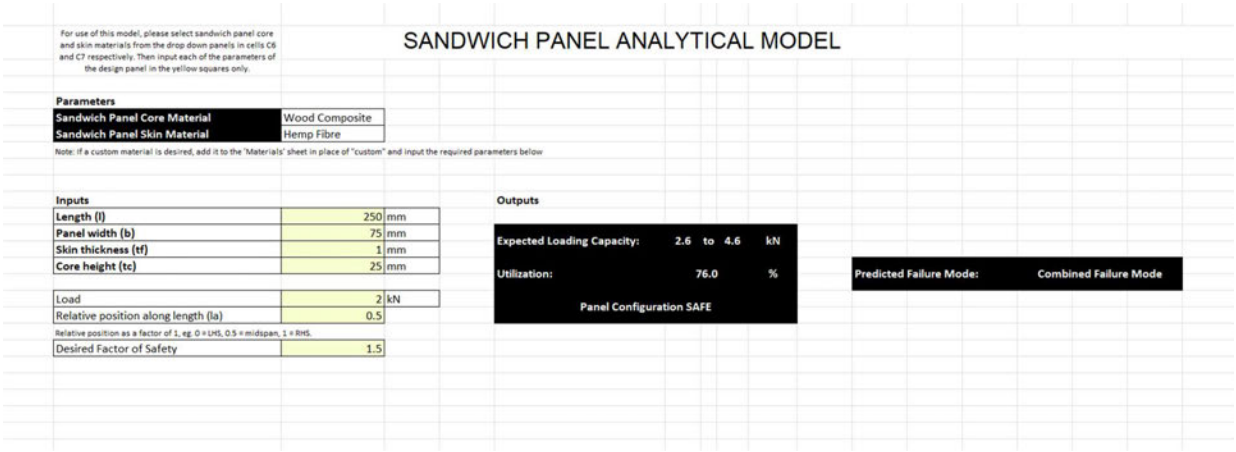

Figure 39: Model overview "Summary" sheet.

To
begin, the materials need to be selected for both the skin and the core. When selecting the cell of the core and skin materials, an arrow will appear next to the cell, which will display a list of material options to be selected from (Figure 40). If the desired material is not in the material options, the "Custom" option can be selected for both the core and skin. If this option is selected, the line below gives the instructions to input the material properties of the custom material on the "Materials" sheet.

After the materials have been selected or inputted under custom, the all the input fields need to be filled out, which are cells highlighted in yellow. This includes the dimensions of the design panel, including the width, core height, and skin thickness, as well as the distance between the supports for the loading scenario. From these inputs the model will return an expected loading capacity in the "Outputs" section on the "Summary" sheet. The expected loading capacity will be affected by the input of the desired factor of safety, being recommended between 1.25 and 2, due to the uncertainties of the model.

Other inputs on this sheet include the load and relative position along the length, for if the loading scenario for the design is known. These two inputs will be used to compare against the expected loading capacity and display a utilisation of the modelled panel for the particular loading scenario.

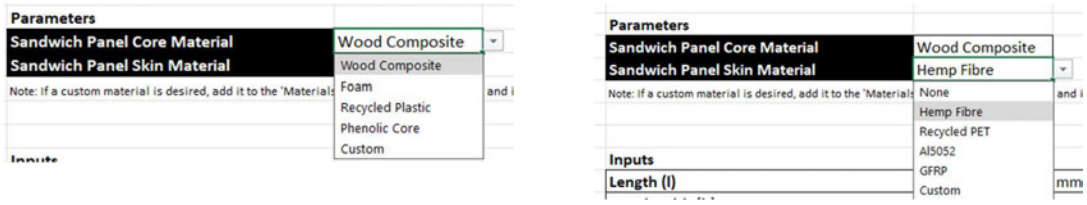

Figure 40: Drop down selection options for core (left) and skin (right) materials on "Summary" sheet.

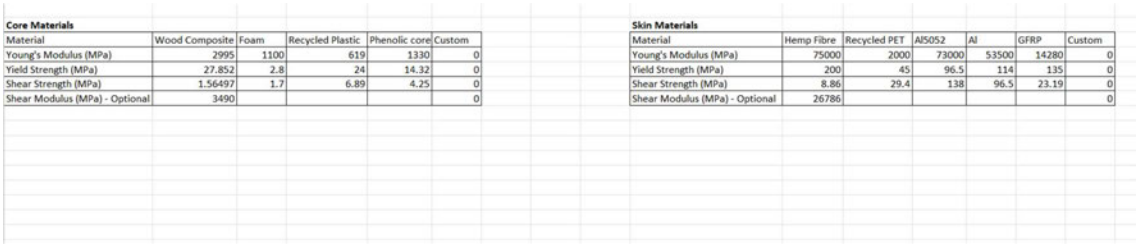

Core Materials					
Material	Wood Composite	Foam	Recycled Plastic	Phenolic core	Custom
Young's Modulus (MPa)	2995	1100	619	1330	0
Yield Strength (MPa)	27.852	2.8	24	14.32	0
Shear Strength (MPa)	1.56497	1.7	6.89	4.25	0
Shear Modulus (MPa) - Optional	3490				0

Skin Materials						
Material	Hemp Fibre	Recycled PET	Al5052	Al	GFRP	Custom
Young's Modulus (MPa)	75000	2000	73000	53500	14280	0
Yield Strength (MPa)	200	45	96.5	114	135	0
Shear Strength (MPa)	8.86	29.4	138	96.5	23.19	0
Shear Modulus (MPa) - Optional	26786					0

Figure 41: Model overview “Materials” sheet.

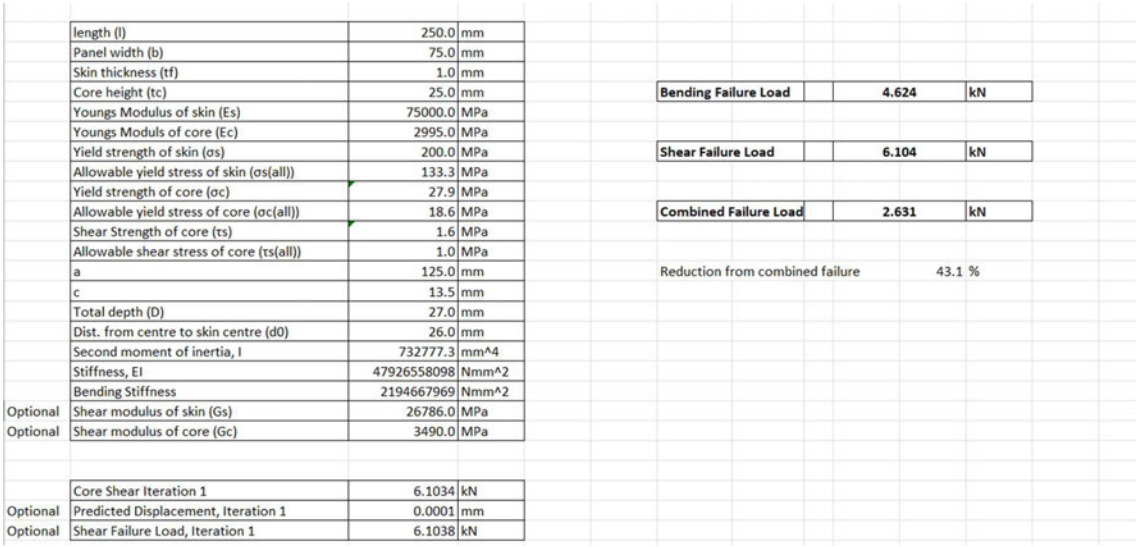

	length (l)	250.0	mm
	Panel width (b)	75.0	mm
	Skin thickness (tf)	1.0	mm
	Core height (tc)	25.0	mm
	Youngs Modulus of skin (Es)	75000.0	MPa
	Youngs Moduls of core (Ec)	2995.0	MPa
	Yield strength of skin (σs)	200.0	MPa
	Allowable yield stress of skin (σs(all))	133.3	MPa
	Yield strength of core (σc)	27.9	MPa
	Allowable yield stress of core (σc(all))	18.6	MPa
	Shear Strength of core (τs)	1.6	MPa
	Allowable shear stress of core (τs(all))	1.0	MPa
	a	125.0	mm
	c	13.5	mm
	Total depth (D)	27.0	mm
	Dist. from centre to skin centre (d0)	26.0	mm
	Second moment of inertia, I	732777.3	mm^4
	Stiffness, EI	47926558098	Nmm^2
	Bending Stiffness	2194667969	Nmm^2
Optional	Shear modulus of skin (Gs)	26786.0	MPa
Optional	Shear modulus of core (Gc)	3490.0	MPa
	Core Shear Iteration 1	6.1034	kN
Optional	Predicted Displacement, Iteration 1	0.0001	mm
Optional	Shear Failure Load, Iteration 1	6.1038	kN

Bending Failure Load		**4.624**	**kN**
Shear Failure Load		**6.104**	**kN**
Combined Failure Load		**2.631**	**kN**
Reduction from combined failure		43.1	%

Figure 42: Model overview “Calculations” sheet.

On the “Materials” sheet, each material is listed, including the required material parameters for the model equations, as well as the ‘Optional’ input of shear modulus. This shear modulus is for use in the Timoshenko calculation of the additional effects of skin on the core shear failure load. This is marked as optional as the additional benefits from this additional calculation are small, slightly increasing the allowable load, so removing this additional benefit will be conservative in the model equation. If this input is not included, the model is able to bypass this step and output the expected shear failure load based on core stress alone.

On the “Calculations” sheet, the model executes all required calculations for display as the outputs on the “Summary” sheet. It calculates all the required parameters for each of the three model equations for the bending, shear and combined failure loads using the model equations, multiplied by the desired factor of safety. From these model equations, the minimum will

always be the combined failure mode, so the model will output a range of which the modelled composite panel is expected to fail. This will be between the combined failure load and the minimum of either the shear or bending failure load predicted by the model. The model will also output the expected failure mode on the "Summary" page, being determined based on the a/D ratio to align with the theory, as well as the amount of contribution each failure mode (bending and shear) has on the combined failure load predicted by the model.

5.6 – EFFECTS OF VARIABLES TO MODEL

The effects of each variable analysed in Section 5.2 of this paper for the stress and stiffness experienced from a sandwich panel will also be analysed in this section, investigating the effects of each parameter on the ultimate failure load and failure mode of a composite sandwich panel. The same standard values of each variable will be used as in Section 5.2, other than the independent variable being altered and investigated in each section.

It should be noted that the predicted load from combined bending and shear will always be less than both bending and shear due to the nature of the prediction equation. This is because the effects from both bending or shear will contribute and reduce the failure load of the panel. While the model will always predict that the failure load will be less in the combined failure mode, the ultimate failure mode will not always be combined failure, as evidence of both methods will not always appear in the physical failure observed of a panel. When one of the failure modes, either bending or shear, is the predominant contributor to the materials failure load, the panel will be assumed to not be failing due combined bending and shear. When both bending and shear are contributing a significant amount to the predicted combined failure load, then the failure mode can be assumed to be combined failure. The level of contribution from each to be considered as combined failure will be investigated further in this chapter.

5.6.1 – Effects of Skin Thickness on Failure Load

The effects of altering the skin thickness of the composite sandwich panel, and the effects of transitioning of the homogenous wood composite to a composite sandwich panel are shown in Figure 43. There is an initial drop in required bending failure load when the material transitions from a homogenous material to a composite sandwich panel. This is due to the failure condition under bending transitioning to be from failure of the core to compressive failure of the top skin material induced via bending moment. Due to the thickness of the skin being very low when the skin thickness is less than 0.5 mm, the load required to cause compressive failure of the top skin layer (caused by bending moment) is less than the load required for bending failure of the

core material, leading to a reduced bending failure load from the model. After this initial drop between 0 and 0.1 mm of skin thickness, the allowable load under bending linearly increases for the design panel, at a rapid rate. The allowable load under the shear failure condition also linearly increases at a rate which is seen as insignificant. From the relation of these two curves, the load required for bending failure of the panel becomes greater than that of shear failure after 1mm of skin thickness on both faces of the panel. Overall, the panel would be likely to fail in bending failure for lower skin thickness (<0.5mm) in this panel configuration and fail via shear at higher skin thicknesses (>2.5mm) and by combined shear-bending failure in-between. Once the bending failure load required surpasses that of shear, the benefits to the composite panel lessen, as the shear failure load does not increase substantially enough to make any difference to the failure load. This makes the only benefit to increasing the skin thickness to reduce the combined failure load.

This makes the optimum skin thickness for this panel to be above 0.5 mm, to have benefit in bending failure over the homogenous core and should be less then 2mm due to the decreasing benefit gained from additional increasing the skin thickness and becoming impractical for a sandwich panel.

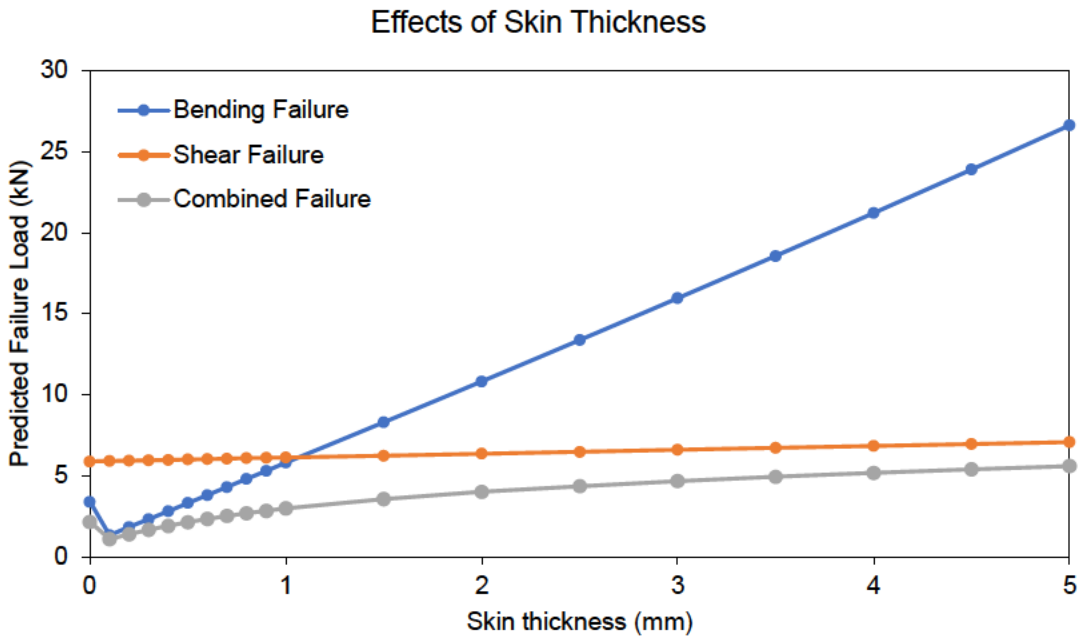

Figure 43: Effects of skin thickness to model equations prediction of failure load.

From the analysis of skin thickness' effects on the ultimate failure load of the test panel composition, the standard value of skin thickness has been selected at 1mm. This is the point where the benefits of increasing the skin thickness lessen from any further increase and provides a decent increase to the base homogenous materials failure load. The failure load

under both shear and bending conditions are most similar at this point, making the analysis of other variables within the model best able to represent the effects on both bending and shear failure load, having the two values origin be at a similar point.

5.6.2 – Effects of Length on Failure Load

For the purposes of analysing the length, the a/D ratio will be mentioned for significant points for the distance between supports. From the standard values, the core height of the panel in this test is 25 mm, and the skin thickness has been decided as 1 mm, making the D = 27 mm as the standard (unless specified elsewhere).

Changing the length of the sandwich panel will have no difference on the ultimate shear load of the panels. Both the materials and their configurations will not be altered, and therefore the amount of shear the panel can withstand will be constant.

The bending moment that will be induced by a load at the midspan will increase as the span increases, making the panel fail at a lesser load without altering the panel itself.

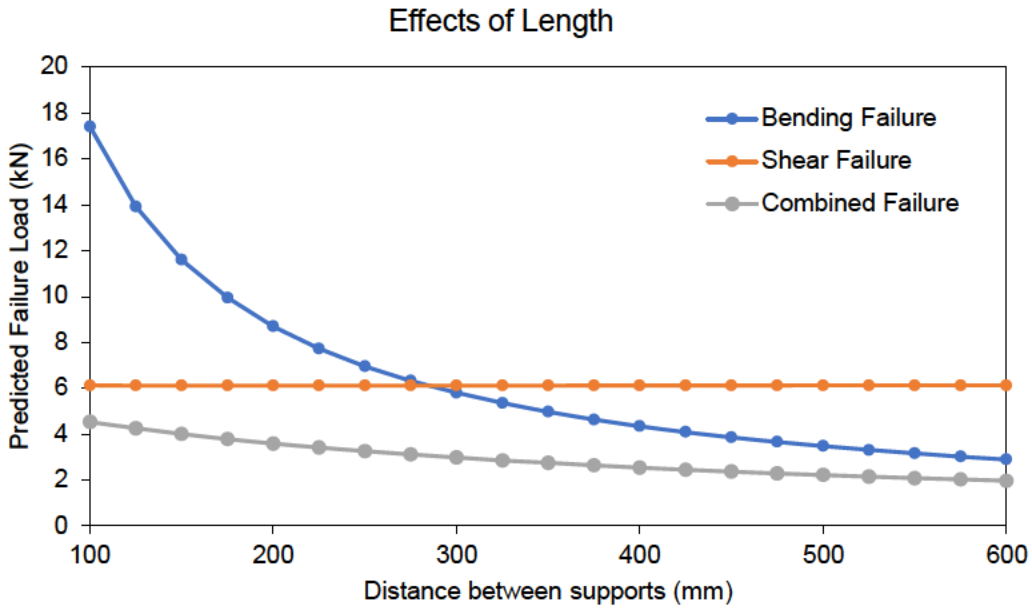

Figure 44: Effects of distance between supports to model equations prediction of failure load.

With the predicted shear failure remaining constant and the required load for bending failure increasing as the distance between support decreases, so the predicted failure load for shear failure is less when the length of the panel reduced beyond 275mm. This would make the a/D ratio be roughly equal to 5, and with an assumed tolerance of ± 1, would make the panel be predicted to fail at an a/D of 6, being 325 mm span, and fail via shear at an a/D of 4, being a span of 216 mm.

The distance between supports is not always controllable in design scenarios for panelling, rather being a determining factor, not an easily changeable material property, however a range will be given for the optimal span that this panel configuration could be designed for, being up to 300 mm before the load required for bending failure becomes less than shear failure. The decrease based on length for bending failure loads does begin to plateau, making the allowable load for any length of the design panel be roughly 3 kN.

5.6.3 – Effects of Width on Failure Load

From increasing the width of the sandwich panel there is a continuous linear increase in the required failure load in both bending and shear. This is due to the stiffness of the panels (EI) increasing from the increase in width of the materials. The increase to both bending and shear failure loads is similar, with bending having a slightly greater increase, while both these increases due to width do not have as great of an effect on the ultimate failure load as altering the length or thickness of the skin. However, if a general increase to both parameters is required then increasing the width of the panels would be a recommended option for exploration, as both skin thickness and length had only significant effects on the bending failure load. With both parameters increasing at a similar rate, increasing the width will have little to no effect on altering the predicted failure mode of the panels.

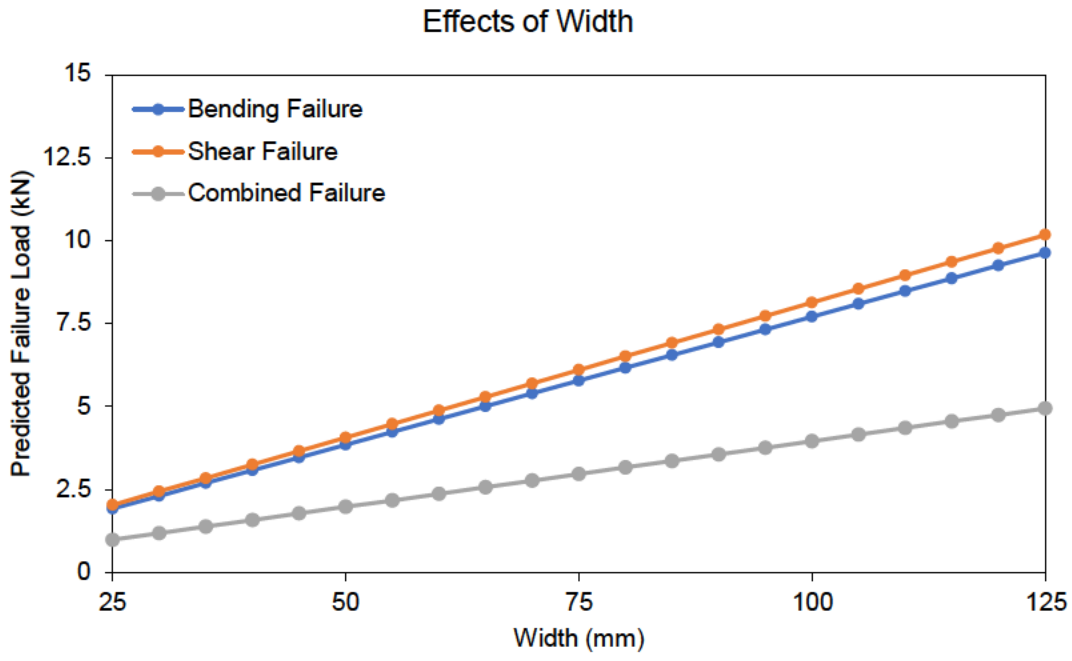

Figure 45: Effects of panel width to model equations prediction of failure load.

5.6.4 – Effects of Core Height on Failure Load

From increasing the core height of the sandwich panels, the cross-sectional area of the panels increases becoming stiffer, increasing both the bending and shear strengths, and making the predicted failure load under both scenarios greater (Figure 46). The increase for this particular panel with a wood composite core is greater than for other traditional panel core types such as foam due to the comparatively high modulus of the material. Even though the affects are significant, they are not as great as increasing the skin thickness due to the higher modulus of the skin. The option of increasing the core height would be desirable in situations where there is allowable room to do so in the design scenario, and the cost of increasing the skin thickness significantly outweighs increasing the core height. Both the shear and bending failure loads are increased from increasing the core height, unlike from increasing the skin thickness, as the failure criteria in shear is directly affected by the cross section of the core and is practically unaffected by the skin layers dimensions and properties. The increase to both bending and shear failure loads is similar compared to the increase in width of the panels, but the shear failure load relationship is linear, while the bending failure relationship is exponential to a small degree. The effects of this exponential relationship would be more greatly seen at higher core heights, greater than 50 mm, however this is seen as unreasonable for this sandwich panel configuration with wood composite products typically coming in long thin boards and planks.

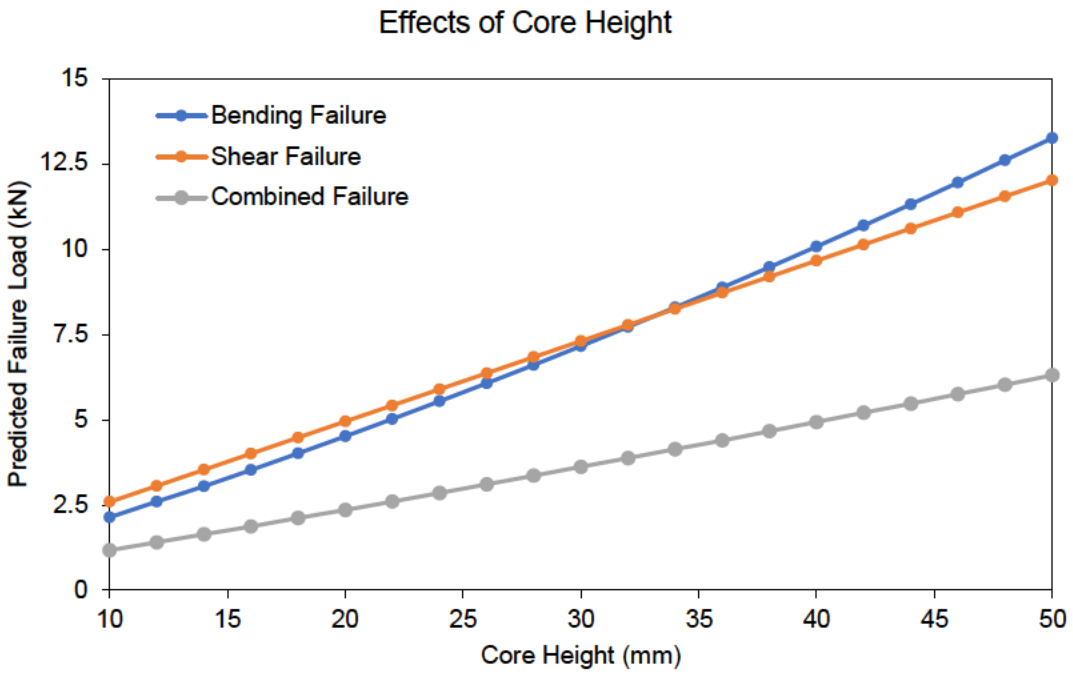

Figure 46: Effects of core height to model equations prediction of failure load.

5.6.5 Effects of Skin Modulus on Failure Load

Altering the modulus of the skin has a minimal effect on the shear failure, as the failure criteria for shear is based on the cores allowable stress. The bending failure load is

seen to be exponentially decreasing, due to the nature of equation, for the increase in second moment of inertia is not great enough due to the small thickness dimension of the skin, making the increase to the modulus of the skin greater, lowering the overall bending failure.

Materials with a greater flexural modulus should intrinsically have a greater resistance to bending moment before failure. From the nature of a sandwich panel, the benefit should be produced from the difference ion modulus between the core and skin materials, if the greater the difference, to a degree, the better the panel would mechanically perform. This is not what is being observed from the model, and the reason behind is presumed to be from the yield strength of the skin remaining constant, which would not be true for if the modulus of elasticity of a material was theoretically increased, then so should the yield strength.

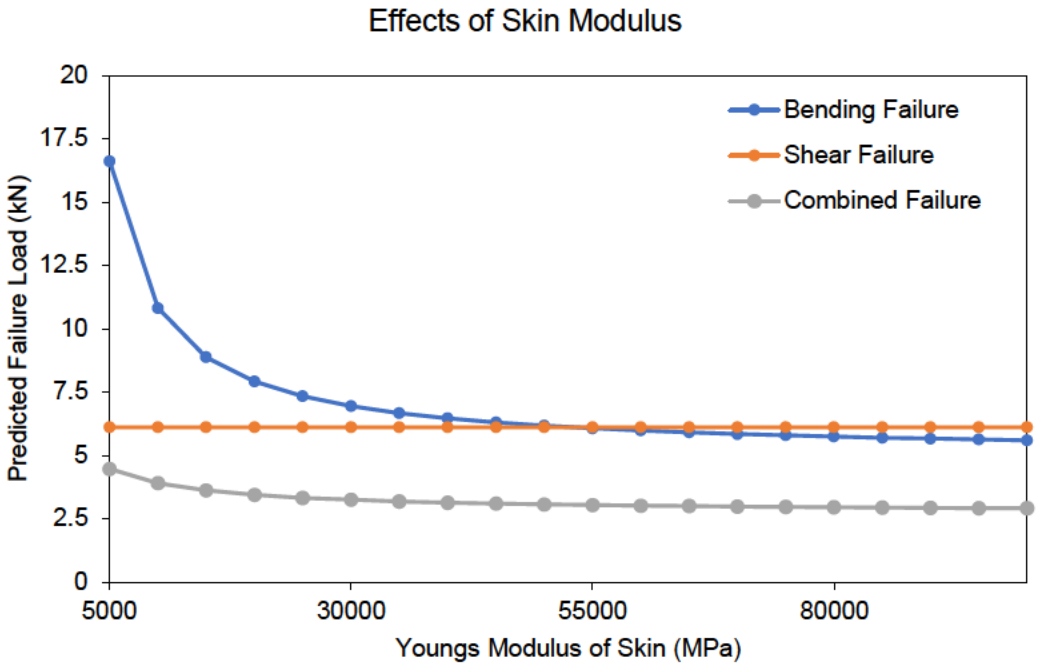

Figure 47: Effects of skin modulus to model equations prediction of failure load.

5.6.6 – Effects of Core Modulus on Failure Load

When the modulus of the core increases, the sandwich panel becomes stronger in bending as the overall stiffness of the panel increases, while the shear of the panel remaining constant under the Timoshenko model. The panel remains constant in shear due to the model equation being based upon the shear strength of the core, however in practice, the shear strength of the core would be likely to increase if the flexural modulus is also increase, but this case is not always true.

From the relationship between bending and shear predicted failure loads, the combined failure load is not greatly affected by the increase to the flexural modulus of the core. This makes any core modulus of a material viable as a sandwich panel, however the potential drawback to a greater modulus giving slight increases to the predicted failure load would be the increase in density of the materials. If a core material is dense, this removes one of the advantages of the panel of being lightweight compared to their mechanical properties, so the density as well as other factors (e.g., shear strength) should be the governing factors over core modulus for selection of a core material in a composite sandwich panel composition.

Foam core panel types typically have a greatly reduced modulus, compared to the skin material, making the performance in bending worse for the panels, but this has little to no impact on the load required for shear failure. Although the performance is lesser, there are several benefits to having a lightweight material, with great properties of heat preservation, sound insulation, and impact resistance, being a highly elastic material compared to solid core panel types.

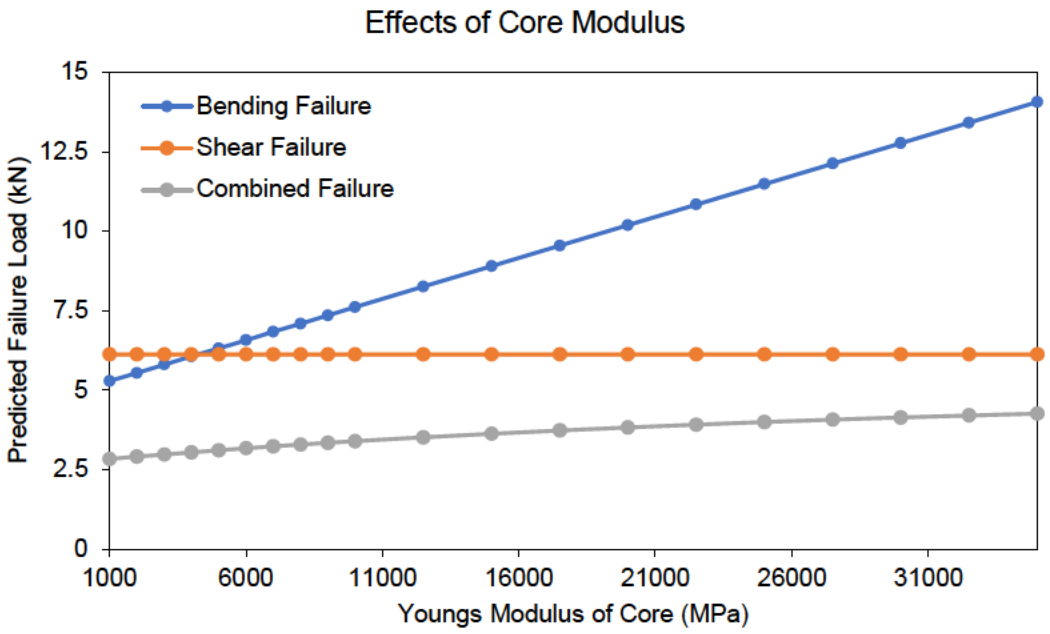

Figure 48: Effects of core modulus to model equations prediction of failure load.

5.6.7 – Effects of Core Shear on Failure Load

From increasing the shear strength of the core in the design sandwich panel, the load required for failure of the panel in shear will linearly increase, while the load required for bending failure will remain constant. The failure load in shear is directly related to the shear strength of the

core as the failure condition in the Timoshenko model is based upon the shear stress exceeding the allowable stress of the core, of which increasing the shear strength directly increases the allowable stress within the panel, with the panel requiring 0 kN of load to fail when the core material has 0 shear strength.

Due to the bending failure load remaining constant, the combined failure load will continually increase from a higher shear strength of the core, but at a lower rate than the shear failure load, being unable to surpass the plateau of the bending failure load. This makes subsequent increases to the core shear strength have a continually diminishing increase on the allowable load in the combined failure equation. The optimum core shear strength is therefore any point greater than where the shear failure load becomes greater than the bending failure load, as the greatest increase can be seen in this zone, which for this design panel is after a core shear strength of 1.5 MPa. The maximum core shear strength would be recommended at 3 MPa for this design panel, due to the diminishing returns. If shear failure is the major issue for a panel being created in the model, increasing the core shear would have a great effect on increasing the failure load of the composite panel.

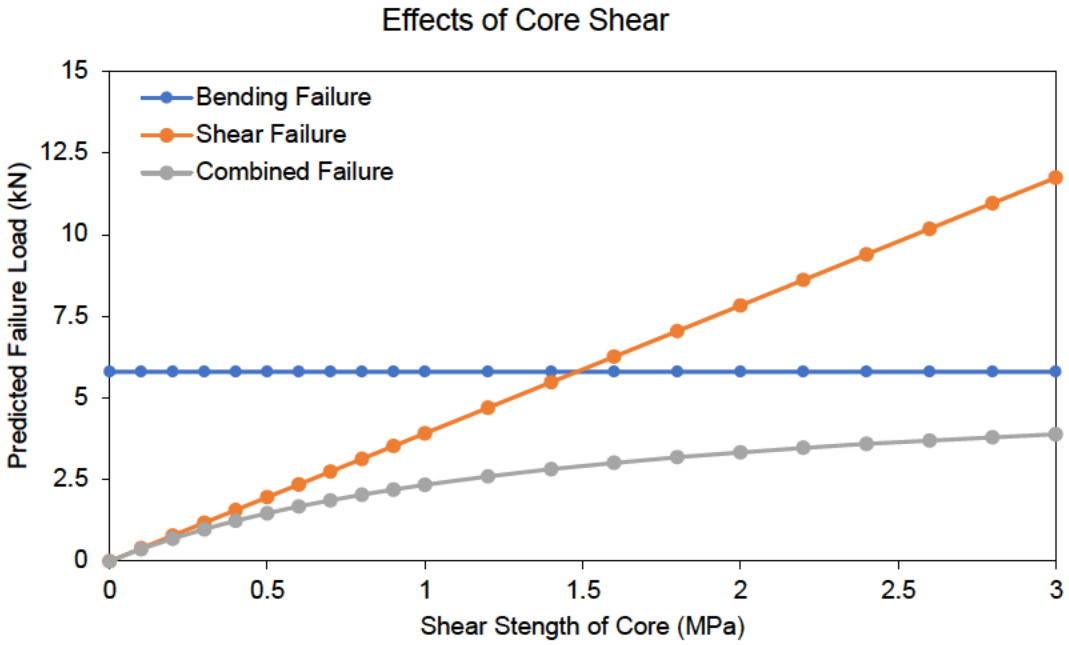

Figure 49: Effects of core shear to model equations prediction of failure load.

5.7 – SUMMARY OF MATERIALS AND PARAMETERS INFLUENCE ON MODEL OUTPUT

Each parameter within the model has the potential to be altered to have a positive influence on the strength and stiffness of the panels, leading to a greater load required to cause failure of the

sandwich panels. If the model predicts the panels to be predominantly failing due to the bending stress being far greater than the allowable limit of the panel, increasing the skin thickness will have the greatest increase to the panels allowable bending stress, for a small amount of extra material and thickness of the panel. The modulus of the skin can also be altered to increase the allowable bending stress of the panel, or the loading scenario can be changed, reducing the distance between supports of the panel within a three-point bending test set-up can reduce the bending load applied to the panel itself. Increasing the width can lead to an increase in load required to cause bending and shear stress, however the increase is not as major compared to the increase in material requirements for the panel. This increase in both failure criteria can be from increasing the core height, however this may not be an applicable solution, due to the panel requirements, which can be used within wall and ceiling panelling, often being restricted in size by the surrounding environment. To greatly increase the load requirement to cause core shear failure within a panel, the core material should be changed to having a higher shear modulus. Using this analysis, the required changes for a design scenario of a sandwich panel can be made based upon the theoretical benefits gained from altering each of the model parameters.

From testing the design panel and altering the core materials (keeping skin material constant), the wood composite material is seen to have the greatest mechanical performance as compared to the other recycled (solid) and foam material options within the model, with the aluminium foam performing the worst (Figures 50 to 53). Recycled plastic lumber is seen to perform on par with foam materials for point loads applied at the midspan. This shows the potential of wood composites to be used as a structural sandwich panel core material, outperforming other panel core types, but have the negatives of the high density and weight of the product and having a brittle nature in failure.

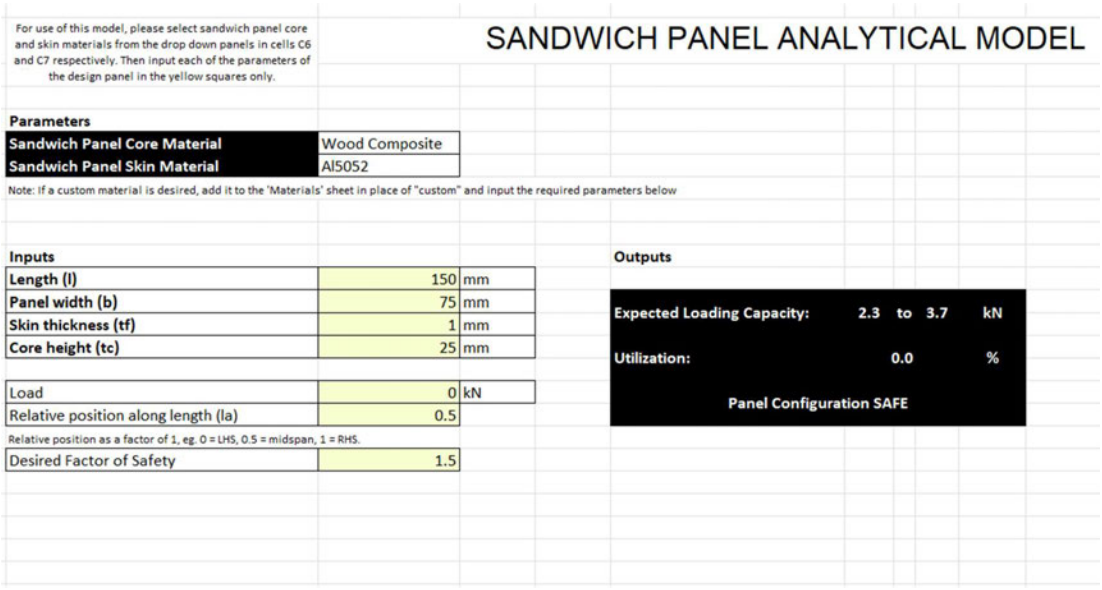

For use of this model, please select sandwich panel core and skin materials from the drop down panels in cells C6 and C7 respectively. Then input each of the parameters of the design panel in the yellow squares only.

SANDWICH PANEL ANALYTICAL MODEL

Parameters

Sandwich Panel Core Material	Wood Composite
Sandwich Panel Skin Material	Al5052

Note: If a custom material is desired, add it to the 'Materials' sheet in place of "custom" and input the required parameters below

Inputs

Length (l)	150	mm
Panel width (b)	75	mm
Skin thickness (tf)	1	mm
Core height (tc)	25	mm
Load	0	kN
Relative position along length (la)	0.5	

Relative position as a factor of 1, eg. 0 = LHS, 0.5 = midspan, 1 = RHS.

Desired Factor of Safety	1.5

Outputs

Expected Loading Capacity:	**2.3**	**to**	**3.7**	**kN**
Utilization:		**0.0**		**%**

Panel Configuration SAFE

Figure 50: Standard panel set-up with wood composite core.

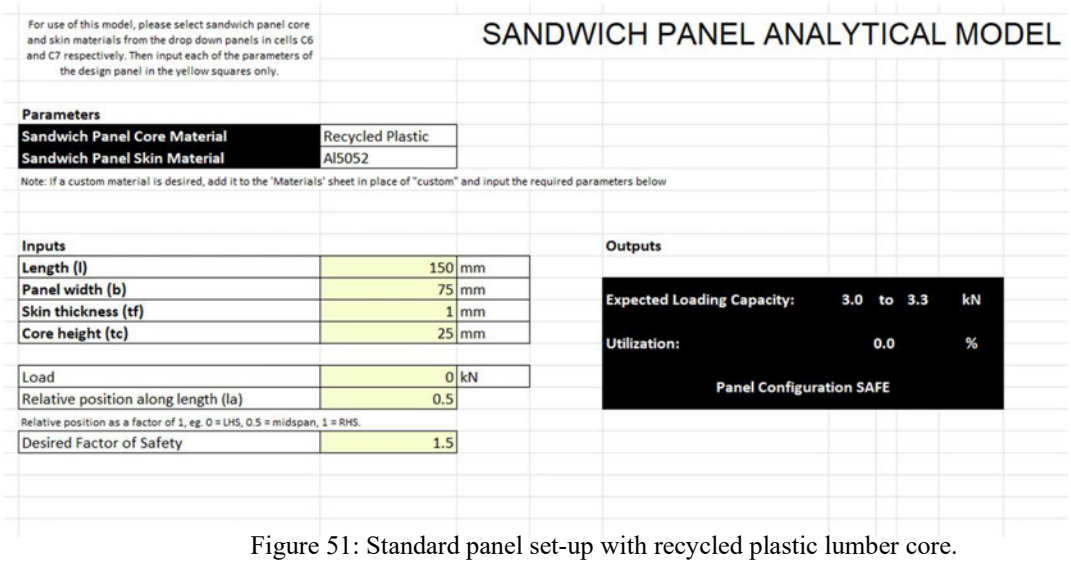

For use of this model, please select sandwich panel core and skin materials from the drop down panels in cells C6 and C7 respectively. Then input each of the parameters of the design panel in the yellow squares only.

SANDWICH PANEL ANALYTICAL MODEL

Parameters

Sandwich Panel Core Material	Recycled Plastic
Sandwich Panel Skin Material	Al5052

Note: If a custom material is desired, add it to the 'Materials' sheet in place of "custom" and input the required parameters below

Inputs

Length (l)	150	mm
Panel width (b)	75	mm
Skin thickness (tf)	1	mm
Core height (tc)	25	mm
Load	0	kN
Relative position along length (la)	0.5	

Relative position as a factor of 1, eg. 0 = LHS, 0.5 = midspan, 1 = RHS.

Desired Factor of Safety	1.5

Outputs

Expected Loading Capacity:	**3.0**	**to**	**3.3**	**kN**
Utilization:		**0.0**		**%**

Panel Configuration SAFE

Figure 51: Standard panel set-up with recycled plastic lumber core.

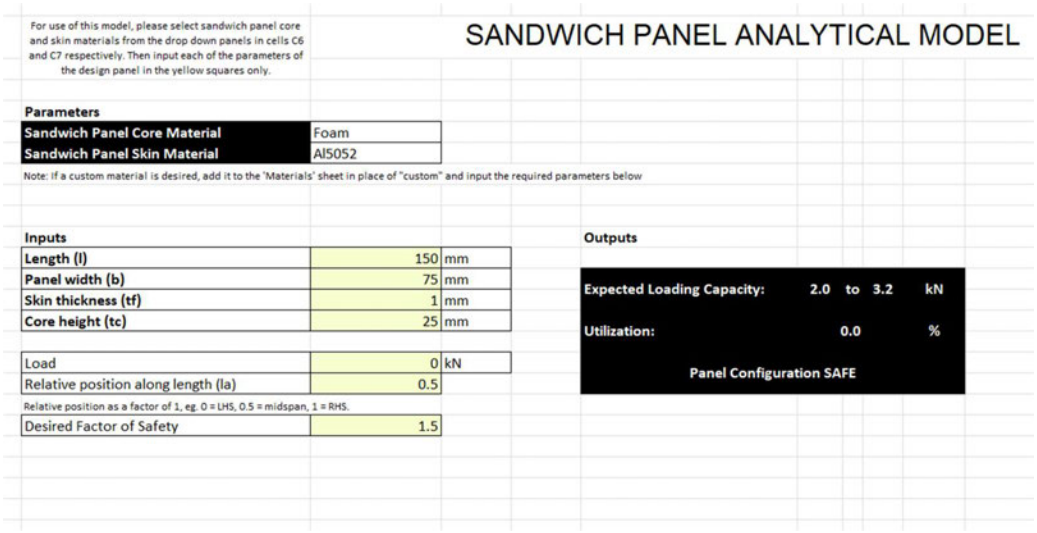

For use of this model, please select sandwich panel core and skin materials from the drop down panels in cells C6 and C7 respectively. Then input each of the parameters of the design panel in the yellow squares only.

SANDWICH PANEL ANALYTICAL MODEL

Parameters	
Sandwich Panel Core Material	Foam
Sandwich Panel Skin Material	Al5052

Note: If a custom material is desired, add it to the 'Materials' sheet in place of "custom" and input the required parameters below

Inputs		
Length (l)	150	mm
Panel width (b)	75	mm
Skin thickness (tf)	1	mm
Core height (tc)	25	mm
Load	0	kN
Relative position along length (la)	0.5	

Relative position as a factor of 1, eg. 0 = LHS, 0.5 = midspan, 1 = RHS.

Desired Factor of Safety	1.5

Outputs

Expected Loading Capacity:	2.0	to	3.2	kN
Utilization:		0.0		%

Panel Configuration SAFE

Figure 52: Standard panel set-up with aluminium foam core.

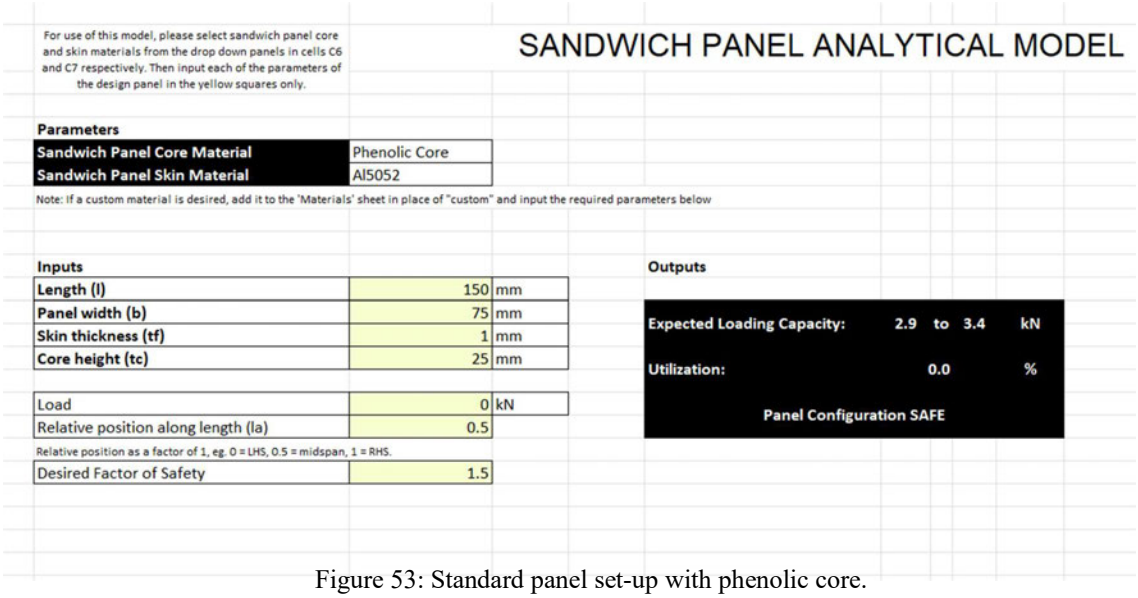

For use of this model, please select sandwich panel core and skin materials from the drop down panels in cells C6 and C7 respectively. Then input each of the parameters of the design panel in the yellow squares only.

SANDWICH PANEL ANALYTICAL MODEL

Parameters	
Sandwich Panel Core Material	Phenolic Core
Sandwich Panel Skin Material	Al5052

Note: If a custom material is desired, add it to the 'Materials' sheet in place of "custom" and input the required parameters below

Inputs		
Length (l)	150	mm
Panel width (b)	75	mm
Skin thickness (tf)	1	mm
Core height (tc)	25	mm
Load	0	kN
Relative position along length (la)	0.5	

Relative position as a factor of 1, eg. 0 = LHS, 0.5 = midspan, 1 = RHS.

Desired Factor of Safety	1.5

Outputs

Expected Loading Capacity:	2.9	to	3.4	kN
Utilization:		0.0		%

Panel Configuration SAFE

Figure 53: Standard panel set-up with phenolic core.

5.8 – MODEL LIMITATIONS

With the model equations being based on solid core panel types, the model is analysed against other sandwich panels with differing core types to see the extent of accuracy from the model. From using the parameters of the experimental testing performed by Xia et al., the results of corrugated core panels, with the corrugations spanning the longitudinal direction (L) and the transverse direction (W), truss core panels, honeycomb core panels, aluminium foam core

panels were calculated separately by the model, as the differing core type panels were made of various materials. All sandwich panels consisted of Al5005-H34 face sheets, with differing core materials with corrugated and truss core types using Al-5005-H34, honeycomb core panels using an Al5005 lattice and the foam core consisting of Al-Ca5-Ti3 aluminium foam. Due to this the model prediction results will be the same for the corrugated and truss panels, as the only differentiation is by core type. The results can be seen in Table 10 below.

Table 10: Comparison of model and experimental results for panels by Xia et al.

	Theoretical Results (kN)	Experimental Results (kN)	Difference
Corrugated Core-L	3.7-3.8	3.1	-0.6
Corrugated Core-T	3.7-3.9	0.5	-3.2
Truss Core	3.7-3.8	0.45	-3.25
Honeycomb Core	2.9-3.0	2	-0.9
Foam Core	0.79-1.4	0.8	0

From these results, the failure mode in this example is heavily dominated by bending failure due to the extreme shear prediction from the model due to the assumption by the model that the core to be differing homogenous aluminium materials. This makes the reduction in the predicted failure load due to shear almost negligible which is not accurate for these various panel core types and would make the predicted range lower if the core shear results were more reasonable. From Table 10, the predictions from the model can be seen to be most accurate for the foam core, being at the minimum of the range (where the model is predicting pure combined failure, which is not true from the experimentation), being an accurate prediction. The results for the longitudinal corrugated core and the honeycomb core are less accurate, due to the high predicted shear failure, but are within a reasonable limit to which an appropriate factor of safety could be applied. The predictions of the transverse corrugated core and the truss core are inaccurate due to the nature of the core types. The transverse corrugated core is much weaker than a longitudinal corrugation in this bending setup due to the direction of the support being in-line with the load applied, having a lower increase to the strength of the panel in a three-point bending set-up. Truss cores also have a substantially lower failure load due to the substantially lesser amount of material being used, being in the same pattern as the longitudinal corrugated core, but only at the edges.

A clear reduction in all sandwich panel core types can be seen as compared to solid core panel types, however the benefits of other core types may outweigh the decrease in strength. Longitudinal corrugated cores and honeycomb cores are highly effective for the reduction in material being used and overall cost of the panel, while still having good mechanical performance. Using foam as a cheaper alternative also provides a solid strength to the panels, while being lightweight and elastic in nature, but features a lower stiffness. Many of these core

types are more suitable to withstand higher distributed loading, which is not able to be seen by the current model.

From this analysis, the model should only be used for solid core panel types without alteration, and is able to be used for foam, honeycomb, and longitudinal corrugated core sandwich panels with an increased factor of safety. With the varying benefits and ideal application of each panel type, being able to model these differing sandwich panel cores will greatly enhance the viability and versatile design tool for modelling and exploring sandwich panels as structurally sound, recyclable construction materials.

5.9 – CHAPTER SUMMARY

In this section of the paper, the experimental results from the three-point bending test on wood composite samples is analysed for failure load and failure mode, with the results from the experimentation being used to obtain required parameters for the analytical model equations. The effects of each of the parameters within the model equations is then analysed, based on the theoretical strength and stiffness of the theoretical composite panel configurations, with the effects also being analysed by how each effects the predicted failure mode within the model.

The model tends to predict bending or combined bending-shear failure as the ultimate failure load when experimental results on honeycomb and core panels were observed to fail by core shear. This is due to solid core panel types have the highest shear strength compared to other traditional sandwich panel cores. Solid panel cores make the panels denser and heavier, requiring the most material, however they are easily constructed and offer the greatest mechanical strength. This material requirement can be offset by using recycled materials for the core, as this can offset the greater material requirement, reducing the environmental impact of the material usage, providing the options are available and at a reasonable cost.

CHAPTER 6 – CONCLUSIONS AND RECOMMENDATIONS

6.1 – SUMMARY OF FINDINGS

This research paper has investigated using wood composite materials as a sandwich panel core to improve the mechanical properties of the material. Based on the material properties of the wood composite from experimental data and previous literature on predictive model equations, an analytical model has been developed for composite sandwich panels. This model uses different model equations to predict the ultimate failure load of a wood composite sandwich panel in bending, shear and combined bending-shear failure modes. From this model, the wood composite panels were investigated to determine how to further improve the performance by altering the properties of the panel materials or dimensions. The panels were found to theoretically have over a 30% decrease in bending stress on the core material from the addition of a hemp fibre skin layer added to each face of the wood composite and increase the failure load required by double from just 1 mm of skin added to each face.

When comparing wood composite to other traditional core materials as a sandwich panel core, a high level of mechanical performance was evident compared to all other core types. Although other core types are lightweight and have differing situational advantages, this study has confirmed the practicality and potential of using solid, dense materials as sandwich panel cores, with the great potential for using recycled materials such as wood composite as the core.

With wood composites strong mechanical performance in shear and flexure as a sandwich core material, the option of using recycled solid sandwich panels is justified to obtain high mechanical properties of the panel. With the high durability and resistivity of wood composites (Section 2.1.3) due to the plastic within the material composition, it makes the product a great option within homes, being termite and fire resistant. The use of recycled plastic within the material matrix also is found to perform on-par with virgin plastics within the wood composite mix (Section 2.1.2). Using recycled polymers within the wood composite material will increase rates of recycling of plastics which contribute a great amount to landfills, having the lowest recovery rate which could be greatly offset if this material gains popularity as a mechanically efficient construction material.

Overall, this study has been successful in determining the viability of solid, homogenous, recycled materials as an alternative as a composite sandwich panel core material. Through the use of the analytical model equations the panel types and materials were able to be investigated in this study, however there is still a lot more to be worked on to further improve this model, to be used as an efficient and effective design tool for more varied applications.

6.2 – RECOMMENDATIONS FOR FUTURE WORK

This model was created with the intentions for experimentation of a fully constructed sandwich panel under three-point testing to compare to the prediction of the model, but due to limitations in time and resources, this was not able to be accomplished, so the model was compared against sandwich panels within the literature to verify the model. By taking other experimentation results, the full details of how these tests were performed and kept unbiased is not known, and the uniformity of testing across differing papers is not applicable, which could lead to outliers and uncertainties when comparing against the analytical prediction equations. Due to this, experimentation under three-point bending should be performed for each of the materials within the model as a homogenous product and as a sandwich panel to validate the information on the "Materials" page and the outputs for expected failure loading. Once this is performed, the reliability of the model equations will be verified further, to reduce uncertainties and not relatively high factors of safety.

The modelling equations for created sandwich panels of many varieties still need to be created for various loading conditions, to be represent a wide range of loading scenarios a panel may undergo in a practical scenario. This would include four-point bending, distributed loads, off-centre point loads, and loads of varying magnitude.

These changes along with investigation of material and fabrication costs associated with differing panel materials and types would allow designers to have a simple way of determining what materials and make-up of a sandwich panel can deliver the requirements needed in an efficient and effective manner. This analytical model can become a very useful tool, saving time and money in construction due to the simplicity of such a tool within engineering design, being able to simply input the parameters of their product to see determine the safety under the intended loading condition.

Future changes to the analytical model can include the variations required of the model in the spreadsheet for different core types, such as corrugated, honeycomb, truss, and foam core sandwich panel types. This study only had the time and resources to study a solid core sandwich panel, but other configurations may provide a greater range of options to select from in a design, and also could provide financial optimisation, through the use of less material in these differing panel types.

Further experimentation on different sandwich panel compositions, dimensions, and materials should be performed and compared against the model to refine what the allowable factor of safety can be within the model for different applications.

A major aspect which should be included to create an effective and useful design tool is a cost per each material included within the model (per m^3). This will allow designers to be able to

compare options against a cost/benefit analysis, as the cost of materials or products has a large importance in design.

6.3 – IMPACT IN INDUSTRY

This research paper has helped contribute to the knowledge of composite sandwich panels and has determined the effectiveness of using non-traditional recycled materials as either the core or the skin of a sandwich panel.

This research and modelling has the potential to have a large impact on the industry if further refinements and enhancements are done to the model with further research. Once refined and tested with practical experimentation for created sandwich panels for validation, this design tool could be used throughout engineering design offices as a quick checking tool to determine options for a design situation in an efficient and effective manner. With the model included many recycled materials, the ability to do design checks of options with these recycled materials would be quick and easy to prove the effectiveness of recycled materials within composite panels compared to traditional sandwich panel materials. This will help improve the rates at which recycled materials are being used, with options for homogenous materials to be checked as well being a versatile design tool. Many traditional non-recycled materials are also being included within the model to increase the useability, as if only recycled options were available as choices, it would not be as desired for use, and then limitations would be placed on designers, being limited in engineering choices, as many traditional products have benefits in particular scenarios, which would limit the choice of designers which is not the desired effect. Without limiting the choices, designers would be more open towards using recycled materials due to their similar, if not better, performance within design scenarios. Although the ultimate decision may be dependent on the cost of materials, the performance, and benefits of using recycled products will be evident and may lead to increased demand of these products, leading to better production methods and lower costs in the future, leading towards an ever-reducing reliance on non-recycled unsustainable materials.

LIST OF REFERENCES

ABS 2020, *Waste Account, Australia, Experimental Estimates,* Australian Government, Canberra, viewed 7 October 2022, <https://www.abs.gov.au/statistics/environment/environmental-management/waste-account-australia-experimental-estimates/latest-release>.

Anwar, H & Najam, F 2017, 'Understanding Cross Sections', in *Structural Cross Sections: Analysis and Design*, Elsevier, Amsterdam, pp. 39-136, ISBN: 978-0-12-804443-8.

ASTM International n.d., *ASTM International,* Pennsylvania, viewed 10 October 2022, <https://www.astm.org/>.

Barbosa, LG, Piaia, M & Ceni, GH 2017, 'Analysis of Impact and Tensile Properties of Recycled Polypropylene', *International Journal of Materials Engineering*, vol. 7, no. 6, pp. 117-20.

Basalp, D, Tihminlioglu, F, Sofuoglu, SC, Inal, F & Sofuoglu, A 2020, 'Utilization of Municipal Plastic and Wood Waste in Industrial Manufacturing of Wood Plastic Composites', in A Nzihou (EIC), *Waste Biomass Valor,* Springer Publishing, New York, vol. 11, pp. 5419–5430, viewed 7 October 2022, <https://doi.org/10.1007/s12649-020-00986-7>.

Caulfield DF, Clemons C, Jacobson RE & Rowell RM 2005, Wood thermoplastic composites', in RM Rowell (ed) *Handbook of wood chemistry and wood composites*, CRC Press, Boca Raton, pp 365–378.

Cavallo, C n.d., *All About 5052 Aluminium (Properties Strengths and Uses*, Thomas Publishing Company, California, viewed 11 August 2023, <https://www.thomasnet.com/articles/metals-metal-products/5052-aluminum>.

Crupi, V & Montanini, R 2007, 'Aluminium foam sandwiches collapse modes under static and dynamic three-point bending', *International Journal of Impact Engineering*, vol. 34, no. 3, pp. 509-21.

Dhaliwal, GS, Dueck, SM & Newaz, GM 2019, 'Experimental and numerical characterization of mechanical properties of hemp fiber reinforced composites using multiscale analysis approach', *SN Applied Sciences*, vol. 1, no. 11.

Ferdous, W, Manalo, A & Aravinthan, T 2017, 'Effect of beam orientation on the static behaviour of phenolic core sandwich composites with different shear span-to-depth ratios', *Composite Structures*, vol. 168, pp. 292-304.

Giglio, M, Gilioli, A & Manes, A 2012, 'Numerical investigation of a three point bending test on sandwich panels with aluminum skins and Nomex™ honeycomb core', *Computational Materials Science*, vol. 56, pp. 69-78.

Gouloubandi, R 1982, 'Wood-plastic composites using woods native to Iran', in *Radiation Physics and Chemistry (1977)*, vol. 19, issue 1, pp. 85-88, viewed 8 October 2022, <https://doi.org/10.1016/0146-5724(82)90052-8>.

Hamel, S, Hermanson, J & Cramer, S 2012, 'Mechanical and time-dependent behaviour of wood-plastic composites subjected to tension and compression', in J Gillespie Jr (ed.) *Journal of Thermoplastic Composite Material,* SAGE Publishers, California, vol. 26, no. 7, pp. 968-87, viewed 9 October 2022, DOI: 10.1177/0892705711432362.

Huang, P, Sun, X, Su, X, Gao, Q, Feng, Z & Zu, G 2022, 'Three-Point Bending Behavior of Aluminum Foam Sandwich with Different Interface Bonding Methods', *Materials (Basel)*, vol. 15, no. 19.

Hugot, F & Cazaurang, G 2008, 'Mechanical Properties of an Extruded Wood Plastic Composite: Analytical Modeling', *Journal of Wood Chemistry and Technology*, vol. 28, no. 4, pp. 283-95.

Hugot, F & Cazaurang, G 2010, 'Mechanical properties of an extruded wood plastic composite', *Mécanique & Industries*, vol. 10, no. 6, pp. 519-24.

Kaymakci, A & Ayrilmis, N 2014, 'Investigation of correlation between Brinell hardness and tensile strength of wood plastic composites', in H Wang & UK Vaidya (EICs), *Composites Part B: Engineering*, vol. 58, pp. 582-585, <https://doi.org/10.1016/j.compositesb.2013.11.009.>.

Keskisaari, A., Kärki, T 2018a, 'The use of waste materials in wood-plastic composites and their impact on the profitability of the product', in M Xu (EIC), *Resources, Conservation and Recycling*, vol. 134, pp. 257-261, viewed 7 October 2022, <https://doi.org/10.1016/j.resconrec.2018.03.023.>.

Klyosov, A 2007, *Wood Plastic Composites,* John Wiley and Sons, New Jersey, viewed 6 October 2022, <https://books.google.com.au/books?id=KmuK4w_D7UUC&newbks=1&newbks_redir=0&printsec=frontcover&pg=PR7&dq=%22wood+plastic+composites%22&hl=en&redir_esc=y#v=onepage&q&f=false>.

Leu, S, Yang, T, Lo, S & Yang, T 2012, 'Optimized material composition to improve the physical and mechanical properties of extruded wood–plastic composites (WPCs)', in M Forde (EIC), *Construction and Building Materials,* Elsevier Ltd., Amsterdam, vol. 29, pp. 120-127, viewed 9 October 2022, <https://doi.org/10.1016/j.conbuildmat.2011.09.013.>.

Liu, J, Liu, J, Mei, J & Huang, W 2018, 'Investigation on manufacturing and mechanical behavior of all-composite sandwich structure with Y-shaped cores', *Composites Science and Technology*, vol. 159, pp. 87-102.

Liu, M, Thygesen, A, Summerscales, J & Meyer, AS 2017, 'Targeted pre-treatment of hemp bast fibres for optimal performance in biocomposite materials: A review', *Industrial Crops and Products*, vol. 108, pp. 660-83.

Ma, M, Yao, W, Jiang, W, Jin, W, Chen, Y & Li, P 2020, 'Fatigue Behavior of Composite Sandwich Panels Under Three Point Bending Load', *Polymer Testing*, vol. 91.

Market Research Report 2020, Report ID: FBI102821, Fortune Business Insights, Maharashtra, India, viewed 7 October 2022, <https://www.fortunebusinessinsights.com/wood-plastic-composite-market-102821>.

Mathieson H, Fam A 2015, 'In-plane bending and failure mechanism of sandwich beams with GFRP skins and soft polyurethane foam core', *Journal of Composites for Construction*, vol. 20, no. 1, DOI:10.1061/(ASCE)CC.1943-5614.0000570.

Matweb n.d. a, *Aluminium 5005-H15*, viewed 12 August, 2023, <https://www.matweb.com/search/datasheet.aspx?matguid=4d68415cc11a4003818339237a515a33>.

Matweb n.d. b, *Overview of materials for PVC, foam grade*, viewed 12 August, 2023, <https://www.matweb.com/search/datasheet_print.aspx?matguid=e19bc7065d1c4836a89d41ff23d47413>.

Mbarek, TB, Robert, L, Hugot, F & Orteu, J-J 2011, 'Mechanical behavior of wood–plastic composites investigated by 3D digital image correlation', *Journal of Composite Materials*, vol. 45, no. 12, pp. 2751-64.

Mei, J, Liu, J & Huang, W 2022, 'Three-point bending behaviors of the foam-filled CFRP X-core sandwich panel: Experimental investigation and analytical modelling', *Composite Structures*, vol. 284.

Mohammadabadi, M, Yadama, V & Dolan, JD 2021, 'Evaluation of Wood Composite Sandwich Panels as a Promising Renewable Building Material', *Materials (Basel)*, vol. 14, no. 8.

Mohammadabadi, M, Jarvis, J, Yadama, V & Cofer, W 2020, 'Predictive Models for Elastic Bending Behavior of a Wood Composite Sandwich Panel', *Forests*, vol. 11, no. 6.

Morell, J, Stark, M, Pendleton, D & McDonald, A 2006, 'Durability of Wood-Plastic Composites', in J Gines (EIC), *Wood Deign Focus*, Forest Products Society, Georgia, vol. 16, no. 3, pp. 7-10.

Najafi, SK 2013, 'Use of recycled plastics in wood plastic composites – A review', in U Arena, P He & D Komilis (EICs), *Waste Management,* Elsevier Ltd., Amsterdam, vol. 33, issue 9, pp. 1898-1905, viewed 6 October 2022, <https://doi.org/10.1016/j.wasman.2013.05.017.>.

Nourbakhsh, A, Ashori, A 2010, 'Wood plastic composites from agro-waste materials: Analysis of mechanical properties', in A Pandey (EIC), *Bioresource Technology*, Elsevier Ltd., Amsterdam, vol. 101, issue 7, pp. 2525-2528, viewed 9 October 2022, <https://doi.org/10.1016/j.biortech.2009.11.040.>.

Ouled Ahmed Ben Ali, R & Chatti, S 2020, 'Failure Mechanism of Sandwich Panels Under Three-Point Bending', in N Aiifaoui (ed.), *Design and Modelling of Mechanical Systems - IV*, Springer, Cham, Switzerland, pp. 533-44.

Pendleton, DE, Theresa, HA, Adcock, T, Woodward, B & Wolcott, MP 2002, 'Durability of an Extruded HDPE/Wood Composite', in B Via (EIC), *Forest Products Journal*, Georgia, vol. 52, no. 6, pp. 21-27.

Polmear, I, St. John, D, Nie, J & Qian, M 2017, 'Novel Materials and Processing Methods', in *Light Alloys*, Elsevier Ltd., Amsterdam, vol. 5, pp. 461-514, viewed 11 May, 2023, ISBN: 978-0-08-099431-4.

Pritchard, G 2004, 'Two Technologies Merge: Wood Plastic Composites', in J Daneshgahi (EIC) *Plastics, Additives and Compounding*, Elsevier Ltd., Amsterdam, vol. 6, issue 4, pp. 18-21, viewed 5 October 2022, <https://doi.org/10.1016/S1464-391X(04)00234-X.>.

Resco Plastics 1997, *Recycled Plastic Lumber Engineering Data*, Portland, Oregon, viewed 10 August, 2023, <https://rescoplastics.com/resources/engineering-and-test-data/>

Rezaeifard, M, Salami, SJ, Dehkordi, MB & Sadighi, M 2016, 'A new nonlinear model for studying a sandwich panel with thin composite faces and elastic–plastic core', *Thin-Walled Structures*, vol. 107, pp. 119-37.

Ror, CK, Negi, S & Mishra, V 2023, 'Development and characterization of sustainable 3D printing filaments using post-consumer recycled PET: processing and characterization', in *Jouranl of Polymer Research,* vol. 30, issue 9, https://doi.org/10.1007/s10965-023-03742-2.

Schirp, A, Ibach, R, Pendleton, D & Wolcott M 2008, 'Biological degradation of wood-plastic composites (WPC) and strategies for improving the resistance of WPC against biological decay' in TP Schultz (ed.) *Development of Commercial Wood Preservatives: Efficacy, Environmental and Health Issues*, American Chemical Society, Washington, pp. 480-507.

Schwarzkopf, M & Bernard, M 2016, 'Wood Plastic Composites-Performance and Environmental Impacts', in A Kutnar & S Muthu (eds) *Environmental Impacts of Traditional and Innovative Forest-based Bioproducts*, Springer Publishing, New York, viewed 7 October 2022, DOI 10.1007/978-981-10-0655-5_2.

Shams, A, Hegger, J & Horstmann, M 2014, 'An analytical model for sandwich panels made of textile-reinforced concrete', *Construction and Building Materials*, vol. 64, pp. 451-9.

Shen, J, Lu, G & Ruan, D 2010, 'Compressive behaviour of closed-cell aluminium foams at high strain rates', *Composites Part B: Engineering*, vol. 41, no. 8, pp. 678-85.

Stark, N 2001, 'Influence of moisture absorption on mechanical properties of woodflour-polypropylene composites', in J Gillepsie Jr., *Thermoplastic Composite Materials*, SAGE Publications, New York, vol. 14, no. 5, pp. 421-432.

Stark, N & Rowlands, R 2003, 'Effects of wood fibre characteristics on mechanical properties of wood/polypropene composites', *Wood and Fibre Science*, US Department of Agriculture, vol. 35, no. 2, pp. 167-174.

Steeves, CA & Fleck, NA 2004a, 'Collapse mechanisms of sandwich beams with composite faces and a foam core, loaded in three-point bending. Part I: analytical models and minimum weight design', *International Journal of Mechanical Sciences*, vol. 46, no. 4, pp. 561-83.

Steeves, CA & Fleck, NA 2004b, 'Collapse mechanisms of sandwich beams with composite faces and a foam core, loaded in three-point bending. Part II: experimental investigation and numerical modelling', *International Journal of Mechanical Sciences*, vol. 46, no. 4, pp. 585-608.

Tapia-Picazo, JC, Luna-Bárcenas, JG, García-Chávez, A, Gonzalez-Nuñez, R, Bonilla-Petriciolet, A & Alvarez-Castillo, A 2014, 'Polyester fiber production using virgin and recycled PET', *Fibers and Polymers*, vol. 15, no. 3, pp. 547-52.

Timber and Forestry eNews 2022, *Australia's Timber Shortage Realities,* Potts Points, NSW, viewed 7 October 2022, <https://www.timberandforestryenews.com/australias-timber-shortage-realities/>.

Trex 2022, trex.com, Winchester, Virginia, viewed 10 October 2022, <https://au.trex.com/>.

Verhey, S, Laks, P & Richter, DL 2001, 'Laboratory decay resistance of woodfiber/thermoplastic composites', in B Via (EIC), *Forest Products Journal*, Georgia, vol. 51, no. 9, pp. 44-49.

Vedrtnam, A, Kumar, S & Chaturvedi, S 2019, 'Experimental study on mechanical behavior, biodegradability, and resistance to natural weathering and ultraviolet radiation of wood-plastic composites', in H Wang & UK Vaidya (EICs), *Composites Part B: Engineering*, vol. 176, 107282, viewed 9 October 2022, <https://doi.org/10.1016/j.compositesb.2019.107282.>.

Wang, Y 2007, *Morphological characterization of wood plastic composite (WPC) with advanced imaging tools: developing methodologies for reliable phase and internal damage characterization*, Oregon State University, Corvallis, Oregon.

Waste Sense 2022, *As Landfills in Melbourne's Southeast run out of Space, Experts Weigh in on the Alternative Solutions,* GlobeNewswire, Los Angeles, California, viewed 7 October 2022, <https://www.globenewswire.com/>.

Wechsler, A & Hiziroglu, S 2007, 'Some of the properties of wood–plastic composites', in Q Chen & X Yang (EICs), *Building and Environment*, Elsevier Ltd., Amsterdam, vol. 42, issue 7, pp. 2637-2644, viewed 6 October 2022, <https://doi.org/10.1016/j.buildenv.2006.06.018.>.

Xia, F, Durandet, Y, Tan, PJ & Ruan, D 2022, 'Three-point bending performance of sandwich panels with various types of cores', *Thin-Walled Structures*, vol. 179.

Xiong, J, Ma, L, Stocchi, A, Yang, J, Wu, L & Pan, S 2014, 'Bending response of carbon fiber composite sandwich beams with three dimensional honeycomb cores', *Composite Structures*, vol. 108, pp. 234-42.

Yin, S, Tuldahar, R, Combe M, Collister T, Jacob, M & Shanks, AR 2013, 'Mechanical Properties of Recycled Plastic Fibres for Reinforced Concrete', *Fibre Concrete 2013*: *Proceedings of the Fibre Concrete*, Prague, Czech Republic.

Zawlocki, M. M 2003, 'Characterization of wood-plastic composites by dissipated `energy', *Washington State University, Department of Civil and Environmental Engineering*.

Zhang, F, Xu, J, Esther, B, Lu, H, Fang, H & Liu, W 2020, 'Effect of shear span-to-depth ratio on the mechanical behavior of composite sandwich beams with GFRP ribs and balsa wood core materials', *Thin-Walled Structures*, vol. 154.

APPENDICES: APPENDIX A – RISK MANAGEMENT PLAN

This Risk Management Plan is for the mechanical testing of the homogenous materials under three-point bending. This experimentation was completed by fellow student Ashiqul Islam, who has completed this Risk Management Plan, and was assisted by the author of this paper, with the experimental results being shared across both papers. The data from the mechanical testing on the wood composite material was vital in the performance analysis of the product and the model creation.

2194	RISK DESCRIPTION	TREND	CURRENT	RESIDUAL
	Laminate preparation, Panel preparation & Mechanical testing		Low	Low

RISK OWNER	RISK IDENTIFIED ON	LAST REVIEWED ON	NEXT SCHEDULED REVIEW
Ashiqul Islam	31/03/2023	03/04/2023	03/04/2024

RISK FACTOR(S)	EXISTING CONTROL(S)	CURRENT	PROPOSED CONTROL(S)	TREATMENT OWNER	DUE DATE	RESIDUAL
Hazard: Recycled PET Polyester Fabric & Hemp Fabric need to be cut into specific dimensions, therefore, the chance of getting hand injury	Control: Safety gloves will be used. Control: The lab technician's assistance will be requested.	Low				Low
Hazards: Risk of the lifting, shifting, and failing objects at the time of sandwich panels; The Risk: The body injuries	Control: Wear safe footwear, heavy-duty gloves, and marks as required. Control: G-Clamp will be utilized to fix panels and plates Control: Ask for help as required from the laboratory technical staff.	Low				Low
Unpleasant smells of resin (Part A) and hardener (Part B), may cause skin irritation, eye irritation and damage, allergic skin reaction and respiratory irritation. Harmfull if swallowed.	Control: Ventilation will be used to reduce the risk of exposure to dust and odor. An eye wash unit and safety shower station is available nearby work place. Control: Training will be provided for the mixing of resin and fillers. MSDS and TDS are attached. Control: Use vapour filter mask, chemical resistant hand gloves, goggles, lab coat and safety boots	Low				Low

Trip hazards due to workplace mess	Control: Plastic cover will be used to keep the area clean. _____ Control: Safety boots, goggles, and hand gloves will be used. Except for part of the face, the entire body will be covered.	Low				Low
Body injuries caused by projectile fragments from failed samples during mechanical testing	Control: Protective shield will be used if necessary. Load will be applied slowly as per standdard guidlines. _____ Control: Training will be provided in the safe operation of equipment. _____ Control: Wear gloves and goggles when testing samples.	Low				Low
Potential for electric shock if equipment is damaged or malfunctioning.	Control: The equipment is RCD protected to mitigate the effect of an electric shock. MTS 100 kN and 10 kN in P11 will be used. _____ Control: Check for current electrical safety tag and perform visual check for any physical damage to machine or electrical connections. Do not use if damage is evident or tag is not in date. Check the status of the power outage before testing samples.	Low				Low
COVID-19: General exposure.	Control: Follow the latest USQ guidelines in relation to COVID-19 and exposure. Maintain social distancing, do not attend work if unwell or after visiting hotspot areas. _____ Control: Wear an appropriate mask if within 1.5m of others.	Low				Low

ATTACHMENTS
MSDS-100% Hemp Yarn.pdf filament & staple fiber - en.pdf MSDS.pdf TDS_-_Part_A_and_Part_B.pdf